Can Information Design Resolve Electric Vehicle Charging Chaos?

Qianni Wang[1], Xiaotong Sun[2], Yu (Marco) Nie*[1], and Jiayang Li[3]

[1]Department of Civil and Environmental Engineering, Northwestern University, Evanston, IL, USA
[2]Intelligent Transportation Thrust, The Hong Kong University of Science and Technology (Guangzhou), Guangzhou, China
[3]Department of Data and Systems Engineering, The University of Hong Kong, Hong Kong SAR, China

December 4, 2025

Abstract

Charging remains an obstacle to the mass adoption of electric vehicles (EVs), especially for long-distance travel. If many EV drivers take to the road around the same time, their "range anxiety" may create a self-fulfilling prophecy. As drivers anticipate uncertainty and congestion at charging stations, they tend to make decisions about when and where to charge that could collectively lead to chaos and inefficiency. Here, we show that information design can persuade drivers to adopt decisions that are better for the system while being consistent with their self-interest as defined by the Bayesian Nash equilibrium. Our stylized model incorporates a congestion effect into drivers' payoffs and assumes that the information designer can leverage its private knowledge about the charging condition to influence heterogeneous drivers whose type is defined by their vehicle's remaining range. We consider both public and private information designs. The former does not depend on the driver type, while the latter does. For the private design problem, we propose a novel cutoff structure that enables us to reformulate an infinite-dimensional problem as a finite one. Our analysis shows that, in a one-station, two-state model equipped with a linear cost function, the optimal public design reduces to full information revelation. Moreover, the optimal private design yields significantly better outcomes and, in some cases, can even attain the system optimum. The model is further extended to a corridor setting to examine the impact of different information release schedules. Numerical results show that the private design with sequential release consistently yields the best performance. Under public design, however, the relative effectiveness of different release schedules depends on the spatial configuration of the corridor, among other factors.

Keywords: Information design; EV charging; Bayesian Nash equilibrium; Information release schedule

1 Introduction

The adoption of electric vehicles (EVs) has grown substantially in recent years. In 2023, EVs accounted for 37%, and 24%, of all new car sales in China and Europe, respectively (Pontes 2024, Kane 2024). Even in the U.S., where the growth of EV sales has lagged behind, 7.2% of new

*Corresponding author, E-mail: y-nie@northwestern.edu

car sales were electric in 2023 (Ewing 2024). The strong growth of the EV market is expected to continue, with the International Energy Agency projecting that by 2035 "every other car sold globally" will be electric (IEA 2024). The current generation of EVs, with a typical range up to 300 miles, are well-suited for intracity travel, especially when their owners have access to home charging. For long-distance intercity travel, however, the need for en-route charging remains a significant obstacle, physically and psychologically. The problem becomes especially acute when big crowds are expected at public charging stations, due to holiday traffic or other special events. For example, many Chinese EV drivers heading home for the Spring Festival in 2024 found themselves spending more time at charging stations than driving (News 2024, Andrews 2024). During the 2024 total solar eclipse in the U.S., many Tesla owners were similarly caught off guard by the long queues at charging stations (Skinner 2024).

The (unknown) possibility of getting stuck in a queue for charging could worsen the so-called "range anxiety" — note that in winter, an EV cannot afford to wait in line for too long because heating can quickly drain an already depleted battery (Jaguemont et al. 2016, Zhang et al. 2018). Anxious EV drivers who seek protection from the peril of running out of fuel may end up going to charge stations more often than needed. This defense charging behavior is bound to exacerbate the shortage of charging capacity relative to the surging demand, creating a vicious cycle that can spin out of control. Our study is inspired by the need to mitigate such chaos.

How do we help drivers trapped between the anxiety about the range of their vehicle on the one hand and the uncertainty in the availability of charging on the other? For many, the first idea that comes to mind may be to eliminate the uncertainty by making real-time information about the charging condition available to all drivers. Indeed, smartphone apps already exist in China that promise to do just that (State Grid Smart Internet of Vehicles Co. 2024). Yet, the question is whether being perfectly transparent is "optimal," in the sense that the system as a whole suffers the least delays and disruptions associated with charging. Plenty of evidence suggests that the answer may be "No." Research in transportation have shown that the benefits gained from providing real-time travel information diminish when the fraction of informed drivers exceeds a certain threshold (Mahmassani and Jayakrishnan 1991, Koutsopoulos et al. 1994, Emmerink et al. 1995), that providing "low-quality" information can be counterproductive (Arnott et al. 1991), and that more information, even when it is of high quality, is not always better (Acemoglu et al. 2018). Similar phenomena have been observed in other application domains (Bergemann and Morris 2019, Wu et al. 2021, De Véricourt et al. 2021). The fundamental insight here is that information provision can be *strategically designed* to maximize impact on user behaviors for a more desirable system outcome. This study aims to examine information design for inducing EV drivers to make charging decisions better aligned with a system objective.

Information design provides a framework for developing and analyzing an information structure — what information should be revealed, to whom, and how — to achieve desirable system outcomes such as improved efficiency, better resource allocation, or enhanced welfare (Kamenica and Gentzkow 2011, Kamenica 2019, Bergemann and Morris 2019). In the past decade, it has attracted much attention in economics and beyond (see Section 2 for details). When adapted to our context, information is transmitted to EV drivers through coded "signals" that indirectly shape their beliefs about the random charging condition through Bayesian updating. These signals are produced according to an information structure that maps each realization of this random variable — referred to as *state* — to a distribution over signals. Having received a particular signal, the drivers then settle for a Bayesian Nash equilibrium (BNE) as they make a charging decision. A

charging information designer can tweak the information structure to influence the BNE, hence the system outcome. Because all drivers know the information structure beforehand, they are *persuaded* rather than coerced or deceived into complying with the designer's goal. Persuasion is a key advantage of information design.

In our base model, EV drivers with different remaining ranges face a trade-off between two options: (i) making a detour to visit a charging station and waiting in a queue for an uncertain amount of time, and (ii) skipping the station to risk enduring a much higher cost later if their remaining range proves insufficient and a detour to a more distant charging facility is necessary. Importantly, the waiting time depends on the collective choices of the drivers: the more drivers choose to charge, the longer the waiting time. Such a congestion effect means each driver's decision has an *externality*. The designer has exclusive knowledge of the charging state, which affects the waiting time. This information asymmetry provides the lever by which the designer persuades drivers to adjust their choices for the good of the system.

Information design can be either public or private. A public design cannot differentiate drivers while a private one can. Intuitively, a private design has greater potential because it gives the designer more freedom. However, because a private design implies sending different signals to different drivers, it has to be justified properly — otherwise, drivers may suspect deception or unfairness, defeating the purpose of persuasion. Existing studies on private information design in congestion games typically impose an i.i.d. information structure across drivers. This means, while information delivery may be "randomized" following a certain population-wide distribution, they are not tied to driver types. In this study, we classify drivers and design information structures based on the remaining range of their vehicles, which naturally introduces heterogeneity through a continuous attribute. Accordingly, the information delivered to drivers depends on this property (type).

We analyze and formulate both public and private information design problems for our base model. To deal with the challenge arising from the infinite number of user types in private design, we propose an information structure based on the concept of cutoff thresholds, which leads to an equivalent mixed integer nonlinear formulation. For a special case with two states and a linear charging cost function, we show that (i) the optimal public design requires full revelation (signal always reveals the true state) and (ii) the optimal private design not only outperforms the full-information scheme in most cases but can achieve the system optimal outcome under certain conditions.

We further extend the base public and private information design models to a two-station corridor. In this setting, drivers' choices include not only whether but also where to charge. We study two information release schedules: (i) sequential release, in which signals are revealed before reaching each station; and (ii) simultaneous release, in which information about both stations is disclosed at the first station. We analyze how different release schedules influence drivers' beliefs about downstream uncertainty and, in turn, their charging decisions. The results show that full information remains optimal under public design. Moreover, while private design consistently favors sequential over simultaneous release, public design does not — its relative performance depends on problem inputs, including the spatial configuration.

Our contributions can be summarized as follows.

- We explore a new class of information design in games where the payoffs of the players (EV drivers in our problem) are influenced by a congestion effect, and their type is represented by a continuous variable. While both aspects have been studied individually, few works,

to the best of our knowledge, have combined them. Although motivated by EV charging, this framework has applications in other domains that involve both externalities and user heterogeneity.

- To address the challenge posed by combining an infinite number of types with externality, we propose a special private information structure that makes recommendations based on a cutoff threshold tied to the state of the system. This approach effectively reduces an infinite dimensional problem to a finite one and, by further simplifying information dissemination and obedience requirements, leads to a formulation that is amenable to analysis.
- We extend the base model to a more realistic corridor setting that allows for both simultaneous and sequential information release. Accordingly, we examine how the outcomes of information design interact with release schedules and the spatial configuration of the corridor.

For the remainder, Section 2 reviews relevant studies. Section 3 first outlines the settings of our base EV charging problem and then formulates the corresponding public and private information design models. Section 4 provides analytical results in a special case and Section 5 further extends the base model to a two-station corridor setting. Numerical results are reported in Section 6. The last section concludes the study and comments on the directions for future research.

2 Related studies

Our review of related studies covers three areas. It begins with the research on EV charging behavior and decision-making problems. Then, an overview of the burgeoning field of information design (ID) is provided, along with a few typical applications. In the final part, we examine the application of ID in congestion games, to which our EV charging problem is closely related.

2.1 EV charging behavior and decision-making

Charging has been identified as a key issue in the push for transportation electrification from early on, with much of the attention being paid to the planning of charging infrastructure (Mak et al. 2013, He et al. 2013, Nie and Ghamami 2013). Given infrastructure planning is not our focus, the reader is referred to Mohammed et al. (2024) and Cui et al. (2023) for recent reviews on the subject. Below we mainly discuss the aspects that concern EV drivers' behaviors and decision-making processes.

Sun et al. (2015) studied EV drivers' choice of when to charge after the last trip of the day. The results, estimated using panel data extracted from a two-year field trial in Japan, suggest that this decision depends on the remaining range, as well as the timing and intensity of the next trip. In a sequel, Sun et al. (2016) considered the choice of fast-charging stations for longer trips (though only one charge per trip is permitted). They found EV drivers prefer charging stations requiring a shorter detour and located at gas stations. Moreover, they confirmed that the remaining range upon approaching a charging station affects the decision to charge there significantly and negatively. Ge and MacKenzie (2022) focused on long-distance trips and allowed for multiple charges per trip, though they relied on stated preference data. Their estimation results identified the remaining range and the ability to reach the next station without changing the original plan

as the most critical factors affecting charging decisions. Wolbertus et al. (2018) explored how the length of charging sessions is affected by factors not directly related to charging. They found that for slower chargers (e.g., level-2), EV drivers tend to leave their vehicles parked at the charging station longer than necessary for a full charge. However, this behavior is much less pronounced at fast-charging facilities.

Recognizing the potential impact of delay caused by a surge in demand on charging time, Hassler et al. (2021) proposed to coordinate the EV drivers' choices of charging stations through vehicle-to-infrastructure communications (V2X). The idea is to make the information on the anticipated delay at charging stations available in real-time to all drivers so that they can choose and announce their best charging plan. In essence, the proposed scheme facilitates the achievement of a Nash equilibrium, which may well be sub-optimal from the perspective of the system. Chakraborty et al. (2022) described a futuristic Peer-to-Peer Car Charging (P2C2) solution that employed high-battery-capacity vehicles to charge other EVs while they are all in motion. To account for uncertainty inherent to the use of EVs, Iversen et al. (2014) modeled EV driving patterns as a Markov process and developed a stochastic dynamic programming model that makes optimal charging decisions using the driving patterns as inputs. Yi and Shirk (2018) adopted an approach similar to that of Iversen et al. (2014), although their application is focused on connected and autonomous EVs and provides the capability to incorporate real-time information into driving patterns for energy consumption prediction. Futalef et al. (2023) studied a version of the electric vehicle routing problem (E-VRP) that accounts for several relevant operational factors, such as nonlinear/partial charging, station capacity, and mass-dependent energy consumption. Their model, solved using a metaheuristic algorithm, updates predetermined routes (obtained by an offline E-VRP variant) according to real-time traffic and charging conditions. Liu et al. (2023) formulated the problem of optimally selecting charging stations and charging duration in a long-distance trip as a finite-horizon Markov decision process. They showed that the optimal charging duration monotonically decreases with the remaining range and increases with travel distance.

2.2 Information design

Information design is a relatively new branch of game theory that addresses the situation where players' payoff in a game depends on system states and a "designer" has an information advantage that he can exploit to achieve a desired outcome (see Bergemann and Morris 2019, for a review). Unlike mechanism design, which focuses on the design of the game's rules, information design focuses on its information structure, specifically how the information about the states is communicated to the players. Another unique feature of information design is that the designer is committed to the information structure *ex-ante*, which can be chosen to ensure the best response of the players aligns with the outcome desired by the designer, per the revelation principle (Myerson 1979). Appendix A summarizes the basic settings of information design. For a more detailed exposition, the reader is referred to Kamenica (2019), Bergemann and Morris (2019).

When the game has only one receiver, information design is often called Bayesian persuasion, where the designer (or sender), is seen as designing an information structure and sending signal accordingly to persuade the player (or receiver) to do his bidding. For a basic setting of such a problem, Kamenica and Gentzkow (2011) characterized the information structure deemed "optimal" by the sender, and provided the conditions under which the optimal information structure

strictly benefits the sender. Despite its simplicity, Bayesian persuasion offers a powerful tool to understand and analyze many social-economic phenomena. The motivating example in Kamenica and Gentzkow (2011) is quite striking: a prosecutor (the sender) may persuade a judge (the receiver) to convict a defendant with a much higher probability than her prior belief, by designing an investigation that slightly overstates the likelihood of the defendant being guilty when they are actually innocent. Rayo and Segal (2010) considered the optimal information disclosure of the sender who randomly draws a "prospect" defined by its profit to the sender and its value to the receiver. In their application, the sender is an internet advertising platform, the receiver an internet user, and the prospect an advertisement. In Ostrovsky and Schwarz (2010), the sender is a school that chooses a grading policy to optimize the job placement of its students, and the receiver is an employer trying to hire the best students from that school.

When the game has multiple players, Bergemann and Morris (2016) demonstrated that the outcomes achievable through information design coincide with Bayesian correlated equilibrium (BCE) — a version of incomplete information equilibrium. These outcomes can be characterized by the players' obedience — they are "obedient" because no better options are available given what they know — to the designer's recommendations. Accordingly, the constraints from the obedience requirement form the feasible set from which the designer selects the most desirable outcome. Bergemann and Morris (2019) highlighted three general insights from information design: (i) it is often optimal to "selectively obfuscate information", (ii) the more prior information the players possess, the less "persuasive" the designer becomes, and (iii) private information design is preferred to public information as long as "perfect correlation between players' actions" is not desired.

Information design and Bayesian persuasion have found numerous applications in understanding and managing socio-technical systems involving strategic agents. Lingenbrink and Iyer (2019) considered the revenue management problem for a service provider, who must decide how to price the service while sharing with potential customers the stochastic state of a queue offering the service. They proved that combining pricing and information design cannot further improve the optimal revenue achievable when the designer only controls price and customers are given full information about the state of the queue. In a follow-up study, Anunrojwong et al. (2023) introduced need-based user heterogeneity into the queuing system. Specifically, high-need users always wait for service due to their lack of alternative options, while low-need users can be persuaded to use their fallback options more frequently than they would if the state of the queue were perfectly observable. They confirmed that information design yields benefits — and can even achieve the system optimum at times — provided that neither class of users dominates the population. Ashlagi et al. (2024) examined the allocation of non-monetary objects (such as organs or public housing) to agents with private preferences over these objects. They demonstrated that, through information design, the optimal mechanism can be implemented via a simple first-come, first-served queue with deferrals, where agents are only informed of a range of an object's quality at the time of the offer. By adjusting this range, a social planner can achieve the desired trade-off between allocative efficiency (which depends on who receives which object) and social welfare (which is negatively impacted by deferrals).

An active strand of information design research concerns the dynamics in decision making. In some applications, the dynamic game unfolds between a manager and a single user through repeated or long-term interactions (Ely 2017, Farhadi and Teneketzis 2022, Gan et al. 2022b). In others, there are multiple users, but in each round only one is engaged, often modeled within a

queuing framework (Renault et al. 2017, Wu et al. 2022, Best and Quigley 2024).

2.3 Information design in congestion games

In transportation, congestion games have been studied since the 1950s (Wardrop 1952, Beckmann et al. 1955). The rise of intelligent transportation systems (ITS) in the late 1980s brought the question of how traffic information promised by ITS can actually benefit drivers (Ben-Akiva et al. 1991, Mahmassani and Jayakrishnan 1991). Using a bottleneck model with stochastic capacities, Arnott et al. (1991) showed that, while providing full and accurate information is always better than not providing information at all, "low-quality" information that affects drivers' beliefs about stochastic capacities may in fact harm efficiency and welfare. Interestingly, the "signal" spoken of in Arnott et al. (1991) plays a similar role as information structures in information design, though they treat this signaling process as given and do not consider designing the information structure itself, nor whether an optimally chosen structure could outperform full and perfect information revelation. Lindsey et al. (2014) considered a similar setting as in Arnott et al. (1991) but focused only on route choice (hence a simpler traffic model). They examined how the adverse effects of full information provision vary depending on factors such as travel cost functions and the stochasticity of traffic states. Instead of exploring how the quality of information provision affects its effectiveness, as done in Arnott et al. (1991), Liu et al. (2016) examined the impact of market penetration. They found that there is a threshold for the market penetration of high-quality information access, beyond which further expansion becomes ineffective and, in some cases, even socially harmful. Like Liu et al. (2016), Acemoglu et al. (2018) also studied the impact of information coverage, focusing specifically on spatial coverage. They assumed that travelers would only use routes for which they had full information. Their analysis revealed that expanding travelers' spheres of knowledge can generally be harmful — what they termed the Informational Braess Paradox — although certain network topologies may prevent this undesirable effect. Wu et al. (2021) studied a Bayesian congestion game with multiple traveler types. In their model, link travel costs in a transportation network are influenced by a stochastic state with a known prior distribution. Travelers, depending on their type (interpreted as the route guidance system they subscribe to), receive private information to update the prior and then settle into a Bayesian Wardrop equilibrium (BWE). By characterizing the BWE, they showed that information benefits a group of travelers relative to others if, and only if, the group's share among all travelers is below a certain threshold.

The studies cited above can largely be seen as sensitivity analyses on information provision. However, they did not address the design question — namely, which information structure and delivery mechanism can maximize benefits. Research aimed at tackling this question has only begun to emerge in recent years. Das et al. (2017) was among the first to investigate both public and private information design in routing games, though they focused on homogeneous travelers. Tavafoghi and Teneketzis (2019) examined information design in a Bayesian congestion game, where homogeneous travelers compete to reach an equilibrium based on their beliefs about uncertain travel times in a road network. They demonstrated that the information designer can enhance social welfare — reducing expected travel time — by tailoring information structures to individual travelers. However, it is unclear whether the differences in information structures are publicly known. If not, the scheme can hardly be called "persuasion." But if the differences are public, the designer may struggle to justify why travelers are treated unequally. Building on this work, Tavafoghi et al. (2019) explored how a profit-driven private designer — such as a

firm like Waze — operates its information provision business. They concluded that competitive pressure would compel such firms to be fully transparent, ultimately leading them to adopt an ad-based rather than a subscription-based business model. Yang et al. (2019) adopted a Bayesian congestion game framework with atomic and homogeneous agents (e.g., Uber drivers) deciding whether to relocate from one zone to another in search of a "resource" (e.g., Uber riders) with a random return. The study considered both private and public information designs, although the authors acknowledged the difficulty of justifying private design for homogeneous agents. Their numerical analysis confirmed that both designs can improve social welfare compared to the no-information and full-information benchmarks. Zhou et al. (2022) studied an atomic and slightly generalized version of the Bayesian congestion game considered by Tavafoghi and Teneketzis (2019). In their setting, all travelers have access to a fixed set of non-overlapping parallel routes, referred to as "resources." Their focus is on developing exact solution algorithms for the optimal public and private information design problems. In Zhu and Savla (2022), the Bayesian congestion game has an identical configuration as Zhou et al. (2022), but with non-atomic agents. They demonstrated that the information design in their setting can be formulated as a convex optimization problem (hence computationally tractable), and that with optimally configured private designs, social welfare is not negatively impacted by the increase in market penetration. For general non-atomic Bayesian congestion games, Griesbach et al. (2022) provided analytical results characterizing the networks where full information provision always aligns with the optimal public information design — note that full information revelation is a special case of public information design. In a follow-up study, Griesbach et al. (2024) explored a different variant of the game, where uncertainty arises from the demand side. They proposed a polynomial-time algorithm to find the optimal public information design and proved that in this setting, full information revelation coincides with the optimal public information design only on series-parallel networks. Building on Das et al. (2017), Matsushita (2024) developed a deep learning–based approximation algorithm applicable to general networks. They also derived lower bounds on the performance of the full-information scheme for specific forms of route cost functions. However, similar to Das et al. (2017), their framework does not explicitly address user heterogeneity — an aspect that is central to the basic setting of the present study.

3 Model

3.1 Basic settings

Our base model of information design for EV drivers is set as a one-shot static game over a simple highway network mimicking a long-distance travel scenario, see Figure 1 for an illustration. EV drivers travel from their home town (the O town) to their destination town (the D town) through a highway. There exists a decision point on the highway where an EV driver has the opportunity to choose an action $a \in \mathbb{A}$, which in our model comprises two options: take a detour to charge (Route C), or continue on the highway so as to skip charging (Route M). Thus, $\mathbb{A} = \{C, M\}$. If the driver takes Route M, then the length of their remaining journey is l; otherwise, the total length increases by Δ_l to $l + \Delta_l$. The existence of the detour highlights that charging is not a default option: the driver will take Route C only if the expected utility gain from charging justifies the additional detour cost.

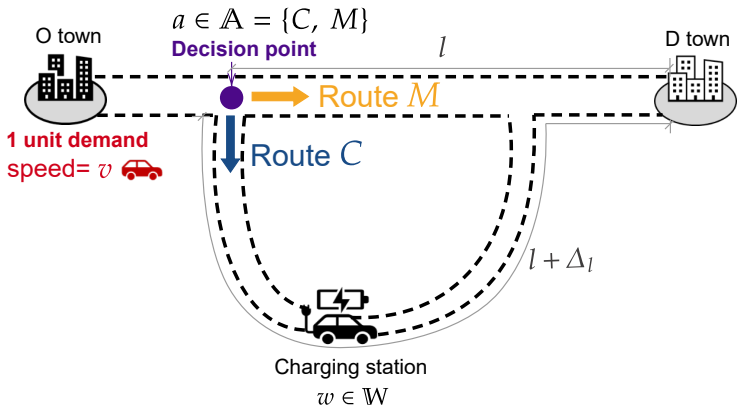

Figure 1: Illustration of the EV charging problem.

For simplicity, we shall assume that the travel speed is independent of the drivers' choices. However, the charging time is subject to a congestion effect: the more drivers choosing Route C, the longer the charging time. The driver's decision is affected by, among other factors, the remaining range of their vehicle at the decision point and the anticipated charging time at the charging station — the latter in turn depends on the state of the charging station. We next discuss these two crucial factors.

The condition of the charging station (hereafter referred to as its *charging condition*) is modeled as an exogenous discrete random variable. A realization of the condition, called a *state*, is denoted by $w \in \mathbb{W}$ where $\mathbb{W}$ is a set of all possible states and $\boldsymbol{\mu}_0$ is the publicly known prior belief. The charging condition may depend on the supply-demand conditions of the local electrical grid, weather, and other contingencies. The information designer (referred to as the designer hereafter) can observe the state, whereas EV drivers cannot. This grants the designer an informational advantage whose exploitation is central to our study.

The remaining range of an EV is assumed to be estimated by the vehicle's on-board computer. This estimate, referred to as the *remaining range estimate* (RRE) and denoted by r, determines the probability of completing the journey without charging, i.e. using Route M, through a function $p(r)$. Note that $p(r)$ should be an increasing function of RRE r. The driver can access their own vehicle's RRE at the decision point (i.e. before they make the charging decision), and the designer is assumed to have information on the distribution of all vehicles' RRE either through historical data or a vehicle-to-vehicle and vehicle-to-infrastructure (V2X) system. The probability density function (PDF) and the cumulative distribution function (CDF) of the RRE distribution are denoted as $g(\cdot)$ and $G(\cdot)$, respectively, over support $\Xi = [\underline{R}, \bar{R}]$, where $\underline{R}$ and $\bar{R}$ represent the minimum and maximum values of the distribution. Throughout the study, we shall assume the distributional information about RRE is public knowledge.

Assumption 1 (RRE distribution)**.** *The distributional information about RRE, represented by the PDF $g(r)$, is common knowledge.*

We posit that EV drivers should have access to the RRE distribution for two reasons. First, such information may be easily obtained through crowdsourcing, prior experience, or historical data. Second, given the goal is persuasion rather than deception, the designer has an incentive to be as transparent as possible.

To define the cost associated with the charging choice, we normalize the total demand for the highway network to 1 unit and let $f \in [0, 1]$ be the flow on Route C. Thus, the flow on Route M is $(1 - f)$ per flow conservation. At each state $w \in \mathbb{W}$ and with a charging flow f, an EV driver with RRE r incurs a non-negative cost depending on their route choice. These costs are regulated by the following conditions.

Assumption 2 (Cost functions)**.** *The cost of choosing Route C is an increasing function of the charging flow f, but independent of the RRE r; the cost of choosing Route M is a decreasing function of $p(r)$ but is independent of the charging flow.*

As mentioned earlier, the charging time is congestible, which contributes to the increase in the cost of choosing Route C when more drivers use Route C. On the other hand, choosing not to charge (Route M) is associated with an inherent risk of not being able to complete the journey, imposing an expected cost that increases as r (hence $p(r)$) decreases. Moreover, both costs are contingent upon the state. Thus, we denote the cost functions associated with Route C and M as $J_C(f|w)$ and $J_M(p(r)|w)$, respectively.

A driver always attempts to minimize their own expected cost, according to their belief about each state and the choices of the other drivers. This brings the system to a Bayesian Nash equilibrium (BNE), from which no one has an incentive to deviate. When drivers' belief is $\boldsymbol{\mu}_0$ (the prior), for example, the expected costs on the two routes can be illustrated in Figure 2. The green dotted line, representing Route M's expected cost, decreases with $p(r)$ (cf. Assumption 2), hence also with the RRE r. In contrast, the solid blue line representing Route C's expected cost is horizontal since it is not a function of r (cf. Assumption 2). The intersection of these two lines identifies a threshold RRE $\bar{r}$. Seeking to minimize expected cost, EV drivers with $r < \bar{r}$ prefer charging (Route C), while those with $r > \bar{r}$ prefer to skip charging (Route M). The driver with $r = \bar{r}$ is indifferent between the two options. As such, the indifferent RRE $\bar{r}$ corresponds to a flow assigned to Route C, i.e, $f = G(\bar{r}) = \int_{\underline{R}}^{\bar{r}} g(r)\,\mathrm{d}r$. When the EV drivers reach BNE, the flow on Route C is denoted as f^*, which, assuming the intersection between the two lines always exists (i.e., excluding the corner solutions), can be solved from the following equilibrium condition:

$$\sum_{w\in\mathbb{W}} \mu_0(w) J_C\left(f^*|w\right) = \sum_{w\in\mathbb{W}} \mu_0(w) J_M\left(p(\bar{r}^*)|w\right). \tag{1}$$

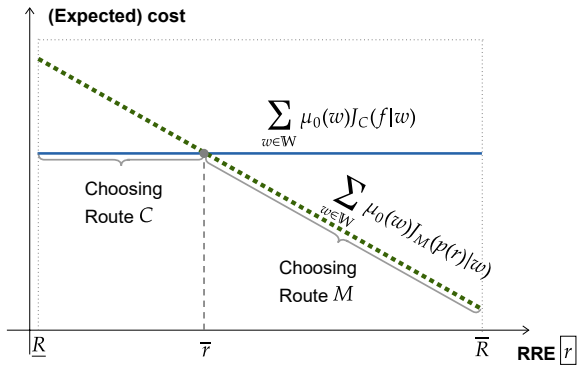

Figure 2: Route choice and Bayesian Nash equilibrium illustration.

The designer can try to move f^* by shifting the drivers' belief away from $\boldsymbol{\mu}_0$ if this equilibrium is deemed undesirable. The designer may always inform the drivers of the true state, hoping that full information leads to a better system outcome. Another option, which is the chief concern in this study, is to shape the drivers' belief to benefit the system as much as possible, by designing an information structure and sharing it with the drivers. Public and private information designs differ in whether all drivers receive the same signal in any given state and thus share the same posterior belief. In our settings, the private design allows the information structure to be differentiated based on drivers' type (i.e., the RRE). In what follows, we first discuss the public option.

3.2 Public information design

In the public design, the designer commits to an information structure $\boldsymbol{\pi} = \{\pi(s \mid w)\}_{w\in\mathbb{W}, s\in\mathbb{S}}$ where $\pi(s \mid w)$ represents the probability of sending signal s given the state w, and $\sum_{s\in\mathbb{S}} \pi(s \mid$

$w) = 1$ $(\forall w \in \mathbb{W})$. Then, after the state w is observed, the designer draws a signal $s \in \mathbb{S}$ according to the information structure $\boldsymbol{\pi}$ and sends it to all drivers. Upon receiving the signal, EV drivers update their beliefs and derive posterior probabilities $\boldsymbol{\mu}_s = \{\mu_s(\dot{w}) = \frac{\mu_0(\dot{w})\pi(s|\dot{w})}{\sum_{w' \in \mathbb{W}} \mu_0(w')\pi(s|w')}\}_{\dot{w} \in \mathbb{W}}$ using the Bayesian rule. Then, the BNE can be determined as in Equation (1), by simply replacing the prior belief $\boldsymbol{\mu}_0$ with the posterior belief $\boldsymbol{\mu}_s$. The equilibrium charging flow and the indifferent RRE, both now dependent on the signal s, are denoted f_s^* and $\bar{r}_s^*$ respectively, with $f_s^* = G\left(\bar{r}_s^*\right) = \int_{\underline{R}}^{\bar{r}_s^*} g(r)\,\mathrm{d}r$ and $\bar{r}_s^* = G^{-1}\left(f_s^*\right)$.

The total expected cost of all EV drivers is employed as a measure of the system performance, which is given in (2).

$$\begin{aligned} Z(\boldsymbol{\pi}) &= \sum_{w \in \mathbb{W}} \mu_0(w) \sum_{s \in \mathbb{S}} \pi(s \mid w) \int_{r \in \Xi} J_{a^*(\boldsymbol{\mu}_s)}\left(f_s^*, p(r)|w\right) g(r)\,\mathrm{d}r \\ &= \sum_{w \in \mathbb{W}} \mu_0(w) \sum_{s \in \mathbb{S}} \pi(s \mid w) \left(f_s^* \cdot J_C(f_s^*|w) + \int_{G^{-1}(f_s^*)}^{\bar{R}} J_M(p(r)|w) g(r)\,\mathrm{d}r \right). \end{aligned} \tag{2}$$

When both routes receive positive flows for all $s \in \mathbb{S}$, the designer's problem can be formulated as follows (Kamenica and Gentzkow 2011):

$$\min \; Z(\boldsymbol{\pi}) \tag{3a}$$

$$\text{subject to: } \sum_{s \in \mathbb{S}} \pi(s \mid w) = 1, \forall w \in \mathbb{W};\; \pi(s \mid w) \geq 0, \forall s \in \mathbb{S}, w \in \mathbb{W}, \tag{3b}$$

$$\sum_{w \in \mathbb{W}} \mu_0(w)\pi(s \mid w) J_C\left(f_s^*|w\right) = \sum_{w \in \mathbb{W}} \mu_0(w)\pi(s \mid w) J_M\left(p(\bar{r}_s^*)|w\right), \forall s \in \mathbb{S}, \text{ where } \bar{r}_s^* = G^{-1}\left(f_s^*\right). \tag{3c}$$

3.3 Private information design

In public information design, the information structure $\boldsymbol{\pi}$ specifies the likelihood of a particular signal $s \in \mathbb{S}$ being sent by the designer to everyone given w. In this section, we explore a private design, whereby the information structure $\boldsymbol{\pi}$ specifies the possibility that action $a \in \mathbb{A}$ is recommended to a driver with RRE r given w per the revelation principle (Gibbard 1973, Dasgupta et al. 1979, Myerson 1979, Bergemann and Morris 2019). As a prerequisite for such a design, we shall assume the designer knows each driver's RRE r through a V2X network.

Assumption 3 (Accessibility of private information)**.** *The designer has access to any EV driver's remaining range estimate r.*

We next impose a specific class of information structures to restrict the design space. The proposed structure has two main features. First, at each state, the recommendation is deterministic rather than probabilistic. Instead of suggesting that a driver with 150 miles of remaining range has an 80% chance of receiving a charge recommendation, for example, the structure simply guarantees that such a driver *will* receive the recommendation to charge. Second, it follows a cutoff rule: at each state, any driver with a remaining range r below a certain threshold is recommended to charge, while those above the threshold are advised to skip charging. This structure is inspired by the characteristics of the Bayesian Nash Equilibrium (BNE) in our problem and aims to improve the practicality of information design. Notably, it eliminates the need for a random draw for each individual driver according to w. A formal statement about the information structure follows.

Assumption 4 (Information structure)**.** *For a given $w \in \mathbb{W}$, the designer makes a route recommendation based on the following rule, which is known by all drivers: pick $\bar{r}_w \in \Xi$ such that*

$$\begin{cases} \pi(C \mid w, r) = 1,\ \pi(M \mid w, r) = 0, \text{ for } r \le \bar{r}_w; \\ \pi(C \mid w, r) = 0,\ \pi(M \mid w, r) = 1, \text{ otherwise}, \end{cases} \tag{4}$$

where $\pi(a \mid w, r)$ denotes the probability of sending recommendation action a given state w and RRE r.

Assumption 4 implies that private information design can be fully specified by a vector of cutoff RRE $\bar{\boldsymbol{r}} = \{\bar{r}_w\}_{w\in\mathbb{W}}$, which, per the property of the BNE, also corresponds to a vector of state-dependent charging flows $\boldsymbol{f} = \{f_w\}_{w\in\mathbb{W}}$. When drivers have no incentive to unilaterally deviate from the designer's recommendation, they reach a Bayesian correlated equilibrium (BCE) (Bergemann and Morris 2019, Goldstein and Leitner 2018). Accordingly, the private information design problem is translated into inducing the BCE by ensuring the obedience of the drivers (i.e., the recommendation matches their best response under posterior beliefs). The formulation reads

$$\min Z(\boldsymbol{f}) = \sum_{w\in\mathbb{W}} \mu_0(w) \int_{r\in\Xi} \left[\pi(C|w,r)\, J_C(f_w|w) + \pi(M|w,r)\, J_M(p(r)|w)\right] g(r)\, \mathrm{d}r, \tag{5a}$$

$$\text{subject to: } \sum_{w\in\mathbb{W}} \mu_0(w)\, \pi(C|w,r) \left[J_C(f_w|w) - J_M(p(r)|w)\right] \le 0, \quad \forall r \in \Xi, \tag{5b}$$

$$\sum_{w\in\mathbb{W}} \mu_0(w)\, \pi(M|w,r) \left[J_M(p(r)|w) - J_C(f_w|w)\right] \le 0, \quad \forall r \in \Xi, \tag{5c}$$

$$f_w \in [0,1], \bar{r}_w = G^{-1}(f_w), \quad \forall w \in \mathbb{W};\ \text{and } \boldsymbol{\pi} \text{ satisfies (4)}. \tag{5d}$$

Similar to the public design problem, the objective here is to minimize the expected total system cost given the private information structure, assuming all EV drivers follow the recommendations. Constraints (5b)-(5c) are the obedience constraints. For example, Constraints (5b) dictate that an EV driver who receives recommendation C has no desire to switch to M because C offers a lower posterior expected cost. Note that the denominator of the posterior belief is omitted here because it appears in both terms on the left hand side of the inequality. Importantly, Constraints (5b)-(5c) must hold for all $r \in \Xi$. Constraints (5d) ensure the feasibility of the charging flow.

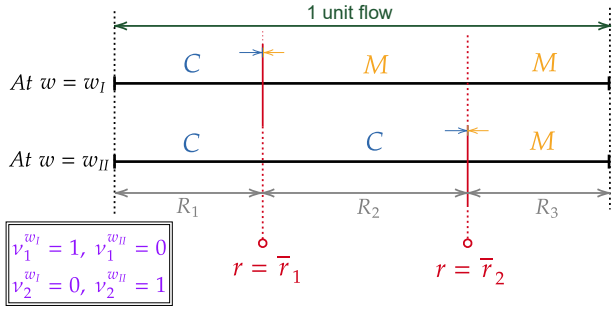

Figure 3: Illustration of type formation in private information design.

The cutoff vector $\bar{\boldsymbol{r}}$ divides the demand into at most $|\mathbb{W}|+1$ intervals. Drivers within each interval can be regarded as the same type since they should receive the same recommendation for any given w. The challenge is that, for any two states w_1 and w_2, the order between $\bar{r}_{w_1}$ and $\bar{r}_{w_2}$ — i.e., whether $\bar{r}_{w_1} > \bar{r}_{w_2}$ — cannot be predetermined. This order, however, is needed to specify the obedience constraint. Thus, we introduce an indicator variable $\boldsymbol{\nu} = \{\nu_i^w\}_{i=1,\dots,|\mathbb{W}|, w\in\mathbb{W}}$, where ν_i^w equals 1 if $\bar{r}_w$ is the i-th smallest among all cutoff thresholds and 0 otherwise. With a slight abuse of notation, we introduce another vector $\hat{\boldsymbol{r}} = \{\underline{R}, \bar{r}_1, \dots, \bar{r}_i, \dots, \bar{r}_{|\mathbb{W}|}, \bar{R}\}$ to denote the sorted RRE thresholds ($\bar{r}_i, \forall i = 1, \dots, |\mathbb{W}|$) augmented

with the lower and upper bounds on RRE. This enables us to define type k drivers as those with RRE $r \in R_k \equiv (\hat{r}_{k-1}, \hat{r}_k], \forall k = 1, \ldots, |\mathbb{W}| + 1$. Note that $\hat{r}_k := \bar{r}_i$ for $k = i \in \{1, \ldots, |\mathbb{W}|\}$, and $\hat{r}_0 := \underline{R}$, $\hat{r}_{|\mathbb{W}|+1} := \bar{R}$. For a given $\boldsymbol{\nu}$ and $\hat{\boldsymbol{r}}$, the recommendation received by all drivers of the same type is set for each w, see Figure 3 for an illustration.

Another difficulty associated with Problem (5) has to do with the dependency of the obedience constraint on r, which renders the problem infinite-dimensional. However, a close look reveals that for any interval, it suffices to require (i) the compliance with a charge recommendation by the driver with the highest RRE among all who receive the same recommendation — for that driver is the least likely to charge; and (ii) the compliance with a skip recommendation by the driver with the least RRE, again because that driver is the most likely to charge.

In light of the above observations, Problem (5) can be reformulated as follows:

$$\min Z(\boldsymbol{f}, \boldsymbol{\nu}) = \sum_{w \in \mathbb{W}} \mu_0(w) \left(f_w \cdot J_C(f_w|w) + \int_{G^{-1}(f_w)}^{\bar{R}} J_M(p(r)|w)\, g(r)\, \mathrm{d}r \right), \tag{6a}$$

$$\text{subject to: } \sum_{i=1}^{|\mathbb{W}|} \nu_i^w = 1, \quad \forall w \in \mathbb{W}, \tag{6b}$$

$$\sum_{w \in \mathbb{W}} \nu_i^w = 1, \quad i = 1, \ldots, |\mathbb{W}|, \tag{6c}$$

$$\sum_{w \in \mathbb{W}} \left(\nu_i^w - \nu_{i+1}^w\right) f_w \leq 0, \quad i = 1, \ldots, |\mathbb{W}| - 1, \tag{6d}$$

$$\bar{r}_i = G^{-1}\left(\sum_{w \in \mathbb{W}} \nu_i^w f_w \right), \quad i = 1, \ldots, |\mathbb{W}|, \tag{6e}$$

$$\sum_{w \in \mathbb{W}} \mu_0(w) \left(\sum_{j=k}^{|\mathbb{W}|} \nu_j^w \right) [J_C(f_w|w) - J_M(p(\hat{r}_k)|w)] \leq 0, \quad k = 1, \ldots, |\mathbb{W}|, \tag{6f}$$

$$\sum_{w \in \mathbb{W}} \mu_0(w) \left(\sum_{j=1}^{k-1} \nu_j^w \right) [J_M(p(\hat{r}_{k-1})|w) - J_C(f_w|w)] \leq 0, \quad k = 2, \ldots, |\mathbb{W}| + 1, \tag{6g}$$

$$f_w \in [0, 1], \quad \forall w \in \mathbb{W}, \tag{6h}$$

$$\nu_i^w = 0 \text{ or } 1, \quad \forall w \in \mathbb{W},\ i = 1, \ldots, |\mathbb{W}|. \tag{6i}$$

This is a mixed integer nonlinear program (MINLP) with $|\mathbb{W}|^2$ binary variables and $|\mathbb{W}|$ continuous variables. Constraints (6b)-(6c) ensure the indicator variables are feasible. Constraints (6d) link the order of RRE to that of the charging flow for each state. Constraints (6e) represent the ith ranked RRE threshold as a function of the charging flow.

Constraints (6f) and (6g) are the obedience constraints rewritten with the new variables. As discussed earlier, for each type and recommendation, we need at most one obedience constraint. In Constraint (6f), the recommendation is charge for type $k = 1, \ldots, |\mathbb{W}|$; the obedience is ensured for everyone in type k if the driver with the highest RRE of that type (i.e., $r = \hat{r}_k$) is obedient. Note that type $k = |\mathbb{W}| + 1$ does not need this constraint because the recommendation is to skip charge regardless of the state (in other words, this type will never receive a charge recommendation). Similarly, Constraint (6g) states that to ensure a skip recommendation is needed by all drivers of type $k = 2, \ldots, |\mathbb{W}| + 1$, we only need to impose the obedience constraint on the driver with the lowest RRE among all drivers of type k (i.e., $r = \hat{r}_{k-1}$). Again, there is no need to impose this constraint for type $k = 1$ drivers as they will never receive a skip recommendation.

Theorem 1. *Problem (6) and Problem (5) are equivalent.*

Proof. See Appendix C for details. □

4 Analytical results

In this section, we attempt to draw useful insights by analyzing the proposed model in finer detail. We first describe a simplified model setting that enables a meaningful analysis, and then provide analytical results for both the public and the private design problems.

4.1 Setting

To maintain tractability, we assume $\mathbb{W} = \{\mathrm{H}, \mathrm{L}\}$. The state H may indicate the electrical grid experiences high loads or other adverse conditions, making it more difficult to maintain the voltage at the charging station at the normal level. On the other hand, the state L signifies normal operation. For simplicity, we shall assume that EV drivers endure an extra wait time β when $w = \mathrm{H}$. Moreover, RRE follows a uniform distribution between $[l, nl]$, i.e., $g(r) = \frac{1}{(n-1)l}$ if $l \leq r < nl$; and 0 otherwise; as depicted in Figure 4(a), where $n > 1$ is a real number.

The probability of completing the journey without charging using Route M is denoted as $p(r)$. For any Route M taker, there is a probability of failing to complete the journey $(1 - p(r))$, which comes with a penalty. For simplicity, we further assume (i) $1 - p(r) = \frac{nl-r}{(n-1)l}$ if $l \leq r < nl$; 1 if $r < l$; and 0 if $r \geq nl$, as illustrated in Figure 4(b); and (ii) the range of any vehicle, when fully charged, is greater than nl. It follows that any Route C taker is guaranteed to complete their journey, regardless of their initial RRE.

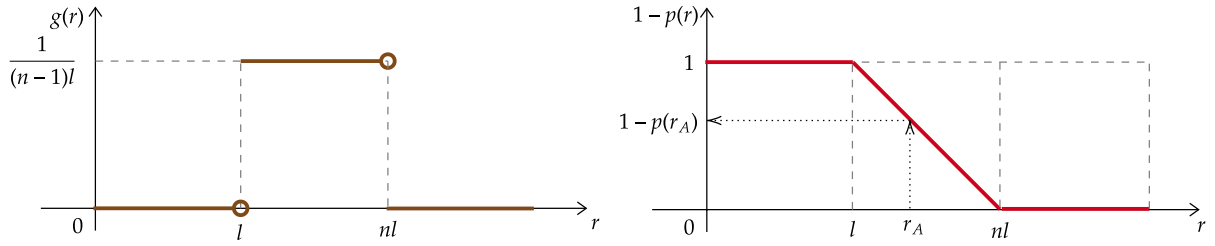

(a) PDF of the RRE distribution $g(r)$.

(b) Probability of failing to complete the journey on Route M.

Figure 4: Common knowledge for the designer and EV drivers.

Per Assumption 2, we define the cost functions as follows:

$$J_C(f|\mathrm{H}) = \frac{l + \Delta_l}{v} + (\alpha f + \beta), \; J_C(f|\mathrm{L}) = \frac{l + \Delta_l}{v} + \alpha f, \; J_M(p(r)|\mathrm{H}) = J_M(p(r)|\mathrm{L}) = \frac{l}{v} + \zeta(1 - p(r)), \quad (7)$$

where v is a constant travel speed. The cost of choosing Route C consists of the travel time with detour Δ_l, and the state-dependent charging time — with the abnormal state H imposing an extra $\beta \geq 0$. For convenience, we introduce $\Delta_t \equiv \Delta_l / v$ to denote the detour in the unit of travel time hereafter. The cost of selecting Route M includes the travel time without detour and a failure penalty, modeled as the product of a failure penalty coefficient $\zeta \geq 0$ and the failure probability. Moreover, these charging costs are assumed to be linear functions of the flow f on Route C, where the coefficient $\alpha \geq 0$ represents the congestion effect. Given Equations (7), the relationship between the charging flow f and the threshold RRE $\bar{r}$ is given as follows: $f = \int_{\underline{R}}^{\bar{r}} g(r)\,\mathrm{d}r = \frac{\bar{r}-l}{(n-1)l}$ and $\bar{r} = G^{-1}(f) = l + (n-1)lf$. Also, $1 - p(\bar{r}) = 1 - \frac{\bar{r}-l}{(n-1)l} = 1 - f$.

For convenience, we summarize the above setting as follows:

Assumption 5 (Simplified single-station settings)**.** *In the simplified single-station model,* $\mathbb{W} = \{\mathrm{H}, \mathrm{L}\}$*; the RRE distribution* $g(r)$ *and the failure probability function* $1 - p(r)$ *are specified as illustrated in Figures 4(a) and 4(b), respectively; and the cost functions associated with each state-action pair are defined in Equations* (7)*.*

4.2 Public information design (PBI)

Given Assumption 5, the detailed analytical results for the public information design (PBI) and benchmark schemes — no information (NI), system optimum (SO), and full information (FI) — are provided in Appendix D.1.1. Importantly, the relationship between the optimal public information design and other information schemes can be stated as follows.

Proposition 1 (Optimal public information design)**.** *Given Assumption 5, disclosing the state truthfully, i.e., providing full information, is optimal under public information design.*

Proof. See Appendix D.3 for details. □

4.3 Private information design (PVI)

Building on the analysis presented in Appendix D.1.2, we summarize the main results of private information design (PVI) in the following proposition.

Proposition 2. *Given Assumption 5, if* $\zeta \geq \Delta_t + \beta$*, the optimal private design outperforms the FI policy, but is always outperformed by the SO policy; otherwise when* $\zeta < \Delta_t + \beta$*:*

(1) if $\underline{\mu_0} \leq \mu_0(\mathrm{H}) \leq \overline{\mu_0}$*, the optimal private design (PVI) policy performs as well as the SO policy;*

(2) else if $\mu_0(\mathrm{H}) \geq \max\left(\overline{\mu_0}, \hat{\mu_0}\right)$ *the PVI policy performs worse than the FI policy;*

(3) else, the PVI policy outperforms all other policies except the SO policy;

where $\underline{\mu_0} \equiv \frac{\alpha(\zeta - \Delta_t)}{-\alpha(\zeta - \Delta_t) + \beta(2\alpha + \zeta)}$ *and* $\overline{\mu_0} \equiv \frac{(\alpha+\zeta)(\zeta - \Delta_t)}{-\alpha(\zeta - \Delta_t) + \beta(2\alpha + \zeta)}$ *and* $\hat{\mu_0} \equiv \frac{\left(\alpha^2 + (\alpha+\zeta)^2\right)(\zeta - \Delta_t)}{-\alpha\zeta(\zeta - \Delta_t) + \beta(2\alpha+\zeta)(\alpha+\zeta)}$.

Proof. See Appendix D.6 for details. □

Proposition 2 enables us to draw useful insights. When $\zeta < \Delta_t$, all threshold values ($\underline{\mu_0}$, $\overline{\mu_0}$, and $\hat{\mu_0}$) are negative, corresponding to Case (2), where an exceedingly small penalty coefficient causes private design to perform worse than full revelation. When $\zeta \in (\Delta_t, \Delta_t + \beta]$, as $\zeta \to \Delta_t + \beta$, we have $\underline{\mu_0} \to \frac{\alpha}{\alpha+\zeta}$, $\overline{\mu_0} \to 1$, $\overline{\mu_0} - \underline{\mu_0} \to \frac{\zeta}{\alpha+\zeta}$, $\hat{\mu_0} \to 1$. Thus, Case (2) becomes unlikely. In this circumstance, the larger ζ is relative to α, the greater the $\overline{\mu_0} - \underline{\mu_0}$, the more likely the private information design achieves SO.

In summary, private information design is the preferred strategy under a wide range of conditions. It is likely to fall behind the full revelation policy only when the failure penalty coefficient is low and the probability of anomaly is high. It performs the best, with a high probability of rivaling the SO policy, when the failure penalty coefficient is less than but close to the extra cost of charging and the probability of anomaly is neither too high nor too low.

5 Two-station corridor model

In this section, we extend our model to analyze a corridor with multiple charging stations. To retain tractability, the extended model is limited to a minimal configuration with two stations (Figure 5), which we believe captures the essential trade-offs that arise from sequential decision-making, while avoiding unnecessary complexity. Models with more than two stations can be formulated similarly.

EV drivers now encounter two charging stations sequentially, each corresponding to a decision point, denoted as D_1 and D_2. At $D_i (i = 1, 2)$, the driver chooses an action a_i from the action set $\mathbb{A}_i$, where $\mathbb{A}_1 = \mathbb{A}_2 = \{C, M\}$. Here, C denotes choosing to charge at the current station, while M denotes choosing to move on without charging. A driver's overall charging strategy across the two stages is represented as an action vector $\boldsymbol{a} = a_1 a_2 \in \mathbb{A} = \{CC, CM, MC, MM\}$, where each element in $\mathbb{A}$ is a shorthand notation for a specific sequence of decisions at the two stations. We denote the distance between the two stations as l_1, and the distance from Station 2 to the final destination as l_2.

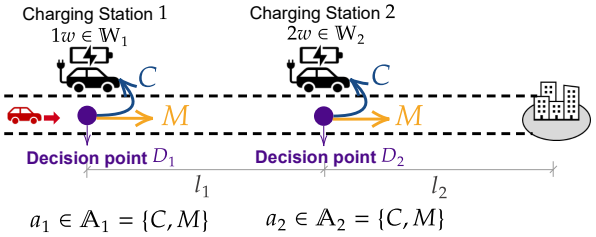

Figure 5: Illustration of a two-station EV charging problem.

As before, travel on the corridor is assumed to be uncongested. Congestion arises only at charging stations, where the cost depends on the charging demand. At the first station, waiting time depends on the total mass of drivers who choose to charge there — that is, those with action $a_1 = C$. At the second station, however, drivers who charge there may have taken different paths: some charged at Station 1 ($\boldsymbol{a} = CC$) while others deferred charging ($\boldsymbol{a} = MC$). These two groups may not compete for charging capacity at Station 2, since their earlier choices at Station 1 assign them to disjoint queues. In addition, the cost at each station is further affected by its charging state $iw \in \mathbb{W}_i$ with prior μ^0_{iw}, and for tractability the two stations' charging conditions are assumed independent.

As EVs travel along the corridor, their remaining range decreases. We assume that each mile traveled reduces the range by a random amount drawn from a distribution with PDF $u(\cdot)$ supported on $[\underline{\delta}, \bar{\delta}]$. Let $p(\hat{r}, l)$ denote the probability that an EV with a remaining range $\hat{r}$ successfully covers distance l, given by $p(\hat{r}, l) = 1 - \int_{\hat{r}/l}^{\bar{\delta}} u(\delta)\, \mathrm{d}\delta$. The expected penalty for attempting to traverse l_i $(i = 1, 2)$ with $\hat{r}$ is then denoted as $J_i^p(\hat{r})$ which decreases as $\hat{r}$ (hence $p(\hat{r}, l_i)$) increases. It represents the expected cost associated with seeking emergency charging or other remedial measures. To characterize the evolution of drivers' RRE as they proceed along the corridor, we generalize the previous single-station setting. As before, the initial RRE of drivers upon arriving at D_1 follows a probability density function $g(\cdot)$ with cumulative distribution $G(\cdot)$ over support $\Xi = [\underline{R}, \bar{R}]$. Each charging action increases the remaining range, while each traveled segment depletes it. Therefore, for a driver with initial RRE $r \in \Xi$, the resulting RRE at each decision point D_i $(i = 1, 2)$ depends on the sequence of actions taken up to that point. To capture these dynamics in a general and policy-adaptive form, we define a set of functions describing the RRE outcomes under different action sequences. Specifically, at Station 1 (D_1), the driver's RRE after making the first decision is represented by $\hat{r}_1^C(r)$ and $\hat{r}_1^M(r)$, corresponding to actions $a_1 = C$

and $a_1 = M$, respectively. At Station 2 (D_2), the driver's RRE further become $\hat{r}_2^{CC}(r)$, $\hat{r}_2^{CM}(r)$, $\hat{r}_2^{MC}(r)$, and $\hat{r}_2^{MM}(r)$, associated with each action sequence $\boldsymbol{a} \in \mathbb{A} = \{CC, CM, MC, MM\}$.

We distinguish two information release schedules: sequential versus simultaneous. In the sequential schedule, the information about each charging station is withheld until the driver is close enough to the station, whereas in the simultaneous schedule all signals are disclosed before the driver arrives at the first station, which mimics the single-station model. For each approach, we consider both public and private information design. In the public information design, let the set of signals for two stations as $\mathbb{S}_1$ and $\mathbb{S}_2$. The information structure is specified by a pair of signal policies $\boldsymbol{\pi} = \{\boldsymbol{\pi}_1, \boldsymbol{\pi}_2\}$, where $\boldsymbol{\pi}_1 = \{\pi_1(1s \mid 1w)\}_{1s\in\mathbb{S}_1, 1w\in\mathbb{W}_1}$ and $\boldsymbol{\pi}_2 = \{\pi_2(2s \mid 2w)\}_{2s\in\mathbb{S}_2, 2w\in\mathbb{W}_2}$. By Carathéodory's theorem (Tyrrell Rockafellar 1970, Bergemann and Morris 2016), we can, without loss of generality, assume that the number of signals equals that of states, i.e., $|\mathbb{S}_1| = |\mathbb{W}_1|, |\mathbb{S}_2| = |\mathbb{W}_2|$. In the private design, we continue to group drivers with identical action recommendations across all states into the same information type. However, a more flexible specification is needed, since a natural ranking of actions does not exist.

5.1 Sequential information release

We begin by assuming information release is sequential. A sequential schedule leads to a multi-stage decision-making process, where the equilibrium is defined recursively across stages. Below, we first discuss public information design.

5.1.1 Public information design

A public information design corresponds to a two-stage decision process. At D_1, drivers observe a public signal $1s \in \mathbb{S}_1$ drawn from $\boldsymbol{\pi}_1$, update their belief about Station 1, and choose the action sequence minimizing expected cost from that point to the destination. At D_2, they observe a new signal $2s \in \mathbb{S}_2$ from $\boldsymbol{\pi}_2$, update their belief about Station 2, and revise their choice by minimizing the remaining expected cost.

Each signal may induce an action sequence for different drivers depending on their initial RRE before D_1. The drivers who choose the same action sequence have RREs within a certain range. For example, upon receiving a signal $1s \in \mathbb{S}_1$, drivers choose subsequent actions $\boldsymbol{a} = a_1a_2 \in \mathbb{A} = \{CC, CM, MC, MM\}$, and their RRE is defined by a range $R_{1s}^{a_1a_2}$. Noting that both CC and CM involve charging at Station 1, while MC and MM do not, we define: $R_{1s}^{C} \equiv R_{1s}^{CC} \cup R_{1s}^{CM}$ and $R_{1s}^{M} \equiv R_{1s}^{MC} \cup R_{1s}^{MM}$, where $R_{1s}^{C} \cup R_{1s}^{M} = \Xi$ for any $1s \in \mathbb{S}_1$. At D_2, upon receiving signal $2s \in \mathbb{S}_2$, drivers take action $a_2 \in \{C, M\}$ conditional on their earlier choice $a_1 \in \{C, M\}$ after receiving $1s$. The range corresponding to these drivers (who follow the full "action path" $\boldsymbol{a}$ under the signal pair $(1s, 2s)$) is denoted $R_{1s2s}^{\boldsymbol{a}}$. Thus, the decision structure across stages and signals can be represented by a set of ranges $\mathbf{R} = \left\{R_{1s}^{C}, R_{1s}^{M}, R_{1s2s}^{CC}, R_{1s2s}^{CM}, R_{1s2s}^{MC}, R_{1s2s}^{MM}\right\}_{1s\in\mathbb{S}_1, 2s\in\mathbb{S}_2}$, where

$$R_{1s}^{C} = R_{1s2s}^{CC} \cup R_{1s2s}^{CM}, \quad R_{1s}^{M} = R_{1s2s}^{MC} \cup R_{1s2s}^{MM}, \ \forall 1s \in \mathbb{S}_1, 2s \in \mathbb{S}_2, \quad R_{1s}^{C} \cup R_{1s}^{M} = \Xi, \ \forall 1s \in \mathbb{S}_1. \tag{8}$$

Note that $\mathbf{R}$ is endogenous and represents the collective decisions of all drivers in response to an information structure, hence also corresponding to the equilibrium of the congestion game.

We further denote the charging cost function at Station 1 in state $1w \in \mathbb{W}_1$ after receiving signal $1s \in \mathbb{S}_1$ as $J_{1C,1w}^{g,1s}$ and that at Station 2 in state $2w \in \mathbb{W}_2$ after receiving signal $2s \in \mathbb{S}_2$ given

signal $1s$ and first-stage choice a_1 as $J^{g,1s2s}_{a_1C,2w}$. Moreover, the former depends on the charging flow $f^C_{1s} = \int_{r\in R^C_{1s}} g(r)\,\mathrm{d}r$ and the latter on $f^{a_1C}_{1s2s} = \int_{r\in R^{a_1C}_{1s2s}} g(r)\,\mathrm{d}r$.

At D_1, after receiving signal $1s \in \mathbb{S}_1$, a driver evaluates the expected cost associated with each of the four possible action sequences. The cost of charging at Station 1 is computed based on the posterior belief μ^{1s}_{1w}, which is updated upon observing $1s$. In contrast, the cost of charging at Station 2 is evaluated using the prior belief μ^0_{2w}, since no information about Station 2 has yet been received. For Station 2, the expected cost under each possible state $2w \in \mathbb{W}_2$ is further weighted by the probability of receiving each signal $2s \in \mathbb{S}_2$, as specified by the information structure $\boldsymbol{\pi}_2$. The expected costs of the four action sequences — denoted as $e^{1s}_{\dot{C}C}$, $e^{1s}_{\dot{C}M}$, $e^{1s}_{\dot{M}C}$, and $e^{1s}_{\dot{M}M}$ — are defined as follows, where the dot accent indicates the location at which the expected cost is incurred:

$$
\begin{aligned}
e^{1s}_{\dot{C}C} &= \sum_{1w\in\mathbb{W}_1} \mu^{1s}_{1w}\cdot J^{g,1s}_{1C,1w} + J^p_1\left(\hat{r}^C_1(r)\right) + \sum_{2w\in\mathbb{W}_2}\mu^0_{2w}\cdot\Big(\sum_{2s\in\mathbb{S}_2}\pi_2\left(2s\mid 2w\right)\cdot J^{g,1s2s}_{CC,2w}\Big) + J^p_2\left(\hat{r}^{CC}_2(r)\right),\\
e^{1s}_{\dot{C}M} &= \sum_{1w\in\mathbb{W}_1} \mu^{1s}_{1w}\cdot J^{g,1s}_{1C,1w} + J^p_1\left(\hat{r}^C_1(r)\right) + J^p_2\left(\hat{r}^{CM}_2(r)\right),\\
e^{1s}_{\dot{M}C} &= J^p_1\left(\hat{r}^M_1(r)\right) + \sum_{2w\in\mathbb{W}_2}\mu^0_{2w}\cdot\Big(\sum_{2s\in\mathbb{S}_2}\pi_2\left(2s\mid 2w\right)\cdot J^{g,1s2s}_{MC,2w}\Big) + J^p_2\left(\hat{r}^{MC}_2(r)\right),\\
e^{1s}_{\dot{M}M} &= J^p_1\left(\hat{r}^M_1(r)\right) + J^p_2\left(\hat{r}^{MM}_2(r)\right),\quad \forall 1s\in\mathbb{S}_1, \text{where } \mu^{1s}_{1w} = \frac{\mu^0_{1w}\pi_1\left(1s\mid 1w\right)}{\sum_{1w'\in\mathbb{W}_1}\mu^0_{1w'}\pi_1\left(1s\mid 1w'\right)}.
\end{aligned}
$$

Note that the expected penalty $J^p_i(\cdot), i = 1, 2$ is state independent and its inputs are the remaining range functions at each decision point we defined earlier.

After arriving at D_2 and observing the second signal $2s \in \mathbb{S}_2$, given that the first-stage signal $1s$ has been received, the driver updates their belief over the state of Station 2 and re-evaluates the expected cost conditional on their prior first-stage decision. The charging cost at Station 2 is now computed using the posterior belief μ^{2s}_{2w}. The second-stage expected costs, denoted as $e^{1s2s}_{C\dot{C}}$, $e^{1s2s}_{C\dot{M}}$, $e^{1s2s}_{M\dot{C}}$, and $e^{1s2s}_{M\dot{M}}$, are given by:

$$
\begin{aligned}
e^{1s2s}_{C\dot{C}} &= \sum_{2w\in\mathbb{W}_2}\mu^{2s}_{2w}\cdot J^{g,1s2s}_{CC,2w} + J^p_2\left(\hat{r}^{CC}_2(r)\right), e^{1s2s}_{M\dot{C}} = \sum_{2w\in\mathbb{W}_2}\mu^{2s}_{2w}\cdot J^{g,1s2s}_{MC,2w} + J^p_2\left(\hat{r}^{MC}_2(r)\right),\\
e^{1s2s}_{C\dot{M}} &= J^p_2\left(\hat{r}^{CM}_2(r)\right), e^{1s2s}_{M\dot{M}} = J^p_2\left(\hat{r}^{MM}_2(r)\right),\ \forall 1s\in\mathbb{S}_1, 2s\in\mathbb{S}_2, \text{where } \mu^{2s}_{2w} = \frac{\mu^0_{2w}\pi_2\left(2s\mid 2w\right)}{\sum_{2w'\in\mathbb{W}_2}\mu^0_{2w'}\pi_2\left(2s\mid 2w'\right)}.
\end{aligned}
$$

Then, in the public information design with sequential information release, for any given information structure $\boldsymbol{\pi}$, a solution $\mathbf{R}^*$ is said to be a BNE, denoted as $\mathbf{R}^* \in \varepsilon(\boldsymbol{\pi})$, if no driver has incentives to deviate from their chosen action at either stage. Mathematically, this condition can be stated as:

> Any driver taking action $\boldsymbol{a}^* \in \arg\min_{\boldsymbol{a}\in\left\{\dot{C}C,\dot{C}M,\dot{M}C,\dot{M}M\right\}} e^{1s}_{\boldsymbol{a}}$, $\forall 1s\in\mathbb{S}_1$ at D_1 must have RRE $r \in R^{a^*}_{1s}$. Similarly, for any driver who has received $1s \in \mathbb{S}_1$ and chosen action $a_1 \in \mathbb{A}_1$ at D_1 and decides at D_2 to take action $\boldsymbol{a}^* \in \arg\min_{\boldsymbol{a}\in\left\{a_1\dot{C},a_1\dot{M}\right\}} e^{1s2s}_{\boldsymbol{a}}, \forall 2s\in\mathbb{S}_2$, their RRE r must fall in $R^{a^*}_{1s2s}$.

Any BNE solution $\mathbf{R}^*$ also satisfies the conservation condition (8).

The system's total expected cost achieved at a given information structure $\boldsymbol{\pi}$ and the corresponding BNE solution $\mathbf{R}^*$ is denoted as $Z_b(\mathbf{R}^*, \boldsymbol{\pi})$. This cost aggregates outcomes across both decision stages. Since the second-stage cost depends on the first-stage signal, it is weighted by the probability of observing each first-stage signal $1s$, which is given by $p_{1s} \equiv \sum_{1w \in \mathbb{W}_1} \mu^0_{1w} \cdot \pi_1(1s \mid 1w)$. This gives rise to:

$$Z_b(\mathbf{R}^*, \boldsymbol{\pi}) = \sum_{1w \in \mathbb{W}_1} \sum_{1s \in \mathbb{S}_1} \mu^0_{1w} \cdot \pi_1(1s|1w) \cdot \left(J^{g,1s}_{1C,1w} \cdot \int_{r \in R^C_{1s}} g(r)\,\mathrm{d}r + \sum_{a_1 \in \{C,M\}} \int_{r \in R^{a_1}_{1s}} J^p_1\left(\hat{r}^{a_1}_1(r)\right) g(r)\,\mathrm{d}r \right)$$
$$+ \sum_{1s \in \mathbb{S}_1} \left[p_{1s} \cdot \sum_{2w \in \mathbb{W}_2} \sum_{2s \in \mathbb{S}_2} \mu^0_{2w} \cdot \pi_2(2s|2w) \cdot \left(\sum_{\boldsymbol{a}' \in \{CC,MC\}} J^{g,1s2s}_{\boldsymbol{a}',2w} \cdot \int_{r \in R^{\boldsymbol{a}'}_{1s2s}} g(r)\,\mathrm{d}r + \sum_{\boldsymbol{a} \in \mathbb{A}} \int_{r \in R^{\boldsymbol{a}}_{1s2s}} J^p_2\left(\hat{r}^{\boldsymbol{a}}_2(r)\right) g(r)\,\mathrm{d}r \right) \right].$$

We are now ready to formulate the sequential public information design problem as follows:

$$\min\ Z_b(\mathbf{R}^*, \boldsymbol{\pi}) \tag{9a}$$
$$\text{subject to: } \sum_{is \in \mathbb{S}_i} \pi_i(is \mid iw) = 1,\ \forall iw \in \mathbb{W}_i, i = 1,2; \tag{9b}$$
$$\pi_i(is \mid iw) \geq 0,\ \forall is \in \mathbb{S}_i, iw \in \mathbb{W}_i, i = 1,2; \tag{9c}$$
$$\mathbf{R}^* \in \varepsilon(\boldsymbol{\pi}), \tag{9d}$$

where Constraints (9b)–(9c) specify the information structure and Constraint (9d) specifies the BNE condition.

5.1.2 Private information design

In the two-station scenario, the cutoff rule used in the single-station setting — where a single threshold at each state separates charging from skipping — no longer applies. Below, we propose a more general modeling framework.

Let $\mathbb{T}$ denote the space of private information types. Each element $t \in \mathbb{T}$ consists of a series of state–action pairs, representing a state-dependent recommendation profile. For instance, an element $t = (1w_1 : C, 1w_2 : C, 2w_1 : M, 2w_2 : C)$ indicates that the driver is recommended to charge in states $1w_1, 1w_2$, and $2w_2$ but to skip in state $2w_1$. The total number of possible types is $|\mathbb{T}| = 2^{(\sum_i |\mathbb{W}_i|)}$. Further, let constant $\eta_{t,w} = 1$ if information type $t \in \mathbb{T}$ receives recommendation C at state $w \in \mathbb{W} = \cup_i \mathbb{W}_i$, and 0 if recommendation is M.

The assignment of a driver with RRE r to an information type is endogenous. To avoid the challenge posed by the infinite dimension, the RRE support Ξ is divided into a set of intervals $\mathbb{K} = \{1, \ldots, K\}$, with $\bar{r}_k, k \in \mathbb{K}$ denoting the upper bound of the kth interval. For each interval $k \in \mathbb{K}$, a binary variable $\iota_{k,t}, t \in \mathbb{T}$ is introduced to indicate that drivers whose RRE falls into kth interval are of information type t. Accordingly, $\bar{\boldsymbol{r}} = [\ldots, \bar{r}_k, \ldots]$ and $\boldsymbol{\iota} = [\ldots, \iota_{k,t}, \ldots]$ are treated as the decision variables.

The cost function at Station 1 in state $1w \in \mathbb{W}_1$ is denoted by $J^g_{1C,1w}$, which depends on the corresponding charging flow $f^{1C}_{1w} = \sum_{k \in \mathbb{K}} \sum_{t \in \mathbb{T}} \int_{\bar{r}_{k-1}}^{\bar{r}_k} \iota_{k,t} \cdot \eta_{t,1w} \cdot g(r)\,\mathrm{d}r$. At Station 2 and given state $(1w, 2w)$, charging flows are distinguished: (i) f^{CC}_{1w2w} representing drivers who charge at both stations and (ii) f^{MC}_{1w2w} representing those who only charge at Station 2. These, defined as, for $1w \in \mathbb{W}_1, 2w \in \mathbb{W}_2$,

$$f^{CC}_{1w2w} = \sum_{k \in \mathbb{K}} \sum_{t \in \mathbb{T}} \int_{\bar{r}_{k-1}}^{\bar{r}_k} \iota_{k,t} \cdot \eta_{t,1w} \cdot \eta_{t,2w} \cdot g(r)\,\mathrm{d}r, \text{ and } \quad f^{MC}_{1w2w} = \sum_{k \in \mathbb{K}} \sum_{t \in \mathbb{T}} \int_{\bar{r}_{k-1}}^{\bar{r}_k} \iota_{k,t} \cdot (1 - \eta_{t,1w}) \cdot \eta_{t,2w} \cdot g(r)\,\mathrm{d}r, \tag{10}$$

Table 1: Stage-wise cost of an action in the two-station sequential private information design problem.

Action $\boldsymbol{a}$	$E^{a_1}_{1w}(r)$	$E^{\boldsymbol{a}}_{1w2w}(r)$
CC	$J^g_{1C,1w} + J^p_1\left(\hat{r}^C_1(r)\right)$	$J^g_{CC,1w2w} + J^p_2\left(\hat{r}^{CC}_2(r)\right)$
CM		$J^p_2\left(\hat{r}^{CM}_2(r)\right)$
MC	$J^p_1\left(\hat{r}^M_1(r)\right)$	$J^g_{MC,1w2w} + J^p_2\left(\hat{r}^{MC}_2(r)\right)$
MM		$J^p_2\left(\hat{r}^{MM}_2(r)\right)$

determine, respectively, $J^g_{CC,1w2w}$ and $J^g_{MC,1w2w}$, the cost experienced by the two distinctive cohorts.

The system's total expected cost for the two-station charging problem can then be expressed as

$$
\begin{aligned}
Z_v(\bar{\boldsymbol{r}}, \boldsymbol{\iota}) = &\sum_{1w\in\mathbb{W}_1} \mu^0_{1w} \cdot \left[J^g_{1C,1w} \cdot f^{1C}_{1w} + \sum_{k\in\mathbb{K}} \sum_{t\in\mathbb{T}} \int_{\bar{r}_{k-1}}^{\bar{r}_k} \iota_{k,t} \cdot \left[\eta_{t,1w} \cdot J^p_1\left(\hat{r}^C_1(r)\right) + (1-\eta_{t,1w}) \cdot J^p_1\left(\hat{r}^M_1(r)\right) \right] \cdot g(r)\,\mathrm{d}r \right] \\
&+ \sum_{1w\in\mathbb{W}_1} \mu^0_{1w} \cdot \sum_{2w\in\mathbb{W}_2} \mu^0_{2w} \cdot \left[J^g_{CC,1w2w} \cdot f^{CC}_{1w2w} + J^g_{MC,1w2w} \cdot f^{MC}_{1w2w} + \sum_{k\in\mathbb{K}} \sum_{t\in\mathbb{T}} \int_{\bar{r}_{k-1}}^{\bar{r}_k} \iota_{k,t} \cdot \left[\eta_{t,1w}\eta_{t,2w} J^p_2\left(\hat{r}^{CC}_2(r)\right) + \right.\right. \\
&\left.\left. + \eta_{t,1w}(1-\eta_{t,2w}) J^p_2\left(\hat{r}^{CM}_2(r)\right) + (1-\eta_{t,1w})\eta_{t,2w} J^p_2\left(\hat{r}^{MC}_2(r)\right) + (1-\eta_{t,1w})(1-\eta_{t,2w}) J^p_2\left(\hat{r}^{MM}_2(r)\right) \right] g(r)\,\mathrm{d}r \right].
\end{aligned}
$$

To simplify the definition of obedience constraints, let us first introduce $E^{a_1}_{1w}(r)$ and $E^{\boldsymbol{a}}_{1w2w}(r)$, which denote, respectively, the first stage cost at state $1w$ given action a_1 at D_1, and the second stage cost at state $(1w, 2w)$ given action sequence $\boldsymbol{a}$, for each driver with intial RRE r, as summarized in Table 1. At D_1, the obedience constraints ensure that drivers follow the recommended action based on posterior beliefs for Station 1 and prior beliefs for Station 2. The charging obedience constraints at D_1 are

$$
\begin{aligned}
&\sum_{1w\in\mathbb{W}_1} \mu^0_{1w} \cdot \iota_{k,t} \cdot \eta_{t,1w} \cdot \left[E^{1C}_{1w}(\bar{r}_k) + \sum_{2w\in\mathbb{W}_2} \mu^0_{2w} \cdot \left(\eta_{t,2w} E^{CC}_{1w2w}(\bar{r}_k) + (1-\eta_{t,2w}) E^{CM}_{1w2w}(\bar{r}_k) \right) \right. \\
&\left. - \left(E^{1M}_{1w}(\bar{r}_k) + \sum_{2w\in\mathbb{W}_2} \mu^0_{2w} \cdot \left(\eta_{t,2w} E^{MC}_{1w2w}(\bar{r}_k) + (1-\eta_{t,2w}) E^{MM}_{1w2w}(\bar{r}_k) \right) \right) \right] \le 0;\ \forall k \in \mathbb{K}, t \in \mathbb{T}.
\end{aligned} \tag{11}
$$

Note that the term $\mu^0_{1w} \cdot \iota_{k,t} \cdot \eta_{t,1w}$ can be interpreted as the (non-normalized) posterior belief for state $1w$ when information type t is recommended to choose action C at Station 1 in interval k. These constraints state that, for each interval–type pair (k,t) that receives a recommendation to charge at Station 1 (i.e., $\eta_{t,1w} = 1$ for some $1w \in \mathbb{W}_1$), the expected total cost of complying with the recommendation must not exceed the cost of skipping. If no charge recommendation is given (i.e., $\eta_{t,1w} = 0$ for all $1w \in \mathbb{W}_1$), the constraint holds trivially as an equality.

Similarly, the skipping obedience constraints at D_1 are:

$$
\begin{aligned}
&\sum_{w\in\mathbb{W}} \mu^0_{1w} \cdot \iota_{k,t} \cdot (1-\eta_{t,w}) \cdot \left[E^{1M}_{1w}(\bar{r}_{k-1}) + \sum_{2w\in\mathbb{W}_2} \mu^0_{2w} \cdot \left(\eta_{t,2w} E^{MC}_{1w2w}(\bar{r}_{k-1}) + (1-\eta_{t,2w}) E^{MM}_{1w2w}(\bar{r}_{k-1}) \right) \right. \\
&\left. - \left(E^{1C}_{1w}(\bar{r}_{k-1}) + \sum_{2w\in\mathbb{W}_2} \mu^0_{2w} \cdot \left(\eta_{t,2w} E^{CC}_{1w2w}(\bar{r}_{k-1}) + (1-\eta_{t,2w}) E^{CM}_{1w2w}(\bar{r}_{k-1}) \right) \right) \right] \le 0; \forall k \in \mathbb{K}, t \in \mathbb{T}.
\end{aligned} \tag{12}
$$

At D_2, after the state of Station 1 is revealed and a signal about Station 2 is received, the belief

about Station 2 is updated to posterior. The charging and skipping obedience constraints are

$$\begin{aligned}&\sum_{2w\in\mathbb{W}_2}\mu^0_{2w}\cdot\iota_{k,t}\cdot\eta_{t,2w}\cdot\Big[\eta_{t,1w}\cdot E^{CC}_{1w2w}\left(\bar{r}_k\right)+\left(1-\eta_{t,1w}\right)\cdot E^{MC}_{1w2w}\left(\bar{r}_k\right)\\&-\Big(\eta_{t,1w}\cdot E^{CM}_{1w2w}\left(\bar{r}_k\right)+\left(1-\eta_{t,1w}\right)\cdot E^{MM}_{1w2w}\left(\bar{r}_k\right)\Big)\Big]\leq 0,\ \forall k\in\mathbb{K},t\in\mathbb{T},1w\in\mathbb{W}_1,\end{aligned}\tag{13}$$

and

$$\begin{aligned}&\sum_{2w\in\mathbb{W}_2}\mu^0_{2w}\cdot\iota_{k,t}\cdot\left(1-\eta_{t,2w}\right)\cdot\Big[\Big(\eta_{t,1w}\cdot E^{CM}_{1w2w}\left(\bar{r}_{k-1}\right)+\left(1-\eta_{t,1w}\right)\cdot E^{MM}_{1w2w}\left(\bar{r}_{k-1}\right)\Big)\\&-\Big(\eta_{t,1w}\cdot E^{CC}_{1w2w}\left(\bar{r}_{k-1}\right)+\left(1-\eta_{t,1w}\right)\cdot E^{MC}_{1w2w}\left(\bar{r}_{k-1}\right)\Big)\Big]\leq 0,\ \forall k\in\mathbb{K},t\in\mathbb{T},1w\in\mathbb{W}_1.\end{aligned}\tag{14}$$

As before, obedience needs only be checked at the boundary types ($\bar{r}_k$ for charging, $\bar{r}_{k-1}$ for skipping), since monotonicity guarantees compliance for all interior types.

We formulate the two-station sequential private information design problem as follows:

$$\min\ Z_v\left(\bar{\boldsymbol{r}},\boldsymbol{\iota}\right)\tag{15a}$$

$$\text{subject to: }\sum_{t\in\mathbb{T}}\iota_{k,t}=1;\ \forall k\in\mathbb{K},\quad \iota_{k,t}=0\text{ or }1;\ \forall k\in\mathbb{K},t\in\mathbb{T},\tag{15b}$$

$$(11)-(14),\tag{15c}$$

$$\bar{r}_0=\underline{R},\bar{r}_K=\bar{R};\quad \bar{r}_k-\bar{r}_{k-1}\geq 0;\ \forall k\in\mathbb{K}.\tag{15d}$$

Constraints (15b) ensure that each interval is assigned to exactly one information type. Constraints (15c) enforce obedience — requiring that drivers prefer the recommended actions. Constraints (15d) ensure the feasibility of the interval boundaries. As a mixed-integer program with nonlinear obedience constraints (11)–(14) and a nonlinear objective function, Problem (15) is difficult to solve. Adding to the challenge is the fact that we also need to choose the "hyperparameter" K through some iterative process. In numerical experiments, we solve the problem by heuristics that leverage commercial solvers.

5.2 Simultaneous information release

For simultaneous release, the states of all stations are assumed to remain fixed throughout the decision process, and the information about both stations is disclosed at the first decision point. Accordingly, drivers form posterior beliefs about both stations before making their first decision. This means that, even at Station 1, a driver's expectation about the state at Station 2 is based on posterior rather than prior beliefs.

5.2.1 Public information design

We only need to redefine the BNE condition, as well as the expected system cost. Let us first define the action-based range set $\hat{\mathbf{R}}=\left\{\hat{R}^{CC}_{1s2s},\hat{R}^{CM}_{1s2s},\hat{R}^{MC}_{1s2s},\hat{R}^{MM}_{1s2s},\forall 1s\in\mathbb{S}_1,2s\in\mathbb{S}_2\right\}$. The expected

Table 2: Expected cost conditional on recommendation in simultaneous release private information design.

Received $\boldsymbol{a}$	Expected cost $V^{k,t}_{\boldsymbol{a},\boldsymbol{a}'}(r)$
CC	$\sum_{1w\in\mathbb{W}_1} \frac{\mu^0_{1w}\cdot\iota_{k,t}\cdot\eta_{t,1w}}{\sum_{1w'\in\mathbb{W}_1}\mu^0_{1w'}\cdot\iota_{k,t}\cdot\eta_{t,1w'}}\left(E^{a'_1}_{1w}(r)+\sum_{2w\in\mathbb{W}_2}\frac{\mu^0_{2w}\cdot\iota_{k,t}\cdot\eta_{t,2w}}{\sum_{2w'\in\mathbb{W}_2}\mu^0_{2w'}\cdot\iota_{k,t}\cdot\eta_{t,2w'}}\cdot E^{\boldsymbol{a}'}_{1w2w}(r)\right)$
CM	$\sum_{1w\in\mathbb{W}_1} \frac{\mu^0_{1w}\cdot\iota_{k,t}\cdot\eta_{t,1w}}{\sum_{1w'\in\mathbb{W}_1}\mu^0_{1w'}\cdot\iota_{k,t}\cdot\eta_{t,1w'}}\left(E^{a'_1}_{1w}(r)+\sum_{2w\in\mathbb{W}_2}\frac{\mu^0_{2w}\cdot\iota_{k,t}\cdot(1-\eta_{t,2w})}{\sum_{2w'\in\mathbb{W}_2}\mu^0_{2w'}\cdot\iota_{k,t}\cdot(1-\eta_{t,2w'})}\cdot E^{\boldsymbol{a}'}_{1w2w}(r)\right)$
MC	$\sum_{1w\in\mathbb{W}_1} \frac{\mu^0_{1w}\cdot\iota_{k,t}\cdot(1-\eta_{t,1w})}{\sum_{1w'\in\mathbb{W}_1}\mu^0_{1w'}\cdot\iota_{k,t}\cdot(1-\eta_{t,1w'})}\left(E^{a'_1}_{1w}(r)+\sum_{2w\in\mathbb{W}_2}\frac{\mu^0_{2w}\cdot\iota_{k,t}\cdot\eta_{t,2w}}{\sum_{2w'\in\mathbb{W}_2}\mu^0_{2w'}\cdot\iota_{k,t}\cdot\eta_{t,2w'}}\cdot E^{\boldsymbol{a}'}_{1w2w}(r)\right)$
MM	$\sum_{1w\in\mathbb{W}_1} \frac{\mu^0_{1w}\cdot\iota_{k,t}\cdot(1-\eta_{t,1w})}{\sum_{1w'\in\mathbb{W}_1}\mu^0_{1w'}\cdot\iota_{k,t}\cdot(1-\eta_{t,1w'})}\left(E^{a'_1}_{1w}(r)+\sum_{2w\in\mathbb{W}_2}\frac{\mu^0_{2w}\cdot\iota_{k,t}\cdot(1-\eta_{t,2w})}{\sum_{2w'\in\mathbb{W}_2}\mu^0_{2w'}\cdot\iota_{k,t}\cdot(1-\eta_{t,2w'})}\cdot E^{\boldsymbol{a}'}_{1w2w}(r)\right)$

cost for each action profile is given by:

$$\begin{aligned}
\rho^{1s2s}_{CC} &= \sum_{1w\in\mathbb{W}_1}\mu^{1s}_{1w}\cdot\hat{J}^{g,1s2s}_{1C,1w}+J^p_1\left(\hat{r}^C_1(r)\right)+\sum_{2w\in\mathbb{W}_2}\mu^{2s}_{2w}\cdot\hat{J}^{g,1s2s}_{CC,2w}+J^p_2\left(\hat{r}^{CC}_2(r)\right),\\
\rho^{1s2s}_{CM} &= \sum_{1w\in\mathbb{W}_1}\mu^{1s}_{1w}\cdot\hat{J}^{g,1s2s}_{1C,1w}+J^p_1\left(\hat{r}^C_1(r)\right)+J^p_2\left(\hat{r}^{CM}_2(r)\right),\\
\rho^{1s2s}_{MC} &= J^p_1\left(\hat{r}^M_1(r)\right)+\sum_{2w\in\mathbb{W}_2}\mu^{2s}_{2w}\cdot\hat{J}^{g,1s2s}_{MC,2w}+J^p_2\left(\hat{r}^{MC}_2(r)\right),\\
\rho^{1s2s}_{MM} &= J^p_1\left(\hat{r}^M_1(r)\right)+J^p_2\left(\hat{r}^{MM}_2(r)\right),\quad \forall 1s\in\mathbb{S}_1, 2s\in\mathbb{S}_2,
\end{aligned}\tag{16}$$

where the charging cost function at Station 1 after receiving signals $(1s,2s)$ in state $1w\in\mathbb{W}_1$ is denoted by $\hat{J}^{g,1s2s}_{1C,1w}$, which depends on the corresponding charging flow $\hat{f}^{1s2s}_{1C,1w}=\int_{r\in\hat{R}^{CC}_{1s2s}\cup\hat{R}^{CM}_{1s2s}}g(r)\,\mathrm{d}r$. Similarly, the charging cost function at Station 2 after receiving $(1s,2s)$ in state $2w\in\mathbb{W}_2$ under action sequence a_1C ($a_1\in\{C,M\}$) is denoted by $\hat{J}^{g,1s2s}_{a_1C,2w}$, which depends on the charging flow $\hat{f}^{1s2s}_{a_1C,2w}=\int_{r\in\hat{R}^{a_1C}_{1s2s}}g(r)\,\mathrm{d}r$.

A solution $\hat{\mathbf{R}}^*$ is a BNE, written as $\hat{\mathbf{R}}^*\in\hat{\varepsilon}(\boldsymbol{\pi})$, if any driver taking action $\boldsymbol{a}^*\in\arg\min_{\boldsymbol{a}\in\{CC,CM,MC,MM\}}\rho^{1s2s}_{\boldsymbol{a}}$, $\forall 1s\in\mathbb{S}_1, 2s\in\mathbb{S}_2$ has RRE $r\in\hat{R}^{\boldsymbol{a}^*}_{1s2s}$.

The system's total expected cost under the simultaneous public information structure is:

$$\hat{Z}_b\left(\hat{\mathbf{R}}^*,\boldsymbol{\pi}\right)=\sum_{1w\in\mathbb{W}_1}\sum_{1s\in\mathbb{S}_1}\sum_{2w\in\mathbb{W}_2}\sum_{2s\in\mathbb{S}_2}\mu^0_{1w}\cdot\pi_1\left(1s\mid 1w\right)\cdot\mu^0_{2w}\cdot\pi_2\left(2s\mid 2w\right)\cdot\left[\left(\hat{J}^{g,1s2s}_{1C,1w}\cdot\int_{r\in\hat{R}^{CC}_{1s2s}\cup\hat{R}^{CM}_{1s2s}}g(r)\,\mathrm{d}r+\right.\right.$$
$$\left.\left.\sum_{a_1\in\{C,M\}}\int_{r\in\hat{R}^{a_1C}_{1s2s}\cup\hat{R}^{a_1M}_{1s2s}}J^p_1\left(\hat{r}^{a_1}_1(r)\right)g(r)\,\mathrm{d}r\right)+\left(\sum_{a_1\in\{C,M\}}\hat{J}^{g,1s2s}_{a_1C,2w}\cdot\int_{r\in\hat{R}^{a_1C}_{1s2s}}g(r)\,\mathrm{d}r+\sum_{\boldsymbol{a}\in\mathbb{A}}\int_{r\in\hat{R}^{\boldsymbol{a}}_{1s2s}}J^p_2\left(\hat{r}^{\boldsymbol{a}}_2(r)\right)g(r)\,\mathrm{d}r\right)\right].$$

5.2.2 Private information design

Similarly, we only need to redefine the obedience constraints and the objective function. To simplify the exposition of the former, we introduce an expected cost function $V^{k,t}_{\boldsymbol{a},\boldsymbol{a}'}(r)$ to represent the expected cost for a driver of type t with RRE r falling into interval k, when she receives the action recommendation $\boldsymbol{a}$ and chooses to take the action $\boldsymbol{a}'$ — see Table 2 for details.

Using the expected cost function we can write the obedience constraints simply as

$$V^{k,t}_{\boldsymbol{a},\boldsymbol{a}}(\bar{r}_k)\le V^{k,t}_{\boldsymbol{a},\boldsymbol{a}'}(\bar{r}_k),\ V^{k,t}_{\boldsymbol{a},\boldsymbol{a}}(\bar{r}_{k-1})\le V^{k,t}_{\boldsymbol{a},\boldsymbol{a}'}(\bar{r}_{k-1}),\ \forall k\in\mathbb{K}, t\in\mathbb{T}, \boldsymbol{a},\boldsymbol{a}'\in\mathbb{A}.\tag{17}$$

The expected system cost in the simultaneous private information structure is given by

$$\begin{aligned}\hat{Z}_v(\bar{\boldsymbol{r}},\boldsymbol{\iota}) = \sum_{1w\in\mathbb{W}_1}\sum_{2w\in\mathbb{W}_2}\mu^0_{1w}\cdot\mu^0_{2w}\cdot\Big[&J^g_{1C,1w2w}f^{1C}_{1w2w}+J^g_{CC,1w2w}f^{CC}_{1w2w}+J^g_{MC,1w2w}f^{MC}_{1w2w}\\ &+\sum_{k\in\mathbb{K}}\sum_{t\in\mathbb{T}}\int_{\bar{r}_{k-1}}^{\bar{r}_k}\iota_{k,t}\cdot\left(\eta_{t,1w}J^p_1\left(\hat{r}^C_1(r)\right)+(1-\eta_{t,1w})J^p_1\left(\hat{r}^M_1(r)\right)\right)g(r)\,dr\\ &+\sum_{k\in\mathbb{K}}\sum_{t\in\mathbb{T}}\int_{\bar{r}_{k-1}}^{\bar{r}_k}\iota_{k,t}\cdot\left(\eta_{t,1w}\eta_{t,2w}J^p_2\left(\hat{r}^{CC}_2(r)\right)+\eta_{t,1w}(1-\eta_{t,2w})J^p_2\left(\hat{r}^{CM}_2(r)\right)\right.\\ &\left.+(1-\eta_{t,1w})\eta_{t,2w}J^p_2\left(\hat{r}^{MC}_2(r)\right)+(1-\eta_{t,1w})(1-\eta_{t,2w})J^p_2\left(\hat{r}^{MM}_2(r)\right)\right)g(r)\,dr\Big],\end{aligned}\tag{18}$$

where the definition of $f^{CC}_{1w2w}, f^{MC}_{1w2w}, J^g_{CC,1w2w}$, and $J^g_{MC,1w2w}$ follow those in the private information design with sequential release (see Equation (10)). The charging flow at Station 1 under states $(1w, 2w)$ is given by $f^{1C}_{1w2w} = \sum_{k\in\mathbb{K}}\sum_{t\in\mathbb{T}}\int_{\bar{r}_{k-1}}^{\bar{r}_k}\iota_{k,t}\cdot\eta_{t,1w}\cdot g(r)\,\mathrm{d}r$, which determines $J^g_{1C,1w2w}$, the charging cost at Station 1.

By replacing the obedience constraints (15c) with (17) and the objective function with (18), Problem (15) can be employed to obtain private information designs with a simultaneous release schedule.

6 Numerical results

Section 6.1 presents the results of the experiments for the single-station model. In Section 6.1.1, we specify a base instance based on the setting presented in Section 4, solve the general formulation numerically, and compare the results with those given by the analysis. Section 6.1.2 conducts a sensitivity analysis on several key input parameters. In Section 6.1.3, by increasing the number of random states from 2 to 3, we create and solve more general instances for which analytical solutions are not available. We also discuss the computational challenge related to the number of states and how to address it in special cases.

Section 6.2 addresses the two-station corridor model. Recall that the public design problem (9) is a bilevel program, where the lower-level BNE constraint represents drivers' best response to a given information structure. To solve it, the lower-level equilibrium is obtained by either the Method of Successive Averages (MSA) — which requires discretizing the support Ξ into a finite number of intervals and can obtain solutions that are arbitrarily close to the true equilibrium provided that the discretization is sufficiently fine — or approximating driver choices using a softmax rule, which trades off solution quality for computational convenience. The upper-level problem is then solved by either a grid search (if MSA is used to solve the lower-level BNE), or a gradient descent via automatic differentiation (if softmax approximation is employed) (Li et al. 2020, 2022). Both methods (MSA + grid search vs. softmax+gradient descent) are implemented, tested, and shown to consistently identify full revelation as the optimal information scheme. For the private design, we employ a two-stage heuristic: (i) Remove the obedience constraints (11)–(14) from Problem (15) and enumerate all unique $(\boldsymbol{\iota}, K)$ pairs that optimally solve the relaxed problem, which equals the system optimal problem given K. Effectively, this means that we solve the relaxed problem many times, each corresponding to a K value chosen between 1 to a preset upper bound, to obtain the optimal $\boldsymbol{\iota}$; (ii) Solve Problem (15) for each $(\boldsymbol{\iota}, K)$ pair identified in Stage 1 and return the best solution as the "optimal" design. While this approach does not guarantee optimality, we note that it consistently yields much better solutions than directly solving Problem

(15) with commercial solvers for the amount of computing time considered reasonable in our study (up to four hours). In our numerical experiment, this two-stage heuristic is implemented using both COIN-OR BONMIN solver (Bonami et al. 2008) and Artelys Knitro solver (Byrd et al. 2006).

6.1 Base model

6.1.1 Base case

Per Assumption 5, we set the safe range factor $n = 2$, the prior belief $\mu_0(\mathrm{H}) = 0.5$, the remaining travel distance $l = 100$ mile, the detour $\Delta_l = 50$ mile, the travel speed $v = 100 mile/h$, and for the coefficients needed to define the cost functions: the coefficient for failure penalty $\zeta = 3$ (hours), the congestion coefficient $\alpha = 3$ (hours per unit flow), and extra delay $\beta = 2$ (hours).

For the parameters chosen here, the obedience-compliant region for the private information design and the corresponding solutions are illustrated in Figure 6. From the figure, we observe the following solutions and objective function values — the percentages in parentheses after the objective function value show the degree of improvement relative to the no-information solution, with the SO solution capping the improvement:

- $\left(f_{\emptyset}^{\mathrm{NI}*}, f_{\emptyset}^{\mathrm{NI}*}\right) = (1/4, 1/4)$, $Z^*\left(\boldsymbol{f}^{\mathrm{NI}*}\right) = 2.406$ $(+0\%)$;
- $\left(f_{\mathrm{H}}^{\mathrm{SO}*}, f_{\mathrm{L}}^{\mathrm{SO}*}\right) = (1/18, 5/18)$, $Z^*\left(\boldsymbol{f}^{\mathrm{SO}*}\right) = 2.319$ $(+100\%)$;
- $\left(f_{\mathrm{H}}^{\mathrm{FI}*}, f_{\mathrm{L}}^{\mathrm{FI}*}\right) = (1/12, 5/12)$, $Z^*\left(\boldsymbol{f}^{\mathrm{FI}*}\right) = 2.365$ $(+48\%)$;
- $\left(f_{\mathrm{H}}^{\mathrm{PVI}*}, f_{\mathrm{L}}^{\mathrm{PVI}*}\right) = (1/12, 11/36)$, $Z^*\left(\boldsymbol{f}^{\mathrm{PVI}*}\right) = 2.323$ $(+96\%)$.

In the base case, the optimal private design not only significantly outperforms the optimal public information design (which equals the full-information solution, as indicated in Proposition 1), but closely tracks the performance of the SO policy (with about 4% efficiency loss).

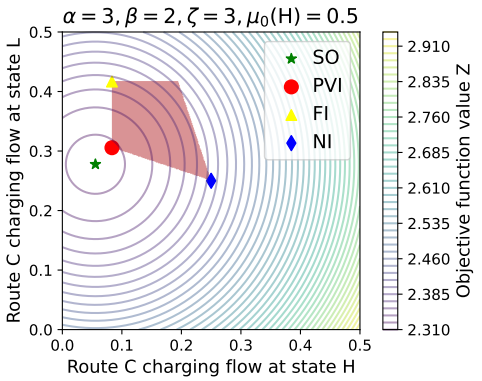

Figure 6: Feasible obedience-compliant region and different solutions.

6.1.2 Sensitivity analysis

We next perform sensitivity analysis over six key parameters: the failure penalty coefficient ζ, the speed v, the extra delay β, the congestion coefficient α, the detour Δ_l, and the prior μ_0. In all cases, the objective function value of the SO policy serves as a benchmark (the lower bound of the system cost), with the deviation from that lower bound being plotted in Figure 7 in all scenarios. Thus, the smaller the deviation, the closer an information design is to the SO policy, the better.

A general trend that holds across all plots is that the blue diamond line (for the NI policy) always lies above the yellow triangle line (for the FI policy), which, with rare exceptions (see the left ends in Figures 7(a) and 7(b)), lies above the red circle line (for the PVI policy). This is expected because our analysis indicates that, in general, private information design is better than full-information revelation, which in turn outperforms the no-information scheme.

The sensitivity results on ζ (Figure 7(a)) and v (Figure 7(b)) are similar. This is because an increase in either parameter tends to favor the charging option (Route C). We can see that the FI policy is preferred to the PVI policy when either parameter takes a sufficiently low value

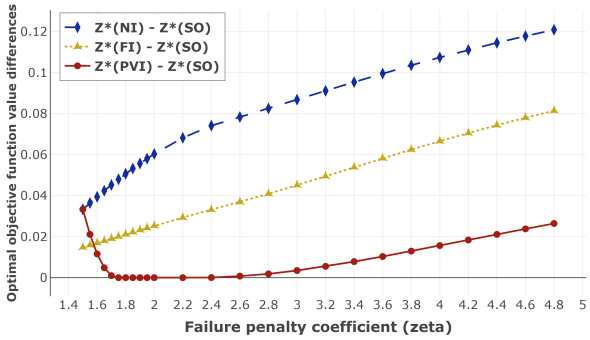

(a) Failure penalty coefficient ζ.

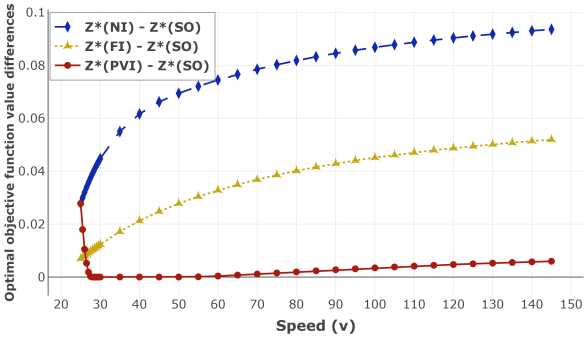

(b) Speed v.

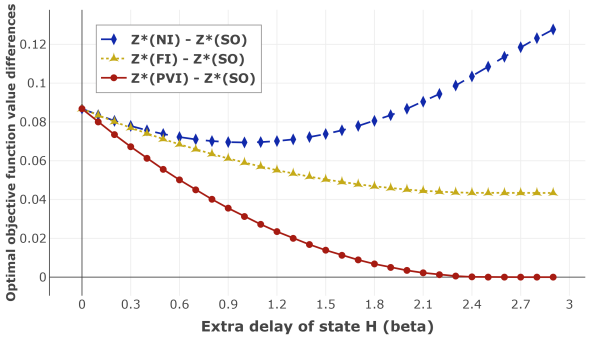

(c) Extra delay β at state H.

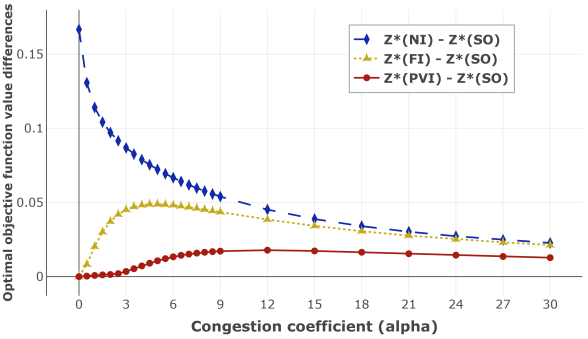

(d) Congestion coefficient α.

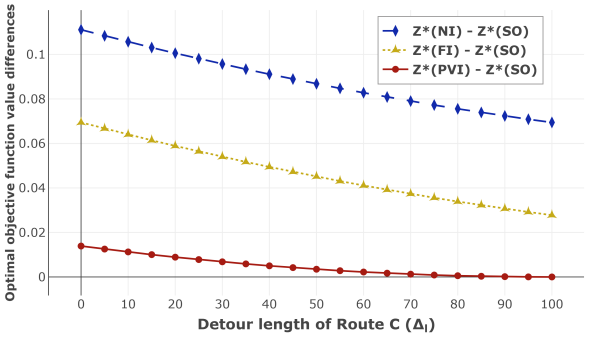

(e) Detour length Δ_l of Route C.

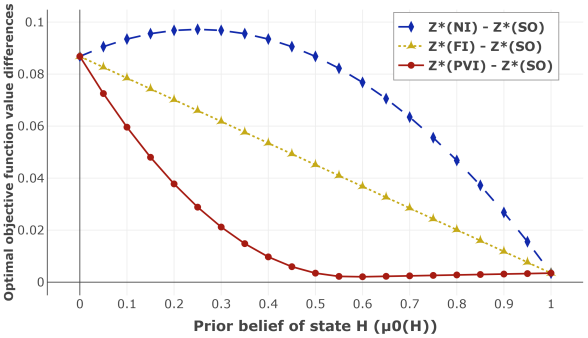

(f) Prior belief $\mu_0(\mathrm{H})$ of state H.

Figure 7: Sensitivity analysis of key model parameters in information design. The y-axis reports the deviation of the system cost from SO.

($\zeta < 1.58$, or $v < 26.5$). Thus, when the charging option is unattractive (due to a small failure penalty or a low speed), it is better to disclose the information fully and publicly than partially and privately. In the intermediate range ($1.75 < \zeta < 2.4$ or $28 < v < 55$), the PVI policy performs as well as the SO policy, highlighting the power of personalized persuasion. When $\zeta \geq 2.4$ or $v \geq 55$, the PVI policy enjoys a significant advantage over the FI policy, with the gap between the two slightly enlarging as ζ and v increase.

As shown in Figure 7(c), an increase in the extra delay associated with the abnormal state (β) pushes the PVI policy toward SO. The FI policy also becomes more effective as β increases, though the gain is more modest. Evidently, as the abnormal state imposes a higher cost, information becomes more valuable and there is greater maneuvering room for the designer. For all β values, the PVI policy consistently outperforms the FI policy. When $\beta \leq 2.5$, the PVI policy begins to deviate from the SO policy (the obedience-compliant region begins to shrink), causing all information designs to slowly converge to the same solution at $\beta = 0$ (where information no longer makes any difference).

Figure 7(d) indicates that the congestion coefficient α, which affects the cost at both states, has a relatively small but positive impact on the effectiveness of information provision. For small α, the NI scheme performs much worse than the other two schemes. In other words, if the waiting at the station is insensitive to the charging flow, there is much to lose by not telling the drivers what is going on. As α increases, however, the gap between the three shrinks quickly. For very large α, the PVI policy still holds a small edge while disclosing information fully or not at all makes no difference whatsoever. This indicates that the benefit of information, regardless of design, diminishes when the waiting time at the charging station is too high.

From Figure 7(e), we can see that increasing the detour length Δ_l brings both FI and PVI policies closer to SO. This suggests that a longer detour, which worsens the charging option, enhances the effectiveness of information provision in general. However, the relative advantage of the PVI policy over other policies is slightly eroded as Δ_l grows.

Figure 7(f) shows that prior belief has a rather dramatic impact on the effectiveness of all three policies, as well as on their effectiveness relative to each other. When nobody initially believes the charging station would operate abnormally ($\mu_0(\mathrm{H}) = 0$), information design makes no difference and all three policies perform poorly compared to SO. On the other extreme, where everyone is predisposed to believe the state is abnormal, information design also matters little. Improvements achieved by either the FI or the PVI policy over the NI policy peak at roughly $\mu_0(\mathrm{H}) = 0.4 \sim 0.6$, highlighting the fact that information design works best when drivers perceive a high level of uncertainty.

6.1.3 Multiple states

In this section, we first conduct experiments with three states to validate the formulation given in Section 3 and to compare the results with analytical results. We then discuss the challenge to deal with an arbitrary number of states. The parameter values in Section 6.1.1 are retained, except (i) ζ is set to 2.35, and (ii) the cost function (7) is slightly generalized to allow both α and β to be state-dependent, i.e., $J_C(f|w) = (l + \Delta_l)/v + (\alpha_w \cdot f + \beta_w)$.

The state set of the charging condition is set to $\mathbb{W} = \{\mathrm{H}, \mathrm{D}, \mathrm{L}\}$ with equal prior probabilities $\mu_0(\mathrm{H}) = \mu_0(\mathrm{D}) = \mu_0(\mathrm{L}) = 1/3$. We consider two scenarios, each corresponding to a different set of values for α_w and β_w. In the first (Scenario A), $\alpha_\mathrm{H} = 5$, $\alpha_\mathrm{D} = 3$, $\alpha_\mathrm{L} = 1$, and $\beta_\mathrm{H} = \beta_\mathrm{D} = \beta_\mathrm{L} = 0$. Under this setting, for any given charging flow f, the charging costs satisfy $J_C(f|\mathrm{H}) \geq J_C(f|\mathrm{D}) \geq$

$J_C(f|\mathrm{L})$. The results are presented in Table 3. We can see that the PBI and the FI policies are still equivalent. Both the PBI and PVI policies are better than the NI policy, though they are still quite far from the SO policy, with a gain of 48.1% and 67.6% respectively.

In Scenario B, we retain all parameter values from Scenario A except that β_{D} is increased from 0 to 1, thereby changing the cost structure across states. As shown in Table 3, somewhat unexpectedly, the PBI policy outperforms the FI policy by pooling states H and D (i.e., the designer issues signal d when the world state is either H or D). Thus, a public information design can still outperform full revelation, even though we have proven this to be impossible per Assumption 5. Under the PVI policy, $f_{\mathrm{D}} < f_{\mathrm{H}}$, confirming that the threshold values cannot be predetermined and that the order indicator $\boldsymbol{\nu}$ in formulation (6) is necessary.

Table 3: Numerical results for the three-state example.

Policy	Scenario A				Scenario B			
	f_{H}	f_{D}	f_{L}	$Z(\boldsymbol{f})$ (+%)	f_{H}	f_{D}	f_{L}	$Z(\boldsymbol{f})$ (+%)
NI	0.346	0.346	0.346	2.035 (+0%)	0.283	0.283	0.283	2.081 (+0%)
SO	0.150	0.222	0.425	1.929 (+100%)	0.150	0.102	0.425	1.983 (+100%)
FI	0.252	0.346	0.552	1.984 (+48.1%)	0.252	0.159	0.552	2.021 (+61.4%)
PVI	0.252	0.317	0.425	1.963 (+67.6%)	0.229	0.159	0.425	2.001 (+82.0%)
PBI	f_h =0.252	f_d =0.346	f_l =0.552	1.984 (+48.1%)		f_d=0.213	f_l=0.552	2.020 (+62.1%)
	$\pi(s \mid w)$	$s=h$	$s=d$	$s=l$	$\pi(s \mid w)$	$s=h$	$s=d$	$s=l$
	$w=\mathrm{H}$	1	0	0	$w=\mathrm{H}$	0	1	0
	$w=\mathrm{D}$	0	1	0	$w=\mathrm{D}$	0	1	0
	$w=\mathrm{L}$	0	0	1	$w=\mathrm{L}$	0	0	1

Note that (+%) denotes $\left(Z\left(\boldsymbol{f}^{\mathrm{NI}*}\right)-Z\left(\boldsymbol{f}\right)\right)/\left(Z\left(\boldsymbol{f}^{\mathrm{NI}*}\right)-Z\left(\boldsymbol{f}^{\mathrm{SO}*}\right)\right)$. In optimal public information design (PBI) policy, the charging flow is determined based on each signal ($s=h,d,l$ in our example) rather than each state, as indicated in the table. f_h is not reported in Scenario B because the states $w=\mathrm{H}$ and $w=\mathrm{D}$ are pooled together, corresponding to signal $s=d$, with $s=h$ never being sent.

With further increase in the number of states $|\mathbb{W}|$, the posterior belief space in the public design problem (3) expands at a rate faster than exponential and the complexity of (6) grows exponentially, rendering both Problems (3) and (6) computationally intractable. The concavification approach (Kamenica and Gentzkow 2011), while elegant, is effective only in low-dimensional settings (up to $|\mathbb{W}|=3$). For public design, the duality approach proposed by Dworczak and Martini (2019) offers a workaround when $|\mathbb{W}|\to\infty$, i.e., the charging condition is represented by a one-dimensional random variable with continuous support on a bounded interval. By considering the designer's problem as finding Walrasian equilibria of a persuasion economy, we can show that the optimal information structure consists of disjoint intervals of the state space that are either fully disclosed or polled as a single signal. To the best of our knowledge, however, the duality approach is not applicable to private design. Thus, addressing the scalability issue associated with the state set remains an open question for private design, even with a finite number of user types.

6.2 Two-station corridor model

We set $\mathbb{W}_i=\{\mathrm{H},\mathrm{L}\}(i=1,2)$, and the distance between the two stations $l_1=60$ miles. The charging cost function at each state $iw\in\mathbb{W}_i$ $(i=1,2)$ is given by $\alpha_{iw}f+\beta_{iw}$ (i.e., the constant travel

times are normalized to zero for simplicity), where f is the corresponding charging flow defined in Section 5. Congestion coefficients are fixed at $\alpha_{1H} = \alpha_{1L} = \alpha_{2H} = \alpha_{2L} = 3$, while congestion intercepts $\beta_{1H} = \beta_{2H} = 2$ and $\beta_{1L} = \beta_{2L} = 0$. The support of the remaining range estimation (RRE) is $\Xi = [\underline{R}, \bar{R}] = [60, 120]$, with a uniform distribution over the interval. The prior probabilities of the station states are symmetric: $\mu^0_{1H} = \mu^0_{1L} = \mu^0_{2H} = \mu^0_{2L} = 0.5$. The expected penalty for attempting to traverse $l_i (i = 1, 2)$ with $\hat{r}$ is given by $J^p_i(\hat{r}) = \zeta \cdot (1 - p(\hat{r}, l_i))$. The penalty coefficient ζ is set to 3. We assume the per-mile range reduction δ follows a distribution over $[\underline{\delta}, \bar{\delta}] = [1, 2]$ with a probability density function given by $u(\delta) = 3/\left(\delta^4 \cdot (\underline{\delta}^{-3} - \bar{\delta}^{-3})\right)$, which is a monotonically decreasing convex function. This results in the probability of successfully covering distance l with remaining range $\hat{r}$ $p(\hat{r}, l) = \max\left(\min\left(1 - \left(8(\hat{r}/l)^{-3} - 1\right)/7, 1\right), 0\right)$, which is monotonically increasing and concave over the interior of its domain (i.e., when $p(\hat{r}, l) \in (0, 1)$). Accordingly, the average range reduction when traveling from D_1 to D_2 is $\delta_1 = l_1 \cdot \int_{\underline{\delta}}^{\bar{\delta}} \delta \cdot u(\delta)\, \mathrm{d}\delta = 1.2857 \cdot l_1$.

In reality, a driver may decide not only whether to charge but also how much to charge. However, the latter decision has to be simplified here since modeling it explicitly would render the current framework intractable. Here, we assume that drives gain a fixed mileage Δ per charge and that their EVs have an identical maximum range $R^{\max}$, which is sufficiently large so that $\max(\bar{R} + \Delta, \bar{R} + 2\Delta - \delta_1) \leq R^{\max}$. This gives us $\hat{r}^C_1(r) = r + \Delta, \hat{r}^M_1(r) = r$, and $\hat{r}^{CC}_2(r) = r + 2\Delta - \delta_1$, $\hat{r}^{CM}_2(r) = r + \Delta - \delta_1$, $\hat{r}^{MC}_2(r) = r - \delta_1 + \Delta$, $\hat{r}^{MM}_2(r) = r - \delta_1$. Unless otherwise specified, we set $\Delta = 70$ miles.

Unlike in the single-station case, drivers' preferences over actions do not follow a predetermined ranking, as these preferences now depend on the spatial configuration. To show this, consider the no-information scenario, fix l_1 and vary l_2. Figure 8 plots the expected cost associated with each action at BNE. We observe that there is no consistent order among the choices. For drivers with lower RRE, charging only at the first station tends to outperform charging only at the second station, and charging at both stations tends to outperform skipping both. However, the relative preferences change as l_2 increases from 20 to 100.

We find that full information consistently yields the best public design outcome in both sequential and simultaneous release schedules — this is in line with the findings from a single-station case. Hence, we report all optimal public information design results simply as full information in this section.

As expected, the relative performance of the two release schedules for public design also depends on the spatial configuration. As shown in Figure 10, when l_2 increases from 10 to 110, simultaneous release leads in two intervals (10 to 25 and 55 to 110) while sequential release leads in the other two. Moreover, as l_2 rises above 110 (not reported in the figure), the discrepancy between the two gradually diminishes. For greater details, the left panel of Figure 9 reports the full information solutions at $l_2 = 40$ for both release schedules. We can see that sequential release directs more drivers to charge at Station 1 when $[1w = \mathrm{H}, 2w = \mathrm{L}]$, but fewer when $[1w = \mathrm{L}, 2w = \mathrm{H}]$ than simultaneous release. This shows how sequential release helps mitigate excessive concentration in response to revealed information. The upper-right panel of Figure 9 reveals how information received at Station 2 affects choices. For example, when drivers learned that Station 1 is at H (the top row in the panel), they are more likely to skip at Station 1 and charge at Station 2 (the green bar). However, upon learning Station 2 is also at H, these same drivers change their mind, choosing instead to skip charging again (the second row in the panel).

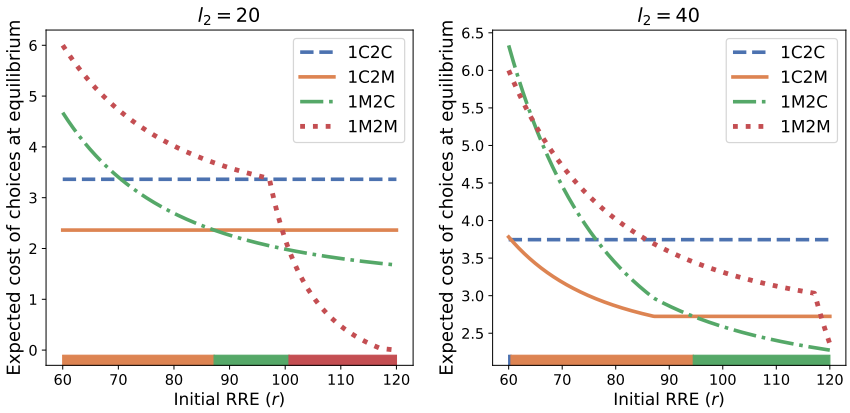

(a) $l_2 = 20$. (b) $l_2 = 40$.

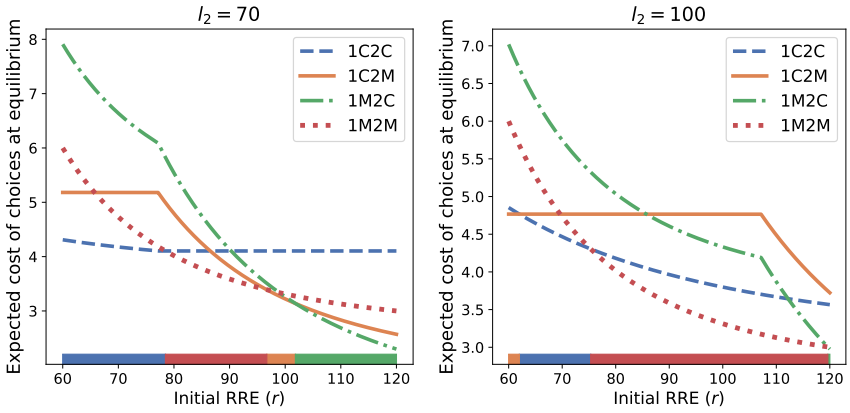

(c) $l_2 = 70$. (d) $l_2 = 100$.

Figure 8: Equilibrium without information in the corridor model: optimal choices, as represented by the colored bars at the bottom, and expected costs (colored curves) for different distances between the second charging station to the destination (l_2).

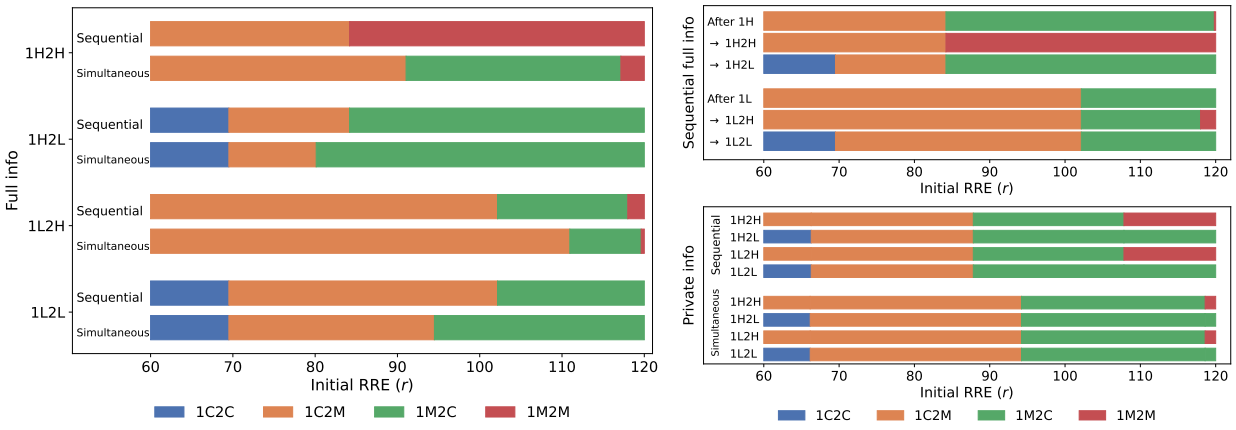

Figure 9: Comparison of optimal choices under different information schemes ($l_2 = 40$).

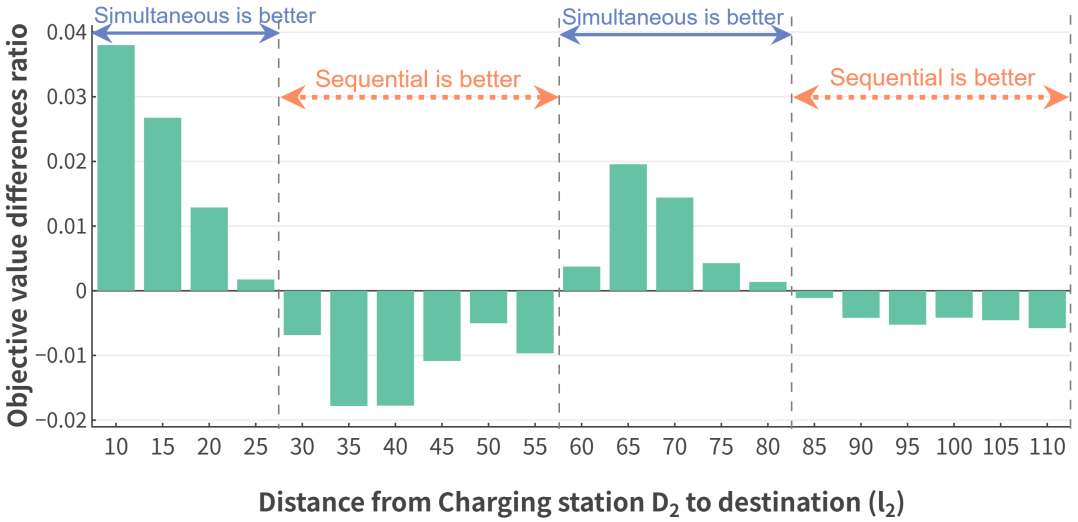

Note: l_1 is set to 60, and the definition of the objective value differences ratio is $(Z_{seq} - Z_{simu}) / (0.5 * (Z_{seq} + Z_{simu}))$, thus the positive value indicates the all-at-once is better.

Figure 10: Comparison of simultaneous (*simu*) and sequential (*seq*) public information designs in the two-station corridor under different distance l_2.

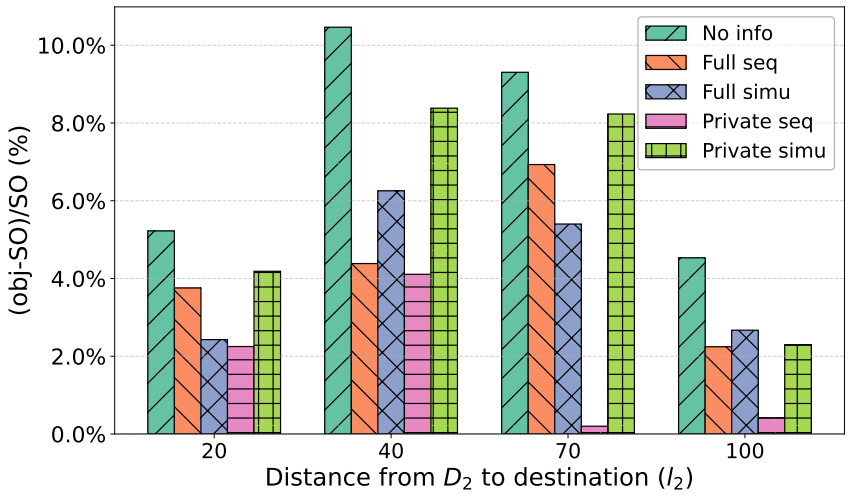

Figure 11: Objective function gap across different information design schemes in the two-station corridor.

The bottom panel of Figure 9 compares the two information release schedules under private information design. For sequential release, the optimal recommendation is primarily driven by the state at Station 2: when that station is in state H, a substantial share of drivers are advised to skip charging at both stations, and none are advised to charge at both; the opposite pattern emerges when Station 2 is in state L. Under simultaneous release, the overall choice pattern appears similar, but fewer drivers can be persuaded to skip charging at both stations when $2w = \mathrm{H}$, with a correspondingly larger proportion opting to charge at the first station. As we shall see below, this small difference contributes to the loss of efficiency in private design with simultaneous release.

Figure 11 reports the excess cost ratio relative to that achieved at the system optimum of the four information design schemes (public design with sequential release, public design with simultaneous release, private design with sequential release, and private design with simultaneous release) and the no-information baseline for four values of l_2. First and foremost, all four information schemes outperform the no-information baseline, though the relative benefits vary significantly with l_2. Second, the private information design with sequential release consistently delivers the best performance and, when l_2 is sufficiently large, tends to achieve outcomes that closely resemble the system optimum. However, with simultaneous release, the performance of private information design degrades below that of the public designs in nearly all cases. This is not surprisingly when we recall that the private design with simultaneous release introduces much more obedience constraints than that with sequential release. The additional constraints both reduce the feasible region (hence the likelihood of achieving a better system outcome) and make it even harder to find high-quality solutions.

7 Conclusions

The rapid adoption of electric vehicles (EVs) has put in the spotlight the inadequacy of charging capacities and the unique challenges it brought to EV drivers, especially for long-distance travel. Recent events have shown that range anxiety, combined with uncertain availability and delays at charging facilities, induce behaviors that can harm the efficiency of the system. In this study, we assume that a designer, who has exclusive knowledge of the state of the charging condition, can guide EV drivers towards a socially desirable outcome, by designing a suitable scheme to disseminate the information.

Building on information design theory, we developed optimization models for designing both public and private information structures. The public model delivers uniform information to all drivers, whereas the private model offer personalized recommendations based on a driver's estimated remaining range. Either way, EV drivers are Bayesian compliant, in that they have no incentive to deviate from the recommendation or the outcome desired by the designer, as their posterior belief, which they form through the Bayesian rule, tells them to take exactly the same action. While the public information design model is largely a direct adaptation of existing Bayesian persuasion models within the specific context that motivates our study, the private information design problem introduces noteworthy methodological innovations that may be generalized to applications beyond the EV charging problem considered herein. First, our private design model simultaneously allows for a congestion effect on the players' payoffs and a representation of their types based on an attribute represented by a continuous variable (the remaining range). Second, we devised a special information structure that reduces an infinite-dimensional problem to a

finite one, which is subsequently formulated as a mixed integer nonlinear program. Last but not least, we extend the framework to a corridor with multiple charging stations, allowing us to analyze, among other things, the impact of information release schedules on information design outcomes.

Our analysis of a single-station two-state model with a linear cost function yields several interesting findings. First, when the information structure is public, consistently revealing the true state of the system fully is the optimal strategy. However, if information can be delivered based on a player's type (represented here by the remaining range of the EV), significantly better outcomes can often be achieved. Under favorable conditions — such as high uncertainty and comparable costs among competing options — even the system-optimal outcome may be attained through strategic persuasion.

Our numerical experiments not only validated the proposed formulation and analytical results, but also yielded more insights. The congestion effect negatively impacts the value of information: if the waiting time at the station is sensitive to the number of drivers choosing to charge, information design is less useful. This occurs because congestion-related delays dilute the impact of the uncertain charging condition. Also, the value of information tends to increase with the level of uncertainty and the cost of charging relative to the other option.

In the multi-state numerical experiments, when the cost function does not render a clear ordering among the states, we find that the optimal public information design tends to obfuscate certain states rather than fully disclose them. This implies that the full-information policy is optimal only under highly restrictive conditions. Experimenting with the corridor model further shows that the private design strongly favors sequential release, which consistently yields the best performance. In contrast, under public design, the effect of the release schedule interacts with the spatial configuration, and no definitive preference appears to exist.

We anticipate that the new private information design model, with both continuous types and congestion externality, will find additional applications in transportation and other domains, such as operating shared mobility platforms, managing traffic, and allocating scarce resources in medical systems or data centers. To broaden its applicability, the current framework could be extended in several ways. For instance, if knowing each player's private type is too restrictive in certain contexts, we might instead assume that drivers are incentivized to share their type. Additionally, the current model considers the congestion effect only on one of the two options; however, in reality, both skipping and charging options may experience congestion. While adding congestion-related costs to both options might seem a straightforward extension, initial analysis suggests this could significantly complicate the model, particularly with a nonlinear congestion function. Extending information design to more general spatial contexts — such as network settings — represents another promising direction for future research. However, such extensions may require a fundamental rethinking not only of the problem formulation and solution algorithms, but also of the underlying modeling structure. Finally, the current cutoff-based obedience constraints were introduced to obtain a restricted version of the original problem. An important open question is under what conditions this structure ensures optimality and, more broadly, what a truly optimal structure may look like. We leave these intriguing questions also for future investigation.

Acknowledgments

This research is funded by US National Science Foundation's Civil Infrastructure System (CIS) Program under the award CMMI #2225087. The authors thank Professor Piotr Dworczak of Northwestern University Department of Economics for his invaluable suggestions.

References

Acemoglu D, Makhdoumi A, Malekian A, Ozdaglar A (2018) Informational braess' paradox: The effect of information on traffic congestion. *Operations Research* 66(4):893–917.

Andrews M (2024) China's electric vehicle infrastructure falls short, as lunar new year holiday woes of ev drivers in hainan and elsewhere showed. https://tinyurl.com/3h9h4k6x, accessed: July 10, 2024.

Anunrojwong J, Iyer K, Manshadi V (2023) Information design for congested social services: Optimal need-based persuasion. *Management Science* 69(7):3778–3796.

Arnott R, De Palma A, Lindsey R (1991) Does providing information to drivers reduce traffic congestion? *Transportation Research Part A: General* 25(5):309–318.

Ashlagi I, Monachou F, Nikzad A (2024) Optimal allocation via waitlists: Simplicity through information design. *Review of Economic Studies* rdae013.

Beckmann MJ, McGuire CB, Winsten CB (1955) *Studies in the economics of transportation* (Yale University Press).

Ben-Akiva M, De Palma A, Isam K (1991) Dynamic network models and driver information systems. *Transportation Research Part A: General* 25(5):251–266.

Bergemann D, Morris S (2016) Bayes correlated equilibrium and the comparison of information structures in games. *Theoretical Economics* 11(2):487–522.

Bergemann D, Morris S (2019) Information design: A unified perspective. *Journal of Economic Literature* 57(1):44–95.

Best J, Quigley D (2024) Persuasion for the long run. *Journal of Political Economy* 132(5):1740–1791.

Bonami P, Biegler LT, Conn AR, Cornuéjols G, Grossmann IE, Laird CD, Lee J, Lodi A, Margot F, Sawaya N, et al. (2008) An algorithmic framework for convex mixed integer nonlinear programs. *Discrete optimization* 5(2):186–204.

Byrd RH, Nocedal J, Waltz RA (2006) Knitro: An integrated package for nonlinear optimization. *Large-scale nonlinear optimization*, 35–59 (Springer).

Chakraborty P, Parker R, Hoque T, Cruz J, Du L, Wang S, Bhunia S (2022) Addressing the range anxiety of battery electric vehicles with charging en route. *scientific reports* 12(1):5588.

Cui D, Wang Z, Liu P, Wang S, Dorrell DG, Li X, Zhan W (2023) Operation optimization approaches of electric vehicle battery swapping and charging station: A literature review. *Energy* 263:126095.

Das S, Kamenica E, Mirka R (2017) Reducing congestion through information design. *2017 55th annual allerton conference on communication, control, and computing (allerton)*, 1279–1284 (IEEE).

Dasgupta P, Hammond P, Maskin E (1979) The implementation of social choice rules: Some general results on incentive compatibility. *The Review of Economic Studies* 46(2):185–216.

De Véricourt F, Gurkan H, Wang S (2021) Informing the public about a pandemic. *Management Science* 67(10):6350–6357.

Dughmi S, Xu H (2016) Algorithmic bayesian persuasion. *Proceedings of the forty-eighth annual ACM symposium on Theory of Computing*, 412–425.

Dworczak P, Martini G (2019) The simple economics of optimal persuasion. *Journal of Political Economy* 127(5):1993–2048.

Ely JC (2017) Beeps. *American Economic Review* 107(1):31–53.

Emmerink RH, Axhausen KW, Nijkamp P, Rietveld P (1995) Effects of information in road transport networks with recurrent congestion. *Transportation* 22:21–53.

Ewing J (2024) Tesla's share of u.s. electric car market falls below 50%. https://www.nytimes.com/2024/07/09/business/tesla-electric-vehicles-market-share.html, accessed: July 10, 2024.

Farhadi F, Teneketzis D (2022) Dynamic information design: A simple problem on optimal sequential information disclosure. *Dynamic Games and Applications* 12(2):443–484.

Futalef JP, Muñoz-Carpintero D, Rozas H, Orchard ME (2023) An online decision-making strategy for routing of electric vehicle fleets. *Information Sciences* 625:715–737.

Gan J, Han M, Wu J, Xu H (2022a) Optimal coordination in generalized principal-agent problems: A revisit and extensions. *arXiv preprint arXiv:2209.01146* .

Gan J, Majumdar R, Radanovic G, Singla A (2022b) Bayesian persuasion in sequential decision-making. *Proceedings of the AAAI Conference on Artificial Intelligence* 36(5):5025–5033.

Ge Y, MacKenzie D (2022) Charging behavior modeling of battery electric vehicle drivers on long-distance trips. *Transportation Research Part D: Transport and Environment* 113:103490.

Gibbard A (1973) Manipulation of voting schemes: a general result. *Econometrica: journal of the Econometric Society* 587–601.

Goldstein I, Leitner Y (2018) Stress tests and information disclosure. *Journal of Economic Theory* 177:34–69.

Griesbach SM, Hoefer M, Klimm M, Koglin T (2022) Public signals in network congestion games. *arXiv preprint arXiv:2205.09823* .

Griesbach SM, Hoefer M, Klimm M, Koglin T (2024) Information design for congestion games with unknown demand. *Proceedings of the AAAI Conference on Artificial Intelligence* 38(9):9722–9730.

Hassler J, Dimitrova Z, Petit M, Dessante P (2021) Optimization and coordination of electric vehicle charging process for long-distance trips. *Energies* 14(13):4054.

He F, Wu D, Yin Y, Guan Y (2013) Optimal deployment of public charging stations for plug-in hybrid electric vehicles. *Transportation Research Part B: Methodological* 47:87–101.

IEA (2024) Global ev outlook 2024. https://www.iea.org/reports/global-ev-outlook-2024, accessed: July 10, 2024, Licence: CC BY 4.0.

Iversen EB, Morales JM, Madsen H (2014) Optimal charging of an electric vehicle using a markov decision process. *Applied Energy* 123:1–12, ISSN 0306-2619, URL http://dx.doi.org/https://doi.org/10.1016/j.apenergy.2014.02.003.

Jaguemont J, Boulon L, Dubé Y (2016) A comprehensive review of lithium-ion batteries used in hybrid and electric vehicles at cold temperatures. *Applied Energy* 164:99–114.

Kamenica E (2019) Bayesian persuasion and information design. *Annual Review of Economics* 11(1):249–272.

Kamenica E, Gentzkow M (2011) Bayesian persuasion. *American Economic Review* 101(6):2590–2615.

Kane M (2024) Europe: Plug-in car sales exceeded 3 million in 2023. https://insideevs.com/news/707425/europe-plugin-car-sales-december2023/, accessed: July 10, 2024.

Koutsopoulos HN, Lotan T, Yang Q (1994) A driving simulator and its application for modeling route choice in the presence of information. *Transportation Research Part C: Emerging Technologies* 2(2):91–107.

Li J, Yu J, Nie Y, Wang Z (2020) End-to-end learning and intervention in games. *Advances in Neural Information Processing Systems* 33:16653–16665.

Li J, Yu J, Wang Q, Liu B, Wang Z, Nie YM (2022) Differentiable bilevel programming for stackelberg congestion games. *arXiv preprint arXiv:2209.07618* .

Lindsey R, Daniel T, Gisches E, Rapoport A (2014) Pre-trip information and route-choice decisions with stochastic travel conditions: Theory. *Transportation Research Part B: Methodological* 67:187–207.

Lingenbrink D, Iyer K (2019) Optimal signaling mechanisms in unobservable queues. *Operations research* 67(5):1397–1416.

Liu B, Ni W, Liu RP, Guo YJ, Zhu H (2023) Optimal electric vehicle charging strategies for long-distance driving. *IEEE Transactions on Vehicular Technology* .

Liu J, Amin S, Schwartz G (2016) Effects of information heterogeneity in bayesian routing games. *arXiv preprint arXiv:1603.08853* .

Mahmassani HS, Jayakrishnan R (1991) System performance and user response under real-time information in a congested traffic corridor. *Transportation Research Part A: General* 25(5):293–307.

Mak HY, Rong Y, Shen ZJM (2013) Infrastructure planning for electric vehicles with battery swapping. *Management science* 59(7):1557–1575.

Matsushita A (2024) Comparison between public and private signals in network congestion games. *International Workshop on Mechanism Design in Social Networks*, 19–35 (Springer).

Mohammed A, Saif O, Abo-Adma M, Fahmy A, Elazab R (2024) Strategies and sustainability in fast charging station deployment for electric vehicles. *Scientific Reports* 14(1):283.

Myerson RB (1979) Incentive compatibility and the bargaining problem. *Econometrica: journal of the Econometric Society* 61–73.

Myerson RB (1986) Multistage games with communication. *Econometrica: Journal of the Econometric Society* 323–358.

News B (2024) Long charging lines, snow stymie ev drivers in china new year. https://www.bloomberg.com/news/articles/2024-02-20/long-charging-lines-snow-stymie-ev-drivers-in-china-new-year, accessed: July 10, 2024.

Nie YM, Ghamami M (2013) A corridor-centric approach to planning electric vehicle charging infrastructure. *Transportation Research Part B: Methodological* 57:172–190.

Ostrovsky M, Schwarz M (2010) Information disclosure and unraveling in matching markets. *American Economic Journal: Microeconomics* 2(2):34–63.

Pontes J (2024) 25% of new car sales in china were 100% electric in 2023! https://tinyurl.com/2wczx37z, accessed: July 10, 2024.

Rayo L, Segal I (2010) Optimal information disclosure. *Journal of political Economy* 118(5):949–987.

Renault J, Solan E, Vieille N (2017) Optimal dynamic information provision. *Games and Economic Behavior* 104:329–349.

Skinner A (2024) Hundreds of tesla owners flood charging station. https://www.newsweek.com/tesla-charging-station-police-solar-eclipse-travel-1888941, accessed: July 10, 2024.

State Grid Smart Internet of Vehicles Co L (2024) Echargenet. http://www.evs.sgcc.com.cn/, accessed: July 19, 2024.

Sun XH, Yamamoto T, Morikawa T (2015) Charge timing choice behavior of battery electric vehicle users. *Transportation Research Part D: Transport and Environment* 37:97–107.

Sun XH, Yamamoto T, Morikawa T (2016) Fast-charging station choice behavior among battery electric vehicle users. *Transportation Research Part D: Transport and Environment* 46:26–39.

Tavafoghi H, Shetty A, Poolla K, Varaiya P (2019) Strategic information platforms in transportation networks. *2019 57th Annual Allerton Conference on Communication, Control, and Computing (Allerton)*, 816–823 (IEEE).

Tavafoghi H, Teneketzis D (2019) Strategic information provision in routing games.

Tyrrell Rockafellar R (1970) Convex analysis. *Princeton mathematical series* 28.

Wardrop JG (1952) Road paper. some theoretical aspects of road traffic research. *Proceedings of the institution of civil engineers* 1(3):325–362.

Wolbertus R, Kroesen M, Van Den Hoed R, Chorus C (2018) Fully charged: An empirical study into the factors that influence connection times at ev-charging stations. *Energy Policy* 123:1–7.

Wu J, Zhang Z, Feng Z, Wang Z, Yang Z, Jordan MI, Xu H (2022) Sequential information design: Markov persuasion process and its efficient reinforcement learning. *arXiv preprint arXiv:2202.10678* .

Wu M, Amin S, Ozdaglar AE (2021) Value of information in bayesian routing games. *Operations Research* 69(1):148–163.

Yang P, Iyer K, Frazier P (2019) Information design in spatial resource competition. *arXiv preprint arXiv:1909.12723* .

Yi Z, Shirk M (2018) Data-driven optimal charging decision making for connected and automated electric vehicles: A personal usage scenario. *Transportation Research Part C: Emerging Technologies* 86:37–58.

Zhang Z, Wang D, Zhang C, Chen J (2018) Electric vehicle range extension strategies based on improved ac system in cold climate–a review. *International Journal of Refrigeration* 88:141–150.

Zhou C, Nguyen TH, Xu H (2022) Algorithmic information design in multi-player games: Possibilities and limits in singleton congestion. *Proceedings of the 23rd ACM Conference on Economics and Computation*, 869–869.

Zhu Y, Savla K (2022) Information design in nonatomic routing games with partial participation: Computation and properties. *IEEE Transactions on Control of Network Systems* 9(2):613–624.

A Preliminaries

As the application of information design in transportation is relatively new, we cover in this section its basics, through an illustrative scenario with two players: a Sender (he) and a Receiver (she). The game is set in a world characterized by a state $w \in \mathbb{W}$, where $\mathbb{W}$ is a finite set. We assume $\boldsymbol{\mu}_0 = \{\mu_0(w)\}_{w\in\mathbb{W}} \in \boldsymbol{\Delta}(\mathbb{W})$ is a vector that represents the Receiver's prior belief about each possible world state. Note that $\boldsymbol{\Delta}$ denotes a probability simplex, i.e., the sum of vector elements is 1. The Receiver has a utility function $u(a, w)$ that depends on her action $a \in \mathbb{A}$ and the world state $w \in \mathbb{W}$. The Sender has his own utility function $v(a, w)$ that also depends on the Receiver's a and w. We assume both $u(a, w)$ and $v(a, w)$ are continuous in a.

The Receiver's action depends on her belief about the world, and the Sender can try to manipulate that belief to maximize his own utility. To do so, the Sender may choose among a finite set of signals $\mathbb{S}$, according to an information structure $\pi : \mathbb{S} \times \mathbb{W} \to [0, 1]$, where $\pi(s \mid w)$ gives the probability that a world state w corresponds to a signal state s. Clearly, we have $\sum_{s\in\mathbb{S}} \pi(s \mid w) = 1$ $(\forall w \in \mathbb{W})$. The Sender shares $\boldsymbol{\pi} = \{\pi(s \mid w)\}_{s\in\mathbb{S},w\in\mathbb{W}}$, with the Receiver, and commits to it before the world state w is realized. Then, for each realized world state, the Sender sends to the Receiver a signal state s rendered based on the information structure $\boldsymbol{\pi}$.

A.1 General information structure

Under a general information structure, upon receiving s, the Receiver forms a posterior belief $\boldsymbol{\mu}_s = \{\mu_s(w)\}_{w\in\mathbb{W}}$ using the Bayesian rule and chooses an action to maximize her expected utility. Specifically, the probability of the world state w, as perceived by the Receiver upon receiving a signal state s, is $\mu_s(w) = \frac{\mu_0(w)\pi(s|w)}{\sum_{w'\in\mathbb{W}} \mu_0(w')\pi(s|w')}$ $(\forall w \in \mathbb{W}, s \in \mathbb{S})$. The optimal action(s) of the Receiver can be written as a set $a^*(\boldsymbol{\mu}_s) = \arg\max_{a\in\mathbb{A}} \mathbb{E}_{w\sim\boldsymbol{\mu}_s}(u(a, w)) = \arg\max_{a\in\mathbb{A}} \sum_{w\in\mathbb{W}} \mu_s(w)u(a, w)$. For notational convenience, let $\hat{a}_s$ be the best response action from $a^*(\boldsymbol{\mu}_s)$ that is preferred by the Sender. Accordingly, the Sender's objective is the maximization of his expected utility

$$V(\boldsymbol{\pi}) = \mathbb{E}_{w\sim\boldsymbol{\mu}_0}\mathbb{E}_{s\sim\pi(\cdot|w)}v(\hat{a}_s, w) = \sum_{w\in\mathbb{W}} \mu_0(w) \sum_{s\in\mathbb{S}} \pi(s \mid w)v(\hat{a}_s, w). \tag{19}$$

Equation (19) indicates that the information structure $\boldsymbol{\pi}$ affects the Sender's payoff directly as well as indirectly, by influencing the Receiver's best response action $\hat{a}_s \in a^*(\boldsymbol{\mu}_s)$ (which depends on the posterior belief $\boldsymbol{\mu}_s$). Accordingly, the Sender's optimization problem can be formulated as follows, with $\boldsymbol{\pi}$ as the decision variable:

$$\max\ V(\boldsymbol{\pi}) \quad \text{subject to:} \sum_{s\in\mathbb{S}} \pi(s \mid w) = 1, \forall w \in \mathbb{W}; \pi(s \mid w) \geq 0, \forall s \in \mathbb{S}, w \in \mathbb{W}. \tag{20}$$

A.2 Direct information structure

Before solving Problem (20), the Sender must choose an appropriate signal set $\mathbb{S}$. For this task, according to the revelation principle (Myerson 1979, 1986, Bergemann and Morris 2019, Gan et al. 2022a), the Sender may focus on direct signaling schemes. A direct information structure assumes $\mathbb{S} = \mathbb{A}$ so that each signal now corresponds to an action recommendation. More specifically, $\pi(a \mid w)$ specifies the probability of sending an action recommendation a according to the realized state w. The Receiver will always follow the recommendation a if it is optimal under the posterior belief, i.e., $\sum_{w\in\mathbb{W}} \mu_0(w)\, \pi(a \mid w)\, [u(a, w) - u(a', w)] \geq 0, \forall a' \in \mathbb{A}$, which are

known as the persuasive or obedience constraints. Thus, the Sender's optimization problem can be formulated as follows (Dughmi and Xu 2016):

$$\max_{\boldsymbol{\pi}} \sum_{w\in\mathbb{W}} \sum_{a\in\mathbb{A}} \mu_0(w)\pi(a \mid w)v(a,w) \tag{21a}$$

$$\text{subject to: } \sum_{w\in\mathbb{W}} \mu_0(w)\,\pi(a \mid w)\left[u(a,w) - u\left(a',w\right)\right] \geq 0, \forall a,a' \in \mathbb{A}, \tag{21b}$$

$$\sum_{a\in\mathbb{A}} \pi(a \mid w) = 1, \forall w \in \mathbb{W};\ \pi(a \mid w) \geq 0, \forall a \in \mathbb{A}, w \in \mathbb{W}. \tag{21c}$$

Here, the objective is the Sender's expected utility, Constraints (21b) enforce the Receiver's obedience to recommendation and Constraints (21c) ensure the feasibility of the information structure.

B Table of notations

Table 4: Notations.

Notation	Definition
	— Base models general settings. —
$a \in \mathbb{A}$	An action a from the action set $\mathbb{A}$.
$\mathbb{A} = \{C, M\}$	Action set $\mathbb{A}$ consisting of Route C (charging) and Route M (non-charging).
$w \in \mathbb{W}$	A state w from the state set $\mathbb{W}$.
$\boldsymbol{\mu}_0 = \{\mu_0(w)\}_{w\in\mathbb{W}}$	Prior belief over all possible state $w \in \mathbb{W}$.
l	The length of the remaining journey from the decision point.
Δ_l	The detour length for using the charging station.
v	The travel speed of the drivers.
$\Delta_t \equiv \Delta_l / v$	Detour expressed in travel time units.
r	The remaining range estimate (RRE) at the decision point.
$p(r)$	The probability of completing the journey without charging.
$g(\cdot)$	The probability density function (PDF) of the RRE distribution across the population.
$G(\cdot)$	The cumulative distribution function (CDF) of the RRE distribution across the population.
$\Xi = [\underline{R}, \bar{R}]$	The support of the RRE distribution.
f	Flow of drivers choosing Route C, also referred to as the charging flow.
$1 - f$	Flow of drivers choosing Route M.
f^*	Bayesian Nash equilibrium (BNE) flow choosing Route C.
$J_C(f\|w)$	The cost function associated with Route C at charging flow level f at state w.
$J_M(p(r)\|w)$	The cost function associated with Route M for driver with RRE r at state w.
$\bar{r}$	Threshold RRE that makes the driver indifferent between C and M under charging flow f.
$\bar{r}^*$	BNE threshold RRE indifferent between choosing Route C and M.
	— Public information design base model. —
$s \in \mathbb{S}$	A signal s from the signal set $\mathbb{S}$.
$\boldsymbol{\pi} = \{\pi(s \mid w)\}_{s\in\mathbb{S},w\in\mathbb{W}}$	Information structure specifying the probability of sending signal s given state w.
$\boldsymbol{\mu}_s = \{\mu_s(w)\}_{w\in\mathbb{W}}$	Posterior belief over states after receiving signal s.
f_s^*	BNE flow choosing Route C after receiving public signal s.
$\bar{r}_s^*$	BNE threshold RRE under public signal s, indifferent between C and M under posterior $\boldsymbol{\mu}_s$.
$Z(\boldsymbol{\pi})$	Expected total system cost for the public information design given $\boldsymbol{\pi}$.
	— Private information design base model. —
$\boldsymbol{\pi} = \{\pi(a \mid w, r)\}_{a\in\mathbb{A},w\in\mathbb{W},r\in\Xi}$	An information structure specifying the probability to recommend action a for r at w.
$\bar{\boldsymbol{r}} = \{\bar{r}_w\}_{w\in\mathbb{W}}$	A vector of state-dependent cutoff RRE thresholds for private information design.
$\{\bar{r}_i\}_{i=1,\ldots,\|\mathbb{W}\|}$	A vector of sorted state-dependent cutoff RRE thresholds for private information design.
$\boldsymbol{f} = \{f_w\}_{w\in\mathbb{W}}$	A vector of state-dependent charging flows for private information design.

$\boldsymbol{\nu} = \{\nu_i^w\}_{i=1,\ldots,\lvert\mathbb{W}\rvert, w\in\mathbb{W}}$	Indicator $\nu_i^w = 1$ if $\bar{r}_w$ is the i-th smallest cutoff; 0 otherwise.
$Z(\boldsymbol{f})$ or $Z(\boldsymbol{f}, \boldsymbol{\nu})$	Expected total system cost for the private information design given $\boldsymbol{f}$ (and indicators $\boldsymbol{\nu}$).
$\hat{\boldsymbol{r}} = \{\underline{R}, \bar{r}_1, \ldots, \bar{r}_i, \ldots, \bar{r}_{\lvert\mathbb{W}\rvert}, \bar{R}\}$ $\equiv \{\hat{r}_0, \hat{r}_1, \ldots, \hat{r}_k, \ldots, \hat{r}_{\lvert\mathbb{W}\rvert}, \hat{r}_{\lvert\mathbb{W}\rvert+1}\}$	The sorted RRE thresholds augmented with the lower and upper bounds on RRE.
$R_k = (\ \hat{r}_{k-1}, \hat{r}_k\ ]$	RRE interval of type k travelers.
	— Parameters used in the base models for analytical results and numerical experiments. —
$\mathbb{W} = \{\mathrm{H}, \mathrm{L}\}$	State H denotes high grid load / adverse conditions; State L denotes normal operation.
α	Coefficient capturing the congestion effect.
β	Additional delay on Route C when $w = \mathrm{H}$.
ζ	Penalty coefficient for Route M.
n	Safe range factor defining the RRE distribution.
Superscript NI	Refers to no information benchmark.
Superscript FI	Refers to full information benchmark.
Superscript SO	Refers to system optimal benchmark.
Superscript PVI	Refers to the private information design.
$\underline{\mu_0}$	Constant given by $(\alpha(\zeta - \Delta_t))/(-\alpha(\zeta - \Delta_t) + \beta(2\alpha + \zeta))$.
$\overline{\mu_0}$	Constant given by $((\alpha + \zeta)(\zeta - \Delta_t))/(-\alpha(\zeta - \Delta_t) + \beta(2\alpha + \zeta))$.
$\hat{\mu_0}$	Constant given by $((\alpha^2 + (\alpha + \zeta)^2)(\zeta - \Delta_t))/(-\alpha\zeta(\zeta - \Delta_t) + \beta(2\alpha + \zeta)(\alpha + \zeta))$.
α_w	Congestion coefficient associated with state w (used in numerical experiments).
β_w	Additional delay associated with state w (used in numerical experiments).
	— Two-station corridor extension general settings: $i = 1, 2$. —
D_i	Decision point D_i on the two-station corridor.
$a_i \in \mathbb{A}_i$	Action a_i taken at decision point D_i, where $a_i \in \mathbb{A}_i$.
$\boldsymbol{a} = a_1 a_2 \in \mathbb{A}$	Driver's overall action sequence $\boldsymbol{a} = a_1 a_2$, where $\boldsymbol{a} \in \mathbb{A}$.
$\mathbb{A} = \{CC, CM, MC, MM\}$	Set of all possible action sequences.
$iw \in \mathbb{W}_i$	A state iw in state set $\mathbb{W}_i$ for Station i.
μ_{iw}^0	Prior belief of each state iw for Station i.
l_1	The distance between the two charging stations.
l_2	The distance from Station 2 to the final destination.
$g(\cdot)$	PDF of the initial RRE distribution.
$G(\cdot)$	CDF of the initial RRE distribution.
$u(\cdot)$	PDF of random range reduction per mile traveled, with support $[\underline{\delta}, \bar{\delta}]$.
$p(\hat{r}, l) = 1 - \int_{\hat{r}/l}^{\bar{\delta}} u(\delta)\,\mathrm{d}\delta$	Probability that a vehicle with RRE $\hat{r}$ can successfully cover distance l.
$J_i^p(\hat{r})$	Expected penalty for attempting to traverse l_i $(i = 1, 2)$ with RRE $\hat{r}$.
$\hat{r}_1^{a_1}(r), a_1 \in \{C, M\}$	Resulting RRE at D_1 after choosing the first action a_1 with the initial RRE r.
$\hat{r}_2^{\boldsymbol{a}}(r), \boldsymbol{a} \in \mathbb{A}$	Resulting RRE at D_2 after choosing the action sequence $\boldsymbol{a} \in \mathbb{A}$ with the initial RRE r.
	— Two-station corridor public information design with sequential release. —
$is \in \mathbb{S}_i$	A signal is at decision point D_i from the set of signals $\mathbb{S}_i$.
$\boldsymbol{\pi} = \{\boldsymbol{\pi}_1, \boldsymbol{\pi}_2\}$	Information structure vector for two stations.
$\boldsymbol{\pi}_i = \{\pi_i(is \mid iw)\}_{is\in\mathbb{S}_i, iw\in\mathbb{W}_i}$	Public information structure at decision point D_i.
$R_{1s}^{a_1 a_2}$	RRE range of drivers who choose actions $a_1 a_2$ after receiving signal $1s$.
R_{1s}^{C}	RRE range of drivers who choose to charge at Station 1 after receiving signal $1s$.
R_{1s}^{M}	RRE range of drivers who choose to skip at Station 1 after receiving signal $1s$.
$R_{1s2s}^{\boldsymbol{a}}$	RRE range of drivers who choose action sequence $\boldsymbol{a}$ after receiving signals $1s$ and $2s$.
$\mathbf{R}$	$\mathbf{R} = \{R_{1s}^{C}, R_{1s}^{M}, R_{1s2s}^{CC}, R_{1s2s}^{CM}, R_{1s2s}^{MC}, R_{1s2s}^{MM}\}_{1s\in\mathbb{S}_1, 2s\in\mathbb{S}_2}$ A set of ranges.
$J_{1C,1w}^{g,1s}$	Charging cost at Station 1 in state $1w \in \mathbb{W}_1$ after receiving signal $1s \in \mathbb{S}_1$.
$J_{a_1C,2w}^{g,1s2s}$	Charging cost at Station 2, conditional on $(1s, a_1)$, given signal $2s$ and state $2w$.
α_{iw}	The congestion coefficient related to state iw at Station i.
β_{iw}	The extra delay related to state iw at Station i.
μ_{1w}^{1s}	Posterior belief about state $1w$ for Station 1 after receiving signal $1s$.
μ_{2w}^{2s}	Posterior belief about state $2w$ for Station 2 after receiving signal $2s$.
$e_{a_1 a_2}^{1s}$	The expected costs for action sequence $a_1 a_2$ at D_1 after receiving signal $1s$.
$e_{a_1 a_2}^{1s2s}$	The expected costs for action a_2 at D_2, conditional on $(1s, a_1)$, after receiving signal $2s$.

$\varepsilon(\boldsymbol{\pi})$	BNE set for public information structure $\boldsymbol{\pi}$ for sequential release.
$Z_b(\mathbf{R}^*, \boldsymbol{\pi})$	The system's total expected cost (in sequential release public design) achieved at $\boldsymbol{\pi}$ and $\mathbf{R}^*$.
p_{1s}	The probability of observing each first-stage signal $1s$: $p_{1s} \equiv \sum_{1w \in \mathbb{W}_1} \mu^0_{1w} \cdot \pi_1(1s \mid 1w)$.
	— Two-station corridor private information design with sequential release. —
$t \in \mathbb{T}$	A private design information type t belongs to $\mathbb{T}$ where $\lvert\mathbb{T}\rvert = 2^{(\sum_i \lvert\mathbb{W}_i\rvert)}$.
$\eta_{t,w}$	Type-state recommendation indicator, $= 1$ if type t receives C at state w, and 0 otherwise.
$\mathbb{K} = \{1, \ldots, K\}$	A set of intervals the range support Ξ is divided into.
$k \in \mathbb{K}$	The kth interval.
$\bar{r}_k$	The upper bound of the kth interval.
$\bar{\boldsymbol{r}} = [\ldots, \bar{r}_k, \ldots]$	The upper bound vector of all intervals.
$\iota_{k,t}$	Binary variable indicating whether drivers in the kth range interval are information type t.
$\boldsymbol{\iota} = [\ldots, \iota_{k,t}, \ldots]$	All interval-type indicating binary variables.
f^{1C}_{1w}	The charging flow at Station 1 under state $1w$.
f^{CC}_{1w2w}	The flow of charging at both stations given state $(1w, 2w)$.
f^{MC}_{1w2w}	The flow of only charging at Station 2 given state $(1w, 2w)$.
$J^g_{1C,1w}$	The charging cost at Station 1 under state $1w$ which depends on f^{1C}_{1w}.
$J^g_{CC,1w2w}$	Charging cost at Station 2 under action CC and states $(1w, 2w)$, dependent on f^{CC}_{1w2w}.
$J^g_{MC,1w2w}$	Charging cost at Station 2 under action MC and states $(1w, 2w)$, dependent on f^{MC}_{1w2w}.
$Z_v(\bar{\boldsymbol{r}}, \boldsymbol{\iota})$	The system's total expected cost (in sequential release private design) achieved at $\bar{\boldsymbol{r}}$ and $\boldsymbol{\iota}$.
$E^{a_1}_{1w}(r)$	The expected cost for RRE r at D_1 given state $1w$ and action a_1.
$E^{\boldsymbol{a}}_{1w2w}(r)$	The expected cost for RRE r at D_2 given states $(1w, 2w)$ and action sequence $\boldsymbol{a}$.
	— Two-station corridor public information design with simultaneous release. —
$\hat{\mathbf{R}}$	$\hat{\mathbf{R}} = \{\hat{R}^{CC}_{1s2s}, \hat{R}^{CM}_{1s2s}, \hat{R}^{MC}_{1s2s}, \hat{R}^{MM}_{1s2s}\}_{1s \in \mathbb{S}_1, 2s \in \mathbb{S}_2}$ A set of ranges for simultaneous release.
$\hat{\varepsilon}(\boldsymbol{\pi})$	BNE set for public information structure $\boldsymbol{\pi}$ for simultaneous release.
$\rho^{1s2s}_{\boldsymbol{a}}$	The expected cost for simultaneous release given public signals $(1s, 2s)$ and action sequence $\boldsymbol{a}$.
$\hat{J}^{g,1s2s}_{1C,1w}$	The charging cost at Station 1 given state $1w$ and public signals $(1s, 2s)$.
$\hat{J}^{g,1s2s}_{a_1C,2w}$	The charging cost at Station 2 given state $2w$ and public signals $(1s, 2s)$ and action a_1.
$\hat{Z}_b(\hat{\mathbf{R}}^*, \boldsymbol{\pi})$	The system's total expected cost (in simultaneous release public design) achieved at $\boldsymbol{\pi}$ and $\mathbf{R}^*$.
	— Two-station corridor private information design with simultaneous release. —
$V^{k,t}_{\boldsymbol{a},\boldsymbol{a}'}(r)$	Expected cost for a type-t driver with RRE r in interval k, receiving recommendation $\boldsymbol{a}$ and choose to take action $\boldsymbol{a}'$.
$\hat{Z}_v(\bar{\boldsymbol{r}}, \boldsymbol{\iota})$	The system's total expected cost (in simultaneous release private design) achieved at $\bar{\boldsymbol{r}}$ and $\boldsymbol{\iota}$.
f^{1C}_{1w2w}	The flow of charging at Station 1 under states $(1w, 2w)$.
$J^g_{1C,1w2w}$	Charging cost at Station 1 under states $(1w, 2w)$, dependent on f^{1C}_{1w2w}.
	— Parameters for two-station corridor extension. —
Δ	The fixed mileage gains from charging at each station.
$\delta_1 = l_1 \cdot \int_{\underline{\delta}}^{\bar{\delta}} \delta \cdot u(\delta)\, \mathrm{d}\delta$	The expected range reduction from traveling between the two stations.

C Proof of Theorem 1

To establish the equivalence between Problems (6) and (5), we first demonstrate the equivalence of their objective functions. Plugging the proposed information structure (4) into (5a), we have

the following which equals (6a).

$$\begin{aligned}
&\sum_{w\in\mathbb{W}} \mu_0(w) \int_{r\in\Xi} \left[\pi(C|w,r)\, J_C(f_w|w) + \pi(M|w,r)\, J_M(p(r)|w)\right] g(r)\,\mathrm{d}r \\
&\quad = \sum_{w\in\mathbb{W}} \mu_0(w) \left(\int_{\underline{R}}^{G^{-1}(f_w)} J_C(f_w|w)\, g(r)\,\mathrm{d}r + \int_{G^{-1}(f_w)}^{\bar{R}} J_M(p(r)|w)\, g(r)\,\mathrm{d}r \right) \\
&\quad = \sum_{w\in\mathbb{W}} \mu_0(w) \left(f_w \cdot J_C(f_w|w) + \int_{G^{-1}(f_w)}^{\bar{R}} J_M(p(r)|w)\, g(r)\,\mathrm{d}r \right).
\end{aligned}$$

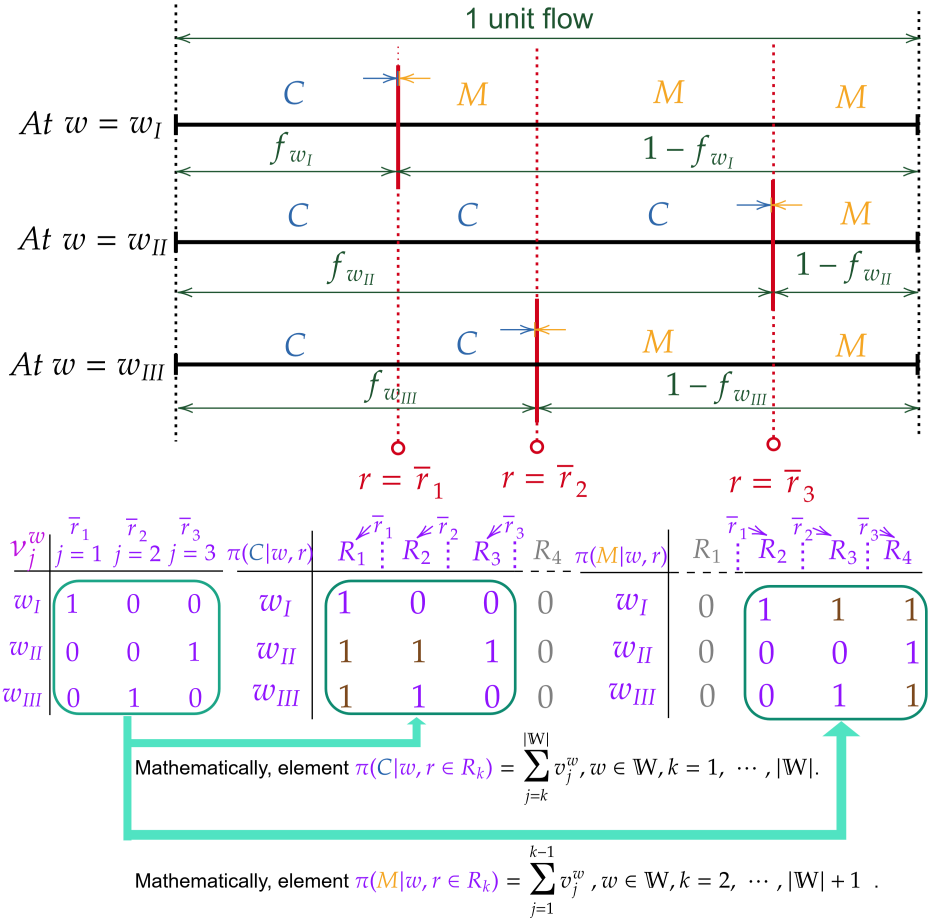

Figure 12: Illustration of the order thresholds and the corresponding information structure.

Recall that the ordered cutoff threshold values are denoted as $\bar{r}_i, i \in 1,\ldots,|\mathbb{W}|$ and a binary variable v_i^w (see (6i)) is used to indicate whether the rank of the cutoff threshold for state w is i (i.e., the i-th smallest among all cutoff thresholds). In Problem (5), Constraint (5d) establishes a one-to-one correspondence between the charging flow f_w and an RRE threshold $\bar{r}_w$ at state w. This relationship is defined in Constraints (6e) using the order indicator variables as $\bar{r}_i = G^{-1}\left(\sum_{w\in\mathbb{W}} v_i^w f_w\right),\ i = 1,\ldots,|\mathbb{W}|$, with the order being enforced in Constraints (6d), i.e., $\sum_{w\in\mathbb{W}} v_i^w f_w \le \sum_{w\in\mathbb{W}} v_{i+1}^w f_w,\ i = 1,\ldots,|\mathbb{W}|-1$.

We next demonstrate the equivalence between the obedience constraints in Problems (6), i.e., Constraints (6f)-(6g), and those in Problem (5), i.e., Constraints (5b)-(5c). The reader is referred

to Figure 12 for illustration. First of all, recall that the RRE of the type k drivers, who receive the same recommendation at each state, falls into $R_k, k = 1, \ldots, |\mathbb{W}|+1$, per the information structure imposed by (4). For any type k driver, only the cost associated with Route M, $J_M(p(r)|w)$ (see (5b)-(5c)), depends on r. Since $p(r)$ is an increasing function of r, and the cost of Route M is a decreasing function of $p(r)$, it suffices to check the compliance with a charging recommendation (Constraint (5b)) for the driver with the highest RRE in R_k (i.e., the upper bound, or $r = \hat{r}_k$), and the compliance with a no-charge recommendation (Constraint (5c)) for the driver with the lowest RRE in R_k (i.e., the lower bound or $r = \hat{r}_{k-1}$). For types 1 and $|\mathbb{W}|+1$, the recommendation is charge and skip, respectively, for all states. Therefore, the obedience to charge can be ensured for everyone in type $k = 1, \ldots, |\mathbb{W}|$ by enforcing the obedience on the driver with $r = \hat{r}_k$, while the obedience to skip can be ensured for all type $k = 2, \ldots, |\mathbb{W}|+1$ drivers by enforcing it on the driver with $r = \hat{r}_{k-1}$.

We proceed to show how the orders of the cutoff thresholds are enforced in the obedience constraints (6f)-(6g). The information structure (4) dictates that, at a given state w, everyone with an $r \leq \bar{r}_w$ is recommended to charge, while others are recommended to skip. This means that $\pi(C \mid w, r \in R_k) = 1$ for any type $k \in [1, l]$ where $\nu_l^w = 1$, and $\pi(M \mid w, r \in R_k) = 1$ for any type $k \in (l, |\mathbb{W}|+1]$ where $\nu_l^w = 1$, see Figure 12. Since $\boldsymbol{\nu}$ is endogenous, we set $\pi(C \mid w, r \in R_k) = \sum_{j=k}^{|\mathbb{W}|} v_j^w, \forall k = 1, \ldots, |\mathbb{W}|$, and $\pi(M \mid w, r \in R_k) = \sum_{j=1}^{k-1} v_j^w, \forall k = 2, \ldots, |\mathbb{W}|+1$.

As a result, by capturing obedience at the cutoff points and replacing the information structure with the elements derived in the "state-interval" matrices, Constraints (5b)-(5c) are transformed into Constraints (6f)-(6g). This process is illustrated in a three-state example in Figure 12. This completes the proof.

D Analytical results and proof for the single-station model

D.1 Analytical results

Assumption 6. *The failure penalty coefficient $\zeta \geq \Delta_t + \beta\mu_0(\mathrm{H})$, which ensures that at least the EV driver with a 100% failure probability chooses Route C based on prior belief.*

D.1.1 Public information design (PBI)

Plugging the cost functions (7) into the BNE condition (3c) and noting $f_s^* \in [0, 1]$, the equilibrium flow corresponding to a public signal s is given by

$$f_s^* = f_s^*(\boldsymbol{\mu}_s) = \max\left(0, \frac{\zeta - \Delta_t - \beta\mu_s(\mathrm{H})}{\alpha + \zeta}\right), \forall s \in \mathbb{S}, \tag{22}$$

where $\mathbb{S} = \mathbb{W}$. Thus, $\pi(s \mid w)$ states the probability of reporting state $s \in \{\mathrm{H}, \mathrm{L}\}$ when the realized state is $w \in \{\mathrm{H}, \mathrm{L}\}$. According to Equation (2), the system's total expected cost can be represented as (see Appendix D.2 for details.)

$$Z(\boldsymbol{f}) = Z(\boldsymbol{\pi}) = \sum_{w \in \mathbb{W}} \mu_0(w) \sum_{s \in \mathbb{W}} \pi(s \mid w) \left[f_s^* \left(\frac{l + \Delta_l}{v} + \alpha f_s^* + \beta\mu_s(\mathrm{H}) \right) + (1 - f_s^*) \frac{l}{v} + 0.5\zeta (1 - f_s^*)^2 \right].$$

The first term within the bracket denotes the total cost associated with charging when the public signal is s, the second term represents the total travel time incurred on Route M, and the third term is the penalty incurred due to running out of power on Route M.

No information (NI) Without any information, i.e., implementing no information policy (NI), EV drivers act on their prior belief, i.e. $\mu_s(w) = \mu_0(w), w \in \mathbb{W}, s = \emptyset$. Thus, per (22), the BNE dictates the charging flow $f_{\emptyset}^{\mathrm{NI}*} = \frac{\zeta - \Delta_t - \beta\mu_0(\mathrm{H})}{\alpha+\zeta}$.

System optimum (SO) If the designer has a coercive power over the EV drivers, he can direct them to achieve a system optimum (SO) charging flow at each state, $f_{\mathrm{H}}^{\mathrm{SO}*}$ and $f_{\mathrm{L}}^{\mathrm{SO}*}$, without relying on persuasion. It is easy to show that, to minimize the expected system cost, the designer should set $f_{\mathrm{H}}^{\mathrm{SO}*} = \max\left(0, \frac{\zeta - \Delta_t - \beta}{2\alpha+\zeta}\right), f_{\mathrm{L}}^{\mathrm{SO}*} = \frac{\zeta - \Delta_t}{2\alpha+\zeta}$. We leave it to the reader to verify that $f_{\emptyset}^{\mathrm{NI}*} \geq f_{\mathrm{H}}^{\mathrm{SO}*}$, which implies that the decision to withhold information from drivers leads to more EV drivers choosing charging when the station is at an abnormal state than what is deemed optimal for the system.

Full information (FI) Under a full information policy (FI), the designer always reveals the true state to all EV drivers, i.e. $\pi(s = \mathrm{H} \mid \mathrm{H}) = 1, \pi(s = \mathrm{H} \mid \mathrm{L}) = 0$. Thus, $\mu_{s=\mathrm{H}}(\mathrm{H}) = 1$ and $\mu_{s=\mathrm{L}}(\mathrm{H}) = 0$. Consequently, we have from (22): $f_{\mathrm{H}}^{\mathrm{FI}*} = \max\left(0, \frac{\zeta - \Delta_t - \beta}{\alpha+\zeta}\right), f_{\mathrm{L}}^{\mathrm{FI}*} = \frac{\zeta - \Delta_t}{\alpha+\zeta}$.

By comparing the solutions, we can show that $f_{\mathrm{H}}^{\mathrm{FI}*} \leq f_{\emptyset}^{\mathrm{NI}*} \leq f_{\mathrm{L}}^{\mathrm{FI}*}$. That is, as expected, providing full information alerts the drivers so that fewer of them would choose to charge in the abnormal state and more would do so in the normal state, compared to the situation when they receive no information. We can also show (details omitted for brevity) that $f_{\mathrm{H}}^{\mathrm{FI}*} \geq f_{\mathrm{H}}^{\mathrm{SO}*}$ and $f_{\mathrm{L}}^{\mathrm{FI}*} \geq f_{\mathrm{L}}^{\mathrm{SO}*}$, which indicates that disclosing full information may not be the best for the system. In the private information design part, we shall show a designer relying on a private information structure can hope to achieve SO in many (if not all) cases.

D.1.2 Private information design (PVI)

We begin by demonstrating that, under our assumptions, the ranking indicator variables $\boldsymbol{\nu}$ in Program (6) are constant — in other words, the cutoff thresholds follow a fixed order.

Lemma 1 (Ranking of cutoff thresholds). *Let $\bar{r}_{\mathrm{H}}^{PVI}$ and $\bar{r}_{\mathrm{L}}^{PVI}$ be the cutoff thresholds for states* H *and* L. *We have $\bar{r}_{\mathrm{H}}^{PVI} \leq \bar{r}_{\mathrm{L}}^{PVI}$.*

Proof. We prove the result by contradiction. Assume that $\bar{r}_{\mathrm{H}}^{\mathrm{PVI}} > \bar{r}_{\mathrm{L}}^{\mathrm{PVI}}$, which implies $f_{\mathrm{H}}^{\mathrm{PVI}} > f_{\mathrm{L}}^{\mathrm{PVI}}$. It follows that there must exist a driver who would receive a recommendation to skip charging in state H but to charge in state L. Let the driver's RRE be r, their obedience constraints read

$$\mu_0(\mathrm{H})\left[J_C(f_{\mathrm{H}}^{\mathrm{PVI}}|\mathrm{H}) - J_M(p(r)|\mathrm{H})\right] \leq 0, \qquad \mu_0(\mathrm{L})\left[J_C(f_{\mathrm{L}}^{\mathrm{PVI}}|\mathrm{L}) - J_M(p(r)|\mathrm{L})\right] \geq 0.$$

Since $J_M(p(r)|\mathrm{H}) = J_M(p(r)|\mathrm{L})$, the above constraints lead to $J_C(f_{\mathrm{H}}^{\mathrm{PVI}}|\mathrm{H}) \leq J_C(f_{\mathrm{L}}^{\mathrm{PVI}}|\mathrm{L})$, or (plugging the cost function) $\alpha f_{\mathrm{H}} + \beta \leq \alpha f_{\mathrm{L}}$, a contradiction with $f_{\mathrm{H}}^{\mathrm{PVI}} > f_{\mathrm{L}}^{\mathrm{PVI}}$ since $\alpha, \beta \geq 0$. □

Thus, there is no need to introduce the ranking indicator $\boldsymbol{\nu}$ in this simplified setting. Accordingly, the two cutoff thresholds divide Ξ into three intervals, as identified by R_1, R_2, and R_3 in Figure 3. This allows us to write the information structure:

$$\begin{aligned}
&\pi(C|\mathrm{H}, r \in R_1) = 1, \quad \pi(C|\mathrm{L}, r \in R_1) = 1, \quad \pi(M|\mathrm{H}, r \in R_1) = 0, \quad \pi(M|\mathrm{L}, r \in R_1) = 0;\\
&\pi(C|\mathrm{H}, r \in R_2) = 0, \quad \pi(C|\mathrm{L}, r \in R_2) = 1, \quad \pi(M|\mathrm{H}, r \in R_2) = 1, \quad \pi(M|\mathrm{L}, r \in R_2) = 0;\\
&\pi(C|\mathrm{H}, r \in R_3) = 0, \quad \pi(C|\mathrm{L}, r \in R_3) = 0, \quad \pi(M|\mathrm{H}, r \in R_3) = 1, \quad \pi(M|\mathrm{L}, r \in R_3) = 1.
\end{aligned}$$

Specifically, EV drivers with $r \in R_1$ are always recommended to take Route C, and those with $r \in R_3$ are always recommended to take Route M. For drivers with $r \in R_2$, the recommendation is Route M when $w = \mathrm{H}$ and Route C when $w = \mathrm{L}$. This approach is equivalent to revealing true information for drivers in R_2, while withholding information from drivers in R_1 and R_3. Without the ranking indicator, the private information design problem can be simplified as:

$$\min\ Z\left(f_{\mathrm{H}}^{\mathrm{PVI}}, f_{\mathrm{L}}^{\mathrm{PVI}}\right) = \mu_0(\mathrm{H})\left(f_{\mathrm{H}}^{\mathrm{PVI}}\left(\frac{l+\Delta_l}{v} + \alpha f_{\mathrm{H}}^{\mathrm{PVI}} + \beta\right) + \left(1 - f_{\mathrm{H}}^{\mathrm{PVI}}\right)\frac{l}{v} + 0.5\zeta(1 - f_{\mathrm{H}}^{\mathrm{PVI}})^2\right)$$
$$+ \mu_0(\mathrm{L})\left(f_{\mathrm{L}}^{\mathrm{PVI}}\left(\frac{l+\Delta_l}{v} + \alpha f_{\mathrm{L}}^{\mathrm{PVI}}\right) + \left(1 - f_{\mathrm{L}}^{\mathrm{PVI}}\right)\frac{l}{v} + 0.5\zeta(1 - f_{\mathrm{L}}^{\mathrm{PVI}})^2\right) \tag{23a}$$

subject to:

$$\mu_0(\mathrm{H})\left[\Delta_t - \zeta\left(1 - f_{\mathrm{H}}^{\mathrm{PVI}}\right) + \left(\alpha f_{\mathrm{H}}^{\mathrm{PVI}} + \beta\right)\right] + \mu_0(\mathrm{L})\left[\Delta_t - \zeta\left(1 - f_{\mathrm{H}}^{\mathrm{PVI}}\right) + \left(\alpha f_{\mathrm{L}}^{\mathrm{PVI}}\right)\right] \le 0, \tag{23b}$$

$$\mu_0(\mathrm{L})\left[\Delta_t - \zeta\left(1 - f_{\mathrm{L}}^{\mathrm{PVI}}\right) + \left(\alpha f_{\mathrm{L}}^{\mathrm{PVI}}\right)\right] \le 0, \tag{23c}$$

$$\mu_0(\mathrm{H})\left[-\Delta_t + \zeta\left(1 - f_{\mathrm{H}}^{\mathrm{PVI}}\right) - \left(\alpha f_{\mathrm{H}}^{\mathrm{PVI}} + \beta\right)\right] \le 0, \tag{23d}$$

$$\mu_0(\mathrm{H})\left[-\Delta_t + \zeta\left(1 - f_{\mathrm{H}}^{\mathrm{PVI}}\right) - \left(\alpha f_{\mathrm{H}}^{\mathrm{PVI}} + \beta\right)\right] + \mu_0(\mathrm{L})\left[-\Delta_t + \zeta\left(1 - f_{\mathrm{L}}^{\mathrm{PVI}}\right) - \left(\alpha f_{\mathrm{L}}^{\mathrm{PVI}}\right)\right] \le 0, \tag{23e}$$

$$f_{\mathrm{H}}^{\mathrm{PVI}}, f_{\mathrm{L}}^{\mathrm{PVI}} \in [0,1]\,. \tag{23f}$$

Problem (23) is a convex optimization problem with linear constraints. Constraints (23b) - (23e) each represent a half space in $\mathbb{R}^2$. For convenience, let b_1, b_2, b_3 and b_4 denote the hyperplane bounding the half space for, respectively, Constraints (23b), (23c), (23d), and (23e). The next result characterizes the feasible set.

Lemma 2. *The set bounded by $b_i, i = 1,2,3,4$ (see Figure 13(a)), referred to as the obedience-compliant region, is a quadrilateral in $\mathbb{R}^2$, with a right angle at the top left corner, a right or obtuse angle at the lower left and upper right corners, and a right or acute angle at the lower right corner. Moreover,*

1. *The hyperplane b_2 is a horizontal line and b_3 is a vertical line. They intersect at $\left(\frac{\zeta-\Delta_t-\beta}{\alpha+\zeta}, \frac{\zeta-\Delta_t}{\alpha+\zeta}\right)$, marked as A in Figure 13(a). When $\zeta \ge \Delta_t + \beta$, point A corresponds to the solution under the FI policy.*
2. *The hyperplanes b_1 and b_4 both have non-positive slopes. In terms of absolute values, the slope and intercept of b_1 are greater than or equal to those of b_4. Also, b_1 and b_4 intersect at $\left(\frac{\zeta-\Delta_t-\beta\mu_0(\mathrm{H})}{\alpha+\zeta}, \frac{\zeta-\Delta_t-\beta\mu_0(\mathrm{H})}{\alpha+\zeta}\right)$, marked as B in Figure 13(a). Point B corresponds to the NI policy.*

Proof. See Appendix D.4 for details. □

With Lemma 2, Problem (23) can be solved analytically by enumerating all possible realizations of the feasible set. Because the solution process is tedious, we report it in Appendix D.5 as Theorem 2. A key driver behind the analysis is the magnitude of ζ, the coefficient of failure on Route M, relative to the sum of Δ_t and β, the extra marginal cost on Route C when the state is abnormal (H). If $\zeta \ge \Delta_t + \beta$ — i.e., the driver with a 100% failure probability prefers Route C to Route M even when the state is always abnormal — Constraints (23f) is never activated even

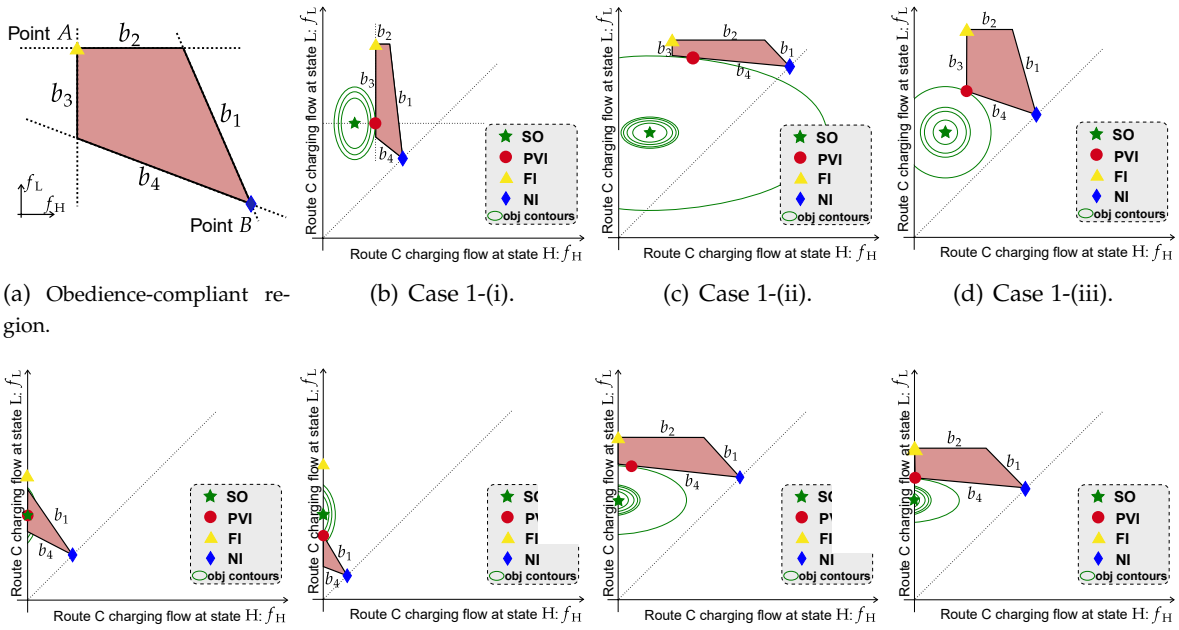

(a) Obedience-compliant region.

(b) Case 1-(i).

(c) Case 1-(ii).

(d) Case 1-(iii).

(e) Case 2-(i).

(f) Case 2-(ii).

(g) Case 2-(iii).

(h) Case 2-(iv).

Figure 13: (a) Obedience-compliant region in private information design (x-axis represents f_{H} and y-axis represents f_{L}). (b)-(d): three cases of optimal solutions when $\zeta \geq \Delta_t + \beta$; (e)-(h): four possible cases of optimal solutions when $\zeta < \Delta_t + \beta$.

with full information. As a result, the feasible set may manifest as one of three cases shown in Figure 13(b)-13(d).

1-(i): When $\mu_0(\mathrm{H}) \geq \frac{\alpha(\alpha+\zeta)(\zeta-\Delta_t)}{\alpha^2(\zeta-\Delta_t)+\beta\zeta(2\alpha+\zeta)}$, the optimal private design occurs on the boundary defined by b_3, giving $\left(f_{\mathrm{H}}^{\mathrm{FI}*}, f_{\mathrm{L}}^{\mathrm{SO}*}\right)$ as the optimal charging flows.

1-(ii) and 1-(iii): Otherwise, the optimal private design either occurs on the boundary defined by b_4, or at the intersection of boundaries defined by b_3 and b_4.

Note that, since $f_{\mathrm{H}}^{\mathrm{FI}*} \geq f_{\mathrm{H}}^{\mathrm{SO}*}$ and $f_{\mathrm{L}}^{\mathrm{FI}*} \geq f_{\mathrm{L}}^{\mathrm{SO}*}$, i.e., the point corresponding to FI policy (the yellow triangle) must lie above and to the right of the SO point (the green star), the optimal solution can never occur on either boundary b_1 or boundary b_2.

If the failure coefficient is not large enough to meet the above condition, the obedience-compliant region will be cut by $f_{\mathrm{H}}^{\mathrm{PVI}} \geq 0$ — in other words, no one should be directed to charging in the abnormal state because of the relatively low failure coefficient. This condition leads to one of the four cases visualized in Figure 13(e)-13(h).

2-(i): SO lies in the obedience-complaint region, thus the private information design coincides with SO solution.

2-(ii): SO lies outside the obedience-complaint region and the optimal private design occurs on the boundary defined by b_1. In this case, the optimal private design may be worse than the FI policy.

2-(iii) and (iv): SO lies outside the obedience-complaint region and the optimal private design is achieved on boundary defined by b_4 with $f_{\mathrm{H}}^{\mathrm{PVI}} > 0$ and $f_{\mathrm{H}}^{\mathrm{PVI}} = 0$, respectively.

D.2 Derivation for public information design

The total expected system cost, as defined in (2), is:

$$Z(\boldsymbol{\mu}) = \sum_{s\in\mathbb{S}} \tau_s \mathbb{E}_{w\sim\boldsymbol{\mu}_s}\left(-v(a^*(\boldsymbol{\mu}_s), w)\right) = \sum_{s\in\mathbb{S}} \tau_s \sum_{w\in\mathbb{W}} \mu_s(w)\left(f_s^*\cdot J_C(f_s^*|w) + \int_{G^{-1}(f_s^*)}^{\bar{R}} J_M(p(r)|w)g(r)\,\mathrm{d}r\right)$$
$$= \sum_{w\in\mathbb{W}}\sum_{s\in\mathbb{S}} \mu_0(w)\pi(s\mid w)\left(f_s^*\cdot J_C(f_s^*|w) + \int_{G^{-1}(f_s^*)}^{\bar{R}} J_M(p(r)|w)g(r)\,\mathrm{d}r\right),$$

where $\tau_s = \sum_{w'\in\mathbb{W}} \mu_0(w')\pi(s\mid w')$ is the probability of receiving signal s given the information structure $\boldsymbol{\pi}$. The last equality holds by substituting the definition of the posterior belief $\mu_s(w)$, in which the denominator is τ_s. Specifically,

$$Z(\boldsymbol{\pi}) = \sum_{w\in\mathbb{W}} \mu_0(w)\sum_{s\in\mathbb{W}} \pi(s\mid w)\left[f_s^*\cdot J_C(f_s^*|w) + \int_{G^{-1}(f_s^*)}^{\bar{R}} J_M(p(r)|w)g(r)\,\mathrm{d}r\right]$$
$$= \sum_{w\in\mathbb{W}} \mu_0(w)\sum_{s\in\mathbb{W}} \pi(s|w)\left[f_s^*\cdot\left(\frac{l+\Delta_l}{v}+\alpha f_s^*\right) + (1-f_s^*)\frac{l}{v} + \int_{G^{-1}(f_s^*)}^{\bar{R}} \zeta\left(1-p\left(r\right)\right)g(r)\,\mathrm{d}r\right] + \sum_{s\in\mathbb{W}} \mu_0(\mathrm{H})\pi(s\mid \mathrm{H})\cdot f_s^*\cdot\beta$$
$$= \sum_{w\in\mathbb{W}} \mu_0(w)\sum_{s\in\mathbb{W}} \pi(s\mid w)\left[f_s^*\cdot\left(\frac{l+\Delta_l}{v}+\alpha f_s^*+\beta\mu_s(\mathrm{H})\right) + (1-f_s^*)\frac{l}{v} + 0.5\zeta\left(1-f_s^*\right)^2\right],$$

where the last equation holds because

$$\sum_{s\in\mathbb{W}} \mu_0(\mathrm{H})\pi(s\mid \mathrm{H})\cdot f_s^*\cdot\beta = \sum_{s\in\mathbb{W}}\sum_{w\in\mathbb{W}} \mu_0(w)\pi(s\mid w)\frac{\mu_0(\mathrm{H})\pi(s\mid \mathrm{H})}{\sum_{w'\in\mathbb{W}}\mu_0(w')\pi(s\mid w')}\cdot f_s^*\cdot\beta$$
$$= \sum_{w\in\mathbb{W}} \mu_0(w)\sum_{s\in\mathbb{W}} \pi(s\mid w)\frac{\mu_0(\mathrm{H})\pi(s\mid \mathrm{H})}{\sum_{w'\in\mathbb{W}}\mu_0(w')\pi(s\mid w')}\cdot f_s^*\cdot\beta = \sum_{w\in\mathbb{W}} \mu_0(w)\sum_{s\in\mathbb{W}} \pi(s\mid w)\cdot\mu_s(\mathrm{H})\cdot f_s^*\cdot\beta,$$

and

$$\int_{G^{-1}(f_s^*)}^{\bar{R}} \zeta\left(1-p\left(r\right)\right)g(r)\,\mathrm{d}r = \frac{\zeta}{(n-1)l}\int_{G^{-1}(f_s^*)}^{\bar{R}} (nl-r)g(r)\,\mathrm{d}r = \frac{\zeta}{(n-1)l}\left[nl(1-f_s^*) - \int_{G^{-1}(f_s^*)}^{\bar{R}} rg(r)\,\mathrm{d}r\right]$$
$$= \frac{\zeta(n(1-f_s^*))}{n-1} - \frac{\zeta\int_{G^{-1}(f_s^*)}^{nl} r\mathrm{d}r}{(n-1)^2l^2} = \frac{\zeta(n(1-f_s^*))}{n-1} - \frac{\zeta(n^2l^2-(l+(n-1)lf_s^*)^2)}{2(n-1)^2l^2} \overset{n=2}{=} 0.5\zeta\left(1-f_s^*\right)^2.$$

D.3 Proof of Proposition 1

Our proof builds on the Bayesian persuasion framework proposed by Kamenica and Gentzkow (2011). We first briefly introduce the concavification method we used for proof. In Corollary 1 of Kamenica and Gentzkow (2011), the designer's problem is formulated as

$$\max_{\boldsymbol{\tau}} \sum_{s\in\mathbb{S}} \tau_s\hat{v}(\boldsymbol{\mu}_s) \quad \text{subject to:} \sum_{s\in\mathbb{S}} \tau_s\mu_s(w) = \mu_0(w), \forall w\in\mathbb{W}, \tag{24a}$$
$$\text{where } \tau_s = \sum_{w'\in\mathbb{W}} \mu_0(w')\pi(s\mid w'), s\in\mathbb{S};\ \hat{v}(\boldsymbol{\mu}_s) = \mathbb{E}_{w\sim\boldsymbol{\mu}_s}\left(v(a^*(\boldsymbol{\mu}_s), w)\right). \tag{24b}$$

Problem (24) has a geometric interpretation if $|\mathbb{W}|\le 3$. When $|\mathbb{W}| = 2$, only one of the two world states, call it w_1, is needed to specify the design objective, as visualized by the $\mu_s(w_1) - \hat{v}(\mu_s(w_1))$ plot in Figure 14. In the plot, the thick black line illustrates $\hat{v}(\mu_s(w_1))$ for a given s. Since the objective of the designer problem is the linear combination of $\hat{v}(\mu_s(w_1)), \forall s$, the decision problem is translated to maximizing that linear combination while ensuring the same

linear combination of $\mu_s(w_1), \forall s$ is Bayesian plausible, i.e., the post and prior beliefs match each other.

Suppose the signal set $S = \{s_1, s_2\}$, then an information structure $\boldsymbol{\pi}$ maps w_1 to $\mu_{s_i}(w_1), i = 1, 2$. The line segment connecting $\hat{v}(\mu_{s_1}(w_1))$ and $\hat{v}(\mu_{s_2}(w_1))$ (visualized as the dotted red line in Figure 14) thus represents the designer's objective function corresponding to all possible choices of τ_{s_1} and τ_{s_2} with $\tau_{s_1} + \tau_{s_2} = 1$. Bayesian plausibility implies that τ_{s_i} must be selected to reach point A, the intersection between that line segment and the dashed vertical line denoting $\mu_0(w_1)$, i.e. $\sum_{i=1}^{2} \tau_{s_i} \mu_{s_i}(w_1) = \mu_0(w_1)$. When $\boldsymbol{\pi}$ contains no useful information, $\mu_{s_i}(w_1) = \mu_0(w_1), \forall i.$, i.e., the posterior beliefs equals the prior belief. Thus, the intersection between the dashed vertical line and the thick black curve, denoted as point B, gives the designer's objective function value without information. Accordingly, the vertical distance between A and B represents the value of information for $\boldsymbol{\pi}$.

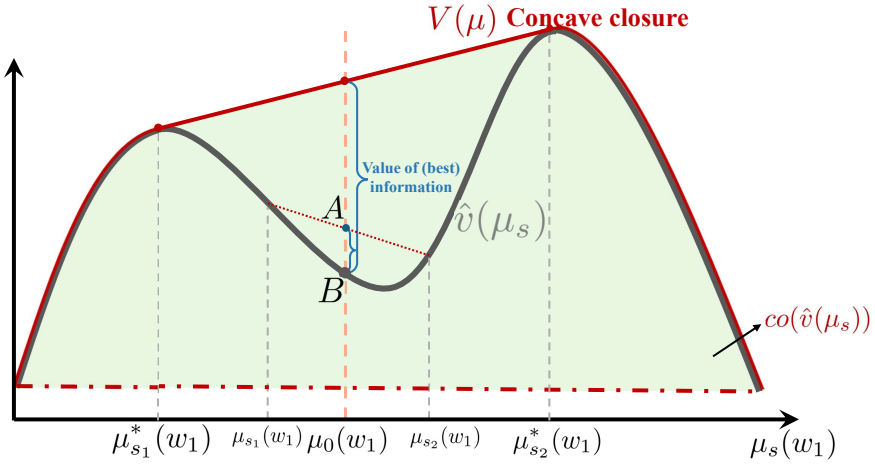

Figure 14: Illustration of the concavification method Kamenica and Gentzkow (2011).

In general, the set of all possible objective values is $\{z|(\mu_0, z) \in co(\hat{v}(\boldsymbol{\mu}_s))\}$, where $co(\hat{v}(\boldsymbol{\mu}_s))$ is the convex hull of the graph $\hat{v}(\boldsymbol{\mu}_s)$, highlighted as the green shaded area in Figure 14. Clearly, z is maximized on the *concave closure* of $\hat{v}(\mu_s(w_1))$, defined as $V(\mu_s(w_1)) \equiv \sup\{z|(\mu_s(w_1), z) \in co(\hat{v}(\boldsymbol{\mu}_s))\}$, which gives the maximum objective function value the designer can achieve for any $\mu_0(w_1)$ and $\boldsymbol{\pi}$. For a given $\mu_0(w_1)$, the optimal value of information is $(V(\boldsymbol{\mu}_0) - \hat{v}(\boldsymbol{\mu}_0))$. Thus, Bayesian persuasion benefits the designer if and only if $V(\boldsymbol{\mu}_0) > \hat{v}(\boldsymbol{\mu}_0)$.

We next apply the analysis to our problem. From (2), the expected persuasion utility for sending s is

$$\begin{aligned}\hat{v}(\boldsymbol{\mu}_s) = \mathbb{E}_{w\sim\boldsymbol{\mu}_s}\left(v(a^*(\boldsymbol{\mu}_s), w)\right) &= -\sum_{w\in\mathbb{W}} \mu_s(w)\left[f_s^* \cdot J_C(f_s^*|w) + \int_{G^{-1}(f_s^*)}^{\bar{R}} J_M(p(r)|w)g(r)\,\mathrm{d}r\right] \\ &= -\left(f_s^*\left(\frac{l+\Delta_l}{v} + \alpha f_s^* + \beta\mu_s(\mathrm{H})\right) + (1-f_s^*)\frac{l}{v} + 0.5\zeta\,(1-f_s^*)^2\right).\end{aligned}$$

Thus, $\hat{v}(\boldsymbol{\mu}_s)$ is expressed as a function of $\mu_s(\mathrm{H})$. When $f_s^* \in (0,1)$, the second order derivative is positive:

$$\frac{\partial^2 \hat{v}(\boldsymbol{\mu}_s)}{\partial\left(\mu_s(\mathrm{H})\right)^2} = \left[(2\alpha+\zeta)\left(\frac{-\beta}{\alpha+\zeta}\right)+\beta\right]\left(\frac{\beta}{\alpha+\zeta}\right) + \frac{\beta^2}{\alpha+\zeta} = \frac{\beta^2}{\alpha+\zeta}\left(2 - \frac{2\alpha+\zeta}{\alpha+\zeta}\right) > 0. \tag{25}$$

Considering the corner solutions (see Equation (22)), we analyze the following three cases separately: (i) $f_s^* = 0$ for any $\mu_s(\mathrm{H}) \in [0,1]$; (ii) $f_s^* > 0$ when $\mu_s(\mathrm{H}) = 0$, and $f_s^* = 0$ when $\mu_s(\mathrm{H}) = 1$; (iii) $f_s^* > 0$ for any $\mu_s(\mathrm{H}) \in [0,1]$. From (22), we know that $f_s^*(\mu_s(\mathrm{H}) = 0) \geq f_s^*(\mu_s(\mathrm{H}) = 1)$, and f_s^* linearly decreases with $\mu_s(\mathrm{H})$ until reaching 0. Therefore, we can easily rule out the case where $f_s^* = 0$ when $\mu_s(\mathrm{H}) = 0$, but $f_s^* > 0$ when $\mu_s(\mathrm{H}) = 1$. Similarly, it is impossible to have $f_s^* = 1$ for all $\mu_s(\mathrm{H})$, since under our assumptions, there are always EV drivers choosing to skip charging.

In Case (i), $\hat{v}(\boldsymbol{\mu}_s)$ does not change with $\mu_s(\mathrm{H})$, the convex hull is reduced to a line, suggesting the value of information is always 0, see Figure 15(a). In Case (ii), $\hat{v}(\boldsymbol{\mu}_s)$ monotonically decreases with $\mu_s(\mathrm{H})$ until it reaches the point after which $f_s^* = 0$ and $\hat{v}(\boldsymbol{\mu}_s)$ remains constant. Until that point (i.e., $f_s^* > 0$), the function is strictly convex per (25), see Figure 15(b). In Case (iii), the function $\hat{v}(\boldsymbol{\mu}_s)$ is always strictly decreasing and convex, see Figure 15(c). In Cases (ii) and (iii), thanks to the convexity of $\hat{v}(\boldsymbol{\mu}_s)$, the value of information, given by the distance between the function $\hat{v}(\boldsymbol{\mu}_s)$ (the purple solid line) and the concave closure (the red dash line for prior $\mu_0(\mathrm{H})$, is always positive. It is easy to see that, in all three cases, the concave closure is the line segment connecting $\hat{v}(\mu_{s=\mathrm{L}}(\mathrm{H}) = 0)$ and $\hat{v}(\mu_{s=\mathrm{H}}(\mathrm{H}) = 1)$. In other words, the optimal information structure $\boldsymbol{\pi}^*$ must render a posterior belief such that for $w = \mathrm{H}$, $\mu_{\mathrm{L}}(\mathrm{H}) = 0$ and $\mu_{\mathrm{H}}(\mathrm{H}) = 1$. This means $\boldsymbol{\pi}^*$ effectively equals the full revelation. This completes the proof.

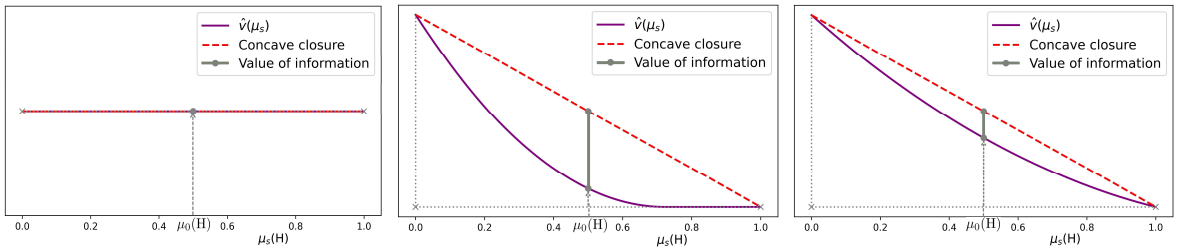

(a) Case (i). (b) Case (ii). (c) Case (iii).

Figure 15: Illustration of concave closure and value of information for public information design.

D.4 Proof of Lemma 2

Proof. We first note that the slope of a hyperplane in $\mathbb{R}^2$ is the negative ratio of the coefficient of the x-coordinate (f_{H} in our case) to that of y-coordinate (f_{L} in our case) in the corresponding constraint. From (23c), b_2 has a slope of 0 (hence it manifests as a horizontal line), while (23d) shows b_3 must be a vertical line. Moreover, the feasible region lies below b_2 and to the right of b_3. Point A, which is where b_2 and b_3 intersect, is given by $\mu_0(\mathrm{L})[\Delta_t - \zeta(1 - f_{\mathrm{L}}) + (\alpha f_{\mathrm{L}})] = 0 \Rightarrow f_{\mathrm{L}}^A = \frac{\zeta - \Delta_t}{\alpha + \zeta}$, $\mu_0(\mathrm{H})[-\Delta_t + \zeta(1 - f_{\mathrm{H}}) - (\alpha f_{\mathrm{H}} + \beta)] = 0 \Rightarrow f_{\mathrm{H}}^A = \frac{\zeta - \Delta_t - \beta}{\alpha + \zeta}$. This proves the first statement.

For the second statement, note that b_1 can be rearranged into $(\alpha\mu_0(\mathrm{H}) + \zeta) f_{\mathrm{H}}^{\mathrm{PVI}} + \alpha\mu_0(\mathrm{L}) f_{\mathrm{L}}^{\mathrm{PVI}} + (\Delta_t - \zeta + \beta\mu_0(\mathrm{H})) = 0$, with a slope $k_1 \equiv -\frac{\alpha\mu_0(\mathrm{H}) + \zeta}{\alpha\mu_0(\mathrm{L})} \leq 0$. Similarly, b_4 is arranged into $-\alpha\mu_0(\mathrm{H}) f_{\mathrm{H}}^{\mathrm{PVI}} + (\alpha\mu_0(\mathrm{L}) + \zeta) f_{\mathrm{L}}^{\mathrm{PVI}} - (\Delta_t - \zeta + \beta\mu_0(\mathrm{H})) = 0$ with a slope $k_4 \equiv -\frac{\alpha\mu_0(\mathrm{H})}{\alpha\mu_0(\mathrm{L}) + \zeta} \leq 0$. The difference in the absolute value of the slopes of b_1 and b_4 is $|k_1| - |k_4| = \frac{\zeta(\alpha + \zeta)}{\alpha\mu_0(\mathrm{L})(\alpha\mu_0(\mathrm{L}) + \zeta)} \geq 0$. The feasible region lies below and to the left of b_1, and above and to the right of b_4. By solving the above two

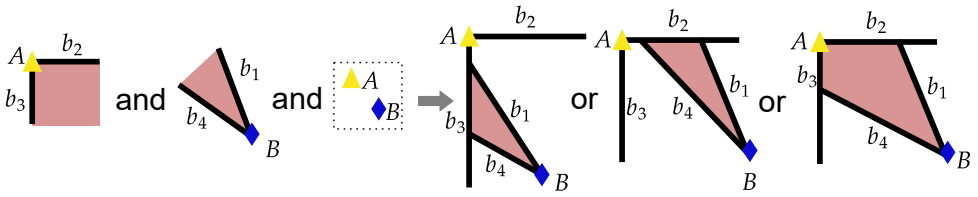

Figure 16: Geometric illustration for the proof of Lemma 2.

equations simultaneously, we find the intersection of b_1 and b_2 as $f_{\mathrm{H}}^B = f_{\mathrm{L}}^B = \frac{\zeta - \Delta_t - \beta\mu_0(\mathrm{H})}{\alpha+\zeta}$ which is the same as the NI policy. Since $f_{\mathrm{H}}^A - f_{\mathrm{H}}^B = \frac{-\beta\mu_0(\mathrm{L})}{\alpha+\zeta} \leq 0$ and $f_{\mathrm{L}}^A - f_{\mathrm{L}}^B = \frac{\beta\mu_0(\mathrm{H})}{\alpha+\zeta} \geq 0$, we know point A is to the upper left of point B.

Combining the above properties implies three possible shapes for the feasible region, as enumerated in Figure 16. To ensure the shape is a quadrilateral as depicted in the lemma (rather than the triangles shown in the figure), we only need to prove that the absolute value of the slope of the line connecting points A and B, which equals $|k_{AB}| \equiv \left|\frac{f_{\mathrm{L}}^B - f_{\mathrm{L}}^A}{f_{\mathrm{H}}^B - f_{\mathrm{H}}^A}\right| = \frac{\mu_0(\mathrm{H})}{\mu_0(\mathrm{L})}$, satisfies $|k_4| \leq |k_{AB}| \leq |k_1|$. This is indeed the case because $|k_{AB}|/|k_4| = \frac{\alpha\mu_0(\mathrm{L})+\zeta}{\alpha\mu_0(\mathrm{L})} \geq 1$ and $|k_1|/|k_{AB}| = \frac{\alpha\mu_0(\mathrm{H})+\zeta}{\alpha\mu_0(\mathrm{H})} \geq 1$. This completes the proof. □

D.5 Optimal private information design

For notational convenience, we introduce the following constants.

$$\Lambda \equiv \left(\zeta - \Delta_t - \beta\mu_0(\mathrm{H}) + \frac{\alpha\mu_0(\mathrm{H})(\Delta_t - \zeta + \beta)}{2\alpha+\zeta} + \frac{(\alpha\mu_0(\mathrm{L}) + \zeta)(\Delta_t - \zeta)}{2\alpha+\zeta}\right)\left(\frac{\mu_0(\mathrm{L})(2\alpha+\zeta)}{\alpha^2\mu_0(\mathrm{H})\mu_0(\mathrm{L}) + (\alpha\mu_0(\mathrm{L}) + \zeta)^2}\right) > 0,$$

$$\tilde{\mu_0} \equiv \frac{\alpha(\alpha+\zeta)(\zeta-\Delta_t)}{\alpha^2(\zeta-\Delta_t) + \beta\zeta(2\alpha+\zeta)}, \quad \underline{\mu_0} \equiv \frac{\alpha(\zeta-\Delta_t)}{-\alpha(\zeta-\Delta_t) + \beta(2\alpha+\zeta)}, \quad \overline{\mu_0} \equiv \frac{(\alpha+\zeta)(\zeta-\Delta_t)}{-\alpha(\zeta-\Delta_t) + \beta(2\alpha+\zeta)}, \quad \Omega \equiv \frac{\Lambda\alpha + (\zeta - \Delta_t - \beta)}{2\alpha+\zeta}.$$

Theorem 2. *The optimal solution of (23) can be described as follows.*

1. *When $\zeta \geq \Delta_t + \beta$, the optimal solution is achieved in one of the following ways:*

   1-(i) When $\mu_0(\mathrm{H}) \geq \tilde{\mu_0}$, we have $\left(f_{\mathrm{H}}^{PVI*}, f_{\mathrm{L}}^{PVI*}\right) = \left(\frac{\zeta-\Delta_t-\beta}{\alpha+\zeta}, \frac{\zeta-\Delta_t}{2\alpha+\zeta}\right)$, and $f_{\mathrm{H}}^{SO*} \leq f_{\mathrm{H}}^{PVI*} = f_{\mathrm{H}}^{FI*}$, and $f_{\mathrm{L}}^{PVI*} = f_{\mathrm{L}}^{SO*} \leq f_{\mathrm{L}}^{FI*}$.

   1-(ii) When $\mu_0(\mathrm{H}) < \tilde{\mu_0}$ and $\Omega > f_{\mathrm{H}}^{FI*} = \frac{\zeta-\Delta_t-\beta}{\alpha+\zeta}$, we have $\left(f_{\mathrm{H}}^{PVI*}, f_{\mathrm{L}}^{PVI*}\right) = \left(\Omega, \Omega + \frac{\beta}{2\alpha+\zeta} + \frac{\Lambda\zeta}{\mu_0(\mathrm{L})(2\alpha+\zeta)}\right)$, and $f_{\mathrm{H}}^{PVI*} \geq f_{\mathrm{H}}^{SO*}$, and $f_{\mathrm{L}}^{PVI*} \geq f_{\mathrm{L}}^{SO*}$.

   1-(iii) When $\mu_0(\mathrm{H}) < \tilde{\mu_0}$ and $\Omega \leq f_{\mathrm{H}}^{FI*} = \frac{\zeta-\Delta_t-\beta}{\alpha+\zeta}$, we have $\left(f_{\mathrm{H}}^{PVI*}, f_{\mathrm{L}}^{PVI*}\right) = \left(\frac{\zeta-\Delta_t-\beta}{\alpha+\zeta}, \frac{\zeta-\Delta_t-\beta\mu_0(\mathrm{H})-\alpha\mu_0(\mathrm{H})f_{\mathrm{H}}^{PVI*}}{\alpha\mu_0(\mathrm{L})+\zeta}\right)$.

2. *When $\zeta < \Delta_t + \beta$, the feasible region is cut by $f_{\mathrm{H}}^{PVI} \geq 0$ in (23f). Accordingly, the optimal solution is achieved in one of the following ways.*

   2-(i) When $\underline{\mu_0} \leq \mu_0(\mathrm{H}) \leq \overline{\mu_0}$, we have $\left(f_{\mathrm{H}}^{PVI*}, f_{\mathrm{L}}^{PVI*}\right) = \left(f_{\mathrm{H}}^{SO*}, f_{\mathrm{L}}^{SO*}\right) = \left(0, \max\left(0, \frac{\zeta-\Delta_t}{2\alpha+\zeta}\right)\right)$.

   2-(ii) When $\mu_0(\mathrm{H}) > \overline{\mu_0}$, we have $\left(f_{\mathrm{H}}^{PVI*}, f_{\mathrm{L}}^{PVI*}\right) = \left(0, \frac{\zeta-\Delta_t-\beta\mu_0(\mathrm{H})}{\alpha\mu_0(\mathrm{L})}\right)$, and $f_{\mathrm{H}}^{PVI*} = f_{\mathrm{H}}^{SO*} = f_{\mathrm{H}}^{FI*} = 0$, and $f_{\emptyset}^{NI*} \leq f_{\mathrm{L}}^{PVI*} \leq f_{\mathrm{L}}^{SO*} \leq f_{\mathrm{L}}^{FI*}$.

2-(iii) When $\mu_0(\mathrm{H}) < \underline{\mu_0}$ and $\Omega \geq 0$, the solution is the same as in 1-(ii).

2-(iv) When $\mu_0(\mathrm{H}) < \underline{\mu_0}$ and $\Omega < 0$, we have $\left(f_{\mathrm{H}}^{PVI*}, f_{\mathrm{L}}^{PVI*}\right) = \left(0, \frac{\zeta - \Delta_t - \beta\mu_0(\mathrm{H})}{\alpha\mu_0(\mathrm{L}) + \zeta}\right)$.

Proof. Let $\lambda_i, i = 1, \ldots, 4$ be the Lagrangian multiplier for Constraints (23b)-(23e), respectively. Based on the shape of the compliant region and the assumption that $\zeta - \Delta_t - \beta\mu_0(\mathrm{H}) \geq 0$, point B must lie on the line segment $f_{\mathrm{H}} = f_{\mathrm{L}}$, where $f_{\mathrm{L}} \in [0, 1]$. To determine whether the compliant region is within $[0, 1] \times [0, 1]$, it is sufficient to check whether $f_{\mathrm{H}}^{A} \geq 0$. This requirement leads to the condition $\zeta \geq \Delta_t + \beta$.

1. When $\zeta \geq \Delta_t + \beta$, from $f_{\mathrm{H}}^{\mathrm{FI}*} \geq f_{\mathrm{H}}^{\mathrm{SO}*}$ and $f_{\mathrm{L}}^{\mathrm{FI}*} \geq f_{\mathrm{L}}^{\mathrm{SO}*}$, we know the SO solution cannot locate inside the compliant region, and either Constraint (23d), or Constraint (23e), or both may be be binding.

   1-(i) When only Constraint (23d) is binding, i.e. $\mu_0(\mathrm{H})\left[\zeta - \Delta_t - \beta - (\alpha + \zeta) f_{\mathrm{H}}^{\mathrm{PVI}*}\right] = 0$, we have $f_{\mathrm{H}}^{\mathrm{PVI}*} = \frac{\zeta - \Delta_t - \beta}{\alpha + \zeta}$. Applying the KKT condition leads to $\mu_0(\mathrm{L})\left[\Delta_t - \zeta + (2\alpha + \zeta) f_{\mathrm{L}}^{\mathrm{PVI}*}\right] + \lambda_3 \cdot 0 = 0$, which gives $f_{\mathrm{L}}^{\mathrm{PVI}*} = \frac{\zeta - \Delta_t}{2\alpha + \zeta}$. It is straightforward to verify that $f_{\mathrm{H}}^{\mathrm{PVI}*} = f_{\mathrm{H}}^{\mathrm{FI}*}$ and $f_{\mathrm{L}}^{\mathrm{PVI}*} = f_{\mathrm{L}}^{\mathrm{SO}*}$.

   1-(ii) When only Constraint (23e) is binding, applying the KKT condition leads to

$$\mu_0(\mathrm{H})\left(\Delta_t - \zeta + \beta + (2\alpha + \zeta) f_{\mathrm{H}}^{\mathrm{PVI}*}\right) + \lambda_4\left(-\alpha\mu_0(\mathrm{H})\right) = 0,$$
$$\mu_0(\mathrm{L})\left(\Delta_t - \zeta + (2\alpha + \zeta) f_{\mathrm{L}}^{\mathrm{PVI}*}\right) + \lambda_4\left(-\alpha\mu_0(\mathrm{L}) - \zeta\right) = 0.$$

   Adding the binding Constraint (23e) and solving the resulting equation system yields $f_{\mathrm{L}}^{\mathrm{PVI}*} = \Omega + \frac{\beta}{2\alpha + \zeta} + \frac{\Lambda\zeta}{\mu_0(\mathrm{L})(2\alpha + \zeta)}, f_{\mathrm{H}}^{\mathrm{PVI}*} = \Omega$ where

$$\lambda_4 = \left(\zeta - \Delta_t - \beta\mu_0(\mathrm{H}) + \frac{\alpha\mu_0(\mathrm{H})(\Delta_t - \zeta + \beta)}{2\alpha + \zeta} + \frac{(\alpha\mu_0(\mathrm{L}) + \zeta)(\Delta_t - \zeta)}{2\alpha + \zeta}\right)\left(\frac{\mu_0(\mathrm{L})(2\alpha + \zeta)}{\alpha^2\mu_0(\mathrm{H})\mu_0(\mathrm{L}) + (\alpha\mu_0(\mathrm{L}) + \zeta)^2}\right) \equiv \Lambda,$$

   1-(iii) When both Constraints (23d) and (23e) are binding, $f_{\mathrm{H}}^{\mathrm{PVI}*}$ is the same as in 1-(i), and $f_{\mathrm{L}}^{\mathrm{PVI}*}$ is obtained by plugging $f_{\mathrm{H}}^{\mathrm{PVI}*}$ into the equation $-\alpha\mu_0(\mathrm{H}) f_{\mathrm{H}}^{\mathrm{PVI}*} - (\alpha\mu_0(\mathrm{L}) + \zeta) f_{\mathrm{L}}^{\mathrm{PVI}*} + (\zeta - \Delta_t - \beta\mu_0(\mathrm{H})) = 0$.

   To derive the conditions for each case, we note first that the solution obtained for Case 1-(i), $\left(f_{\mathrm{H}}^{\mathrm{FI}*}, f_{\mathrm{L}}^{\mathrm{SO}*}\right)$, is optimal if and only if it lies above b_4. The condition is necessary because if it is not satisfied, the solution would fall out of the feasible region; it is sufficient because from geometry, b_3 is the closest boundary to the optimal solution, see Figure 13(b). Requiring $\left(f_{\mathrm{H}}^{\mathrm{FI}*}, f_{\mathrm{L}}^{\mathrm{SO}*}\right)$ lies above b_4 leads to $\mu_0(\mathrm{H}) \geq \frac{\alpha(\alpha+\zeta)(\zeta-\Delta_t)}{\alpha^2(\zeta-\Delta_t)+\beta\zeta(2\alpha+\zeta)} = \tilde{\mu_0}$. To obtain the additional condition that separates Case 1-(ii) from 1-(iii), we check whether the solution in Case 1-(ii) lies to the right of b_3, i.e., $\Omega > f_{\mathrm{H}}^{\mathrm{FI}*} = \frac{\zeta - \Delta_t - \beta}{\alpha + \zeta}$. If it does, then the solution does not fall on b_3, which corresponds to Case 1-(ii), see Figure 13(c); otherwise, it is Case 1-(iii), see Figure 13(d).

2. When $\zeta < \Delta_t + \beta$, the compliant region is cut by $f_{\mathrm{H}}^{\mathrm{PVI}} \geq 0$, thus $f_{\mathrm{H}}^{\mathrm{SO}*} = f_{\mathrm{H}}^{\mathrm{FI}*} = 0$ in this case.

   2-(i) When the SO solution is feasible, it is evident that $\left(f_{\mathrm{H}}^{\mathrm{PVI}*}, f_{\mathrm{L}}^{\mathrm{PVI}*}\right) = \left(f_{\mathrm{H}}^{\mathrm{SO}*}, f_{\mathrm{L}}^{\mathrm{SO}*}\right)$, see Figure 13(e).

2-(ii) When the SO solution is infeasible and Constraint (23b) is binding, we must have $f_{\mathrm{H}}^{\mathrm{PVI}*} = f_{\mathrm{H}}^{\mathrm{SO}*} = 0$, see Figure 13(f). Then, solving $(\alpha\mu_0(\mathrm{H}) + \zeta) \cdot 0 + \alpha\mu_0(\mathrm{L}) f_{\mathrm{L}}^{\mathrm{PVI}*} - (\zeta - \Delta_t - \beta\mu_0(\mathrm{H})) = 0$, we obtain $f_{\mathrm{L}}^{\mathrm{PVI}*} = \frac{\zeta - \Delta_t - \beta\mu_0(\mathrm{H})}{\alpha\mu_0(\mathrm{L})}$. From Figure 13(f) we can easily infer $f_{\emptyset}^{\mathrm{NI}*} \le f_{\mathrm{L}}^{\mathrm{PVI}*} \le f_{\mathrm{L}}^{\mathrm{SO}*}$.

2-(iii) When the SO solution is infeasible and only (23e) is binding, the proof follows 1-(ii), omitted here for brevity.

2-(iv) When the SO solution is infeasible, and both $f_{\mathrm{H}}^{\mathrm{PVI}*} \ge 0$ and Constraint (23e) are binding (see Figure 13(h)), we have $f_{\mathrm{H}}^{\mathrm{PVI}*} = 0$. Then, from $-\alpha\mu_0(\mathrm{H}) \cdot 0 - (\alpha\mu_0(\mathrm{L}) + \zeta) f_{\mathrm{L}}^{\mathrm{PVI}*} + (\zeta - \Delta_t - \beta\mu_0(\mathrm{H})) = 0$, we obtain $f_{\mathrm{L}}^{\mathrm{PVI}*} = \frac{\zeta - \Delta_t - \beta\mu_0(\mathrm{H})}{\alpha\mu_0(\mathrm{L}) + \zeta}$.

It is worth noting that Constraint (23c) can never be active at optimum, when the SO solution is infeasible. This is because activating it requires $f_{\mathrm{L}}^{\mathrm{PVI}*} = f_{\mathrm{L}}^{\mathrm{FI}*} < f_{\mathrm{L}}^{\mathrm{SO}*}$. However, we have shown $f_{\mathrm{L}}^{\mathrm{FI}*} \ge f_{\mathrm{L}}^{\mathrm{SO}*}$ in Section D.1.1.

To derive the conditions for each case, we note that Case 2-(i) arises when $\left(f_{\mathrm{H}}^{\mathrm{SO}*}, f_{\mathrm{L}}^{\mathrm{SO}*}\right)$ lies below b_1 and above b_4. The former condition leads to $\mu_0(\mathrm{H}) \le \overline{\mu_0}$ and latter to $\mu_0(\mathrm{H}) \ge \underline{\mu_0}$. Case 2-(ii) occurs when $\left(f_{\mathrm{H}}^{\mathrm{SO}*}, f_{\mathrm{L}}^{\mathrm{SO}*}\right)$ lies above both b_1 and b_4, which leads to $\mu_0(\mathrm{H}) \ge \overline{\mu_0}$. Case 2-(iii) and (iv) occurs when $\left(f_{\mathrm{H}}^{\mathrm{SO}*}, f_{\mathrm{L}}^{\mathrm{SO}*}\right)$ lies below both b_1 and b_4, which leads to $\mu_0(\mathrm{H}) \le \underline{\mu_0}$. The difference between 2-(iii) and 2-(iv) is $\Omega = f_{\mathrm{H}}^{\mathrm{PVI}*} \ge 0$ in 2-(iii) and $\Omega < f_{\mathrm{H}}^{\mathrm{PVI}*} = 0$ in 2-(iv).

This completes the proof. □

D.6 Proof of Proposition 2

Proof. We need to show the following (the cases are defined in the proof for Theorem 2):

(a) The FI policy always outperforms the NI policy.

(b) In Cases 1-(i), 1-(ii), 1-(iii), the optimal private design (PVI) policy outperforms the FI policy.

(c) In Cases 2-(iii), 2-(iv), the PVI policy outperforms the FI policy.

(d) In Case 2-(ii), when $\mu_0(\mathrm{H}) \ge \hat{\mu_0}$, the FI policy outperforms the PVI policy, while when $\overline{\mu_0} \le \mu_0(\mathrm{H}) < \hat{\mu_0}$ the PVI policy outperforms the FI policy.

Only in Case 2-(i), the SO solution lies in the obedience-complaint region, thus the PVI policy works as well as the SO policy. In all other cases, the SO policy outperforms the PVI policy.

To prove (a), we need to show that $\delta = Z\left(f_{\emptyset}^{\mathrm{NI}*}, f_{\emptyset}^{\mathrm{NI}*}\right) - Z\left(f_{\mathrm{H}}^{\mathrm{FI}*}, f_{\mathrm{L}}^{\mathrm{FI}*}\right) \ge 0$, where $Z(\cdot)$ is defined in (23a). When $f_{\mathrm{H}}^{\mathrm{FI}*} > 0$, $\delta = \frac{\beta^2\zeta\mu_0(\mathrm{H})\mu_0(\mathrm{L})}{2(\alpha+\zeta)^2} \ge 0$. Otherwise, i.e., when $f_{\mathrm{H}}^{\mathrm{FI}*} = 0$, $\delta = \frac{-\zeta\mu_0(\mathrm{H})}{2(\alpha+\zeta)^2}\left[(\zeta - \Delta_t - \beta)^2 - \beta^2\mu_0(\mathrm{L})\right]$, which is non-negative as

$$\underbrace{\frac{-\zeta\mu_0(H)}{2\left(\alpha+\zeta\right)^2}}_{\le 0}\underbrace{\left(\zeta - \Delta_t - \beta\left(1 - \sqrt{\mu_0(\mathrm{L})}\right)\right)}_{\ge \zeta - \Delta_t - \beta\mu_0(\mathrm{H}) \ge 0}\underbrace{\left(\zeta - \Delta_t - \beta\left(1 + \sqrt{\mu_0(\mathrm{L})}\right)\right)}_{\le \zeta - \Delta_t - \beta \le 0} \ge 0.$$

To prove (b) and (c), we show that the designer's objective function must strictly improves as the solution moves from the FI policy $\boldsymbol{f}^{\mathrm{FI}*} = \left(f_{\mathrm{H}}^{\mathrm{FI}*}, f_{\mathrm{L}}^{\mathrm{FI}*}\right)$ to the PVI policy $\boldsymbol{f}^{\mathrm{PVI}*} = \left(f_{\mathrm{H}}^{\mathrm{PVI}*}, f_{\mathrm{L}}^{\mathrm{PVI}*}\right)$.

Let $\boldsymbol{d} = \boldsymbol{f}^{\text{PVI}*} - \boldsymbol{f}^{\text{FI}^*}$ and $\mathbb{F} = \{\boldsymbol{f} | \boldsymbol{f} = s\boldsymbol{f}^{\text{FI}*} + (1-s)\boldsymbol{f}^{\text{PFI}*}, \forall s \in [0,1]\}$ We proceed to prove that for any $\boldsymbol{f} \in \mathbb{F}$ we have $\langle d, -\nabla Z(\boldsymbol{f})\rangle \geq 0$.

To begin, we note that

$$\nabla Z(\boldsymbol{f}) = \begin{bmatrix} \frac{\partial Z(\boldsymbol{f})}{\partial f_{\text{H}}^{\text{PVI}}} \\ \frac{\partial Z(\boldsymbol{f})}{\partial f_{\text{L}}^{\text{PVI}}} \end{bmatrix} = \begin{bmatrix} \mu_0(\text{H})\left((\zeta - \Delta_t - \beta) - (2\alpha + \zeta) f_{\text{H}}^{\text{PVI}}\right) \\ \mu_0(\text{L})\left((\zeta - \Delta_t) - (2\alpha + \zeta) f_{\text{L}}^{\text{PVI}}\right) \end{bmatrix}.$$

It is easy to verify that $-\frac{\partial Z(\boldsymbol{f})}{\partial f_{\text{H}}^{\text{PVI}}}$ decreases with $f_{\text{H}}^{\text{PVI}}$ and $-\frac{\partial Z(\boldsymbol{f})}{\partial f_{\text{L}}^{\text{PVI}}}$ decreases with $f_{\text{L}}^{\text{PVI}}$.

- In Case 1-(i), 1-(ii), and 1-(iii),

$$-\nabla Z(\boldsymbol{f}) = \begin{bmatrix} -\frac{\alpha\mu_0(\text{H})(\zeta - \Delta_t - \beta)}{\alpha+\zeta} \\ -\frac{\alpha\mu_0(\text{L})(\zeta - \Delta_t)}{\alpha+\zeta} \end{bmatrix} \leq 0$$

  at $\left(f_{\text{H}}^{\text{FI}*}, f_{\text{L}}^{\text{FI}*}\right)$, since $\zeta \geq \Delta_t + \beta$. At $\left(f_{\text{H}}^{\text{PVI}*}, f_{\text{L}}^{\text{PVI}*}\right)$,

  1-(i) we have

$$-\nabla Z(\boldsymbol{f}^{\text{PVI}*}) = \begin{bmatrix} -\frac{\alpha\mu_0(\text{H})(\zeta - \Delta_t - \beta)}{\alpha+\zeta} \\ 0 \end{bmatrix}.$$

  Thus, as the solution moves along $\boldsymbol{d}$ from the FI policy to the PVI policy, $-\frac{\partial Z(\boldsymbol{f})}{\partial f_{\text{H}}^{\text{PVI}}}$ remains a constant while $-\frac{\partial Z(\boldsymbol{f})}{\partial f_{\text{L}}^{\text{PVI}}}$ increases from a non-positive value to zero. Moreover, $\boldsymbol{d}$ can be written as $\tau[-1,0]^T$ for $\tau \in \mathbb{R}^+$. Thus, we have $\langle d, -\nabla Z(\boldsymbol{f})\rangle \geq 0$. From Figure 17 we can see that this means $\boldsymbol{d}$ and $-\nabla Z(\boldsymbol{f})$ always form an acute angle until $\boldsymbol{f}$ reaches $\boldsymbol{f}^{\text{PVI}*}$.

  1-(ii) we have

$$-\nabla Z(\boldsymbol{f}^{\text{PVI}*}) = \begin{bmatrix} -\Lambda\alpha\mu_0(\text{H}) \\ -\Lambda\left(\alpha\mu_0(\text{L}) + \zeta\right) \end{bmatrix} \leq 0,$$

  which, per the KKT condition, must be perpendicular to b_4. Since $f_{\text{H}}^{\text{PVI}*} \geq f_{\text{H}}^{\text{FI}*}$, $f_{\text{L}}^{\text{PVI}*} \leq f_{\text{L}}^{\text{FI}*}$ (see Figure 13(c)), we can show that $-\frac{\partial Z(\boldsymbol{f})}{\partial f_{\text{H}}^{\text{PVI}}}$ decreases and $-\frac{\partial Z(\boldsymbol{f})}{\partial f_{\text{L}}^{\text{PVI}}}$ increases while the solution moves from the FI policy to the PVI policy. Consequently, the angle between $\boldsymbol{d}$ and $-\nabla Z(\boldsymbol{f})$ also increases. However, since $\boldsymbol{d}$ has a greater absolute slope than that of b_4 and $-\nabla Z(\boldsymbol{f})$ is perpendicular to b_4 at the PVI policy, the angle between the vectors at the terminal point of $\boldsymbol{d}$ can not be obtuse, again see Figure 17. Thus, $\langle d, -\nabla Z(\boldsymbol{f})\rangle \geq 0$ for any $\boldsymbol{f} \in \mathbb{F}$.

  1-(iii) it is difficult to derive the closed-form expression for $-\nabla Z(\boldsymbol{f})$. However, the result is similar to Case 1-(i): $-\frac{\partial Z(\boldsymbol{f})}{\partial f_{\text{H}}^{\text{PVI}}}$ remains unchanged, while $-\frac{\partial Z(\boldsymbol{f})}{\partial f_{\text{L}}^{\text{PVI}}}$ increases monotonically as the solution moves along $\boldsymbol{d}$. Since this means the angle between $\boldsymbol{d}$ and $-\nabla Z(\boldsymbol{f})$ will grow along $\boldsymbol{d}$, we only need to show that the angle cannot be an obtuse one at the PVI policy. Per the KKT condition, $-\nabla Z(\boldsymbol{f})$ must lie in the normal cone of the feasible set at the intersection between b_3 and b_4 (formed by the two vectors perpendicular to b_3 and b_4, see Figure 17. Its angle with $\boldsymbol{d}$, which points downward vertically and overlaps with b_3, must be acute.

- In Case 2-(iii), the proof is identical to Case 1-(ii), hence omitted for brevity. For Case 2-(iv), since $f_{\text{H}}^{\text{SO}*} = f_{\text{H}}^{\text{PVI}*} = f_{\text{H}}^{\text{FI}*} = 0$ and $f_{\text{L}}^{\text{SO}*} \leq f_{\text{L}}^{\text{PVI}*} \leq f_{\text{L}}^{\text{FI}*}$, it follows that $Z(\boldsymbol{f}^{\text{PVI}*}) \leq Z(\boldsymbol{f}^{\text{FI}*})$ — note that $Z(\cdot)$ is a quadratic function with respect to f_{L}, which peaks at $f_{\text{L}}^{\text{SO}*}$ and have both $f_{\text{L}}^{\text{PVI}*}$ and $f_{\text{L}}^{\text{FI}*}$ lie at the same side of the peak.

To prove (d), note tht in Case 2-(ii), $f_{\mathrm{H}}^{\mathrm{SO}*} = f_{\mathrm{H}}^{\mathrm{PVI}*} = f_{\mathrm{H}}^{\mathrm{FI}*} = 0$ and $f_{\mathrm{L}}^{\mathrm{PVI}*} \leq f_{\mathrm{L}}^{\mathrm{SO}*} \leq f_{\mathrm{L}}^{\mathrm{FI}*}$. Whether the FI policy is better than the PVI policy depends on the distance between the corresponding f_{L} and $f_{\mathrm{L}}^{\mathrm{SO}*}$, where the quadratic function $Z(\cdot)$ peaks. The FI policy is better than the PVI policy when $f_{\mathrm{L}}^{\mathrm{FI}*} - f_{\mathrm{L}}^{\mathrm{SO}*} < f_{\mathrm{L}}^{\mathrm{SO}*} - f_{\mathrm{L}}^{\mathrm{PVI}*}$, which leads to the following condition $\mu_0(\mathrm{H}) \geq \left(\alpha^2 + (\alpha+\zeta)^2\right)(\zeta - \Delta_t) \,/\, [-\alpha\zeta(\zeta - \Delta_t) + \beta(2\alpha+\zeta)(\alpha+\zeta)] = \hat{\mu_0}$. This completes the proof. □

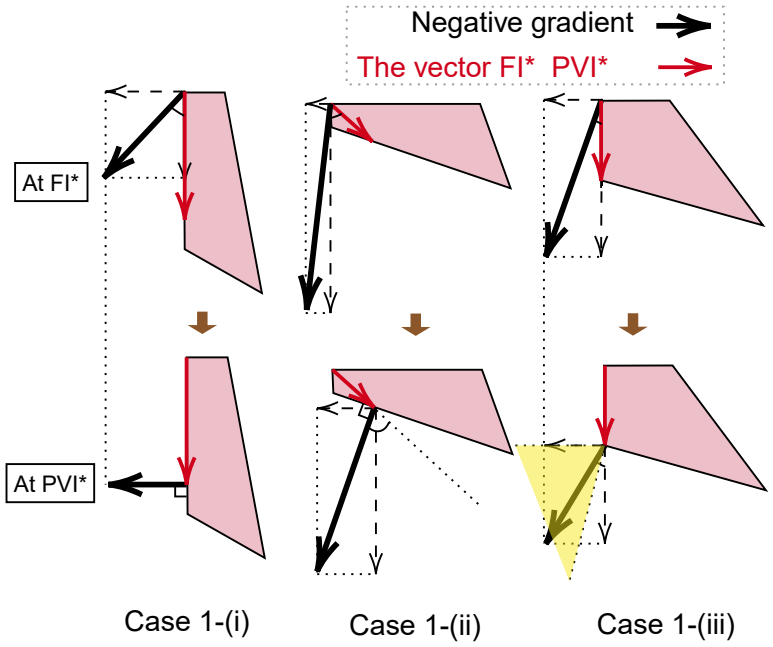

Figure 17: Illustration of the proof of Proposition 2.